Naval Command,
Control and Ocean
Surveillance Center RDT&E Division San Diego, CA
92152-5001

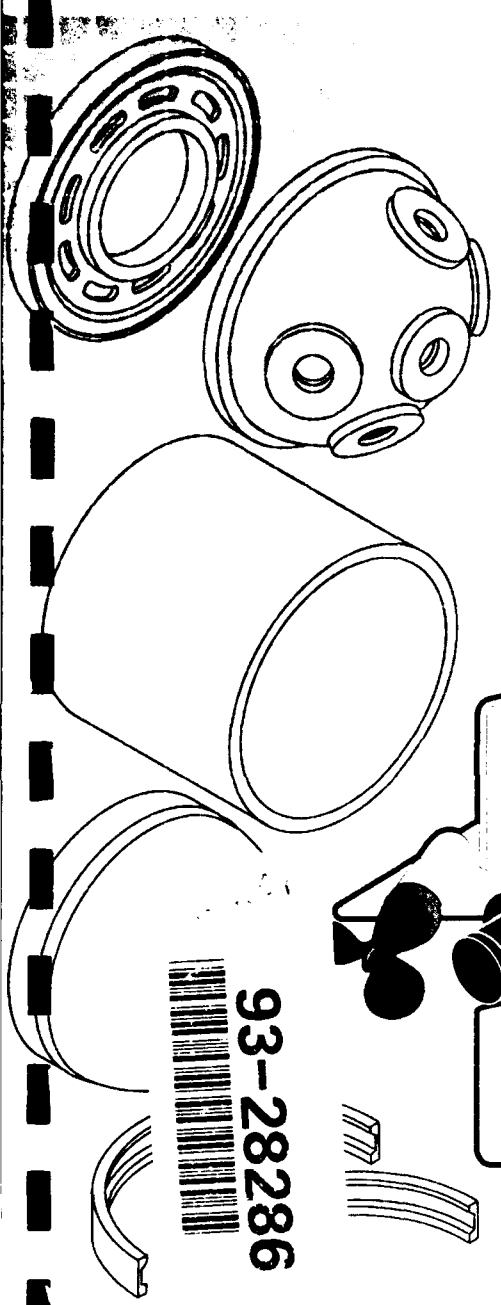

Adhesive Bonded Joint With Improved Cyclic Fa for Alumina-Ceramic Cy and Hemispheres

Fourth Generation Housings

Technical Report 1587
August 1993

J. D. Stachiw

Technical Report 1587
August 1993

Adhesive Bonded Joint With Improved Cyclic Fatigue Life for Alumina-Ceramic Cylinders and Hemispheres

Fourth Generation Housings

J. D. Stachiw

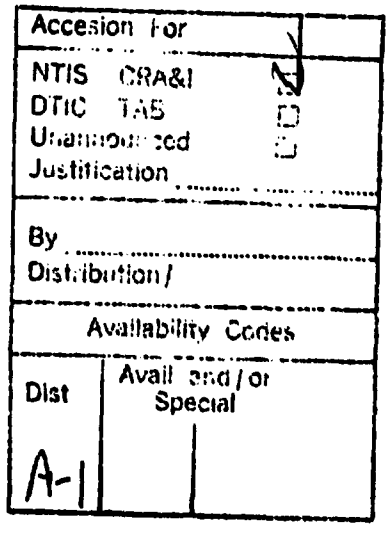

NAVAL COMMAND, CONTROL AND OCEAN SURVEILLANCE CENTER
RDT&E DIVISION
San Diego, California 92152–5001

K. E. EVANS, CAPT, USN
Commanding Officer

R. T. SHEARER
Executive Director

ADMINISTRATIVE INFORMATION

This work was performed by the Marine Materials Technical Staff, RDT&E Division of the Naval Command, Control and Ocean Surveillance Center, for the Naval Sea Systems Command, Washington, DC 20362.

Released by
J. D. Stachiw, Head
Marine Materials
Technical Staff

Under authority of
N. B. Estabrook, Head
Ocean Engineering
Division

ES

SUMMARY

OBJECTIVE

The study was conceived to resolve three problems raised by previous Naval Ocean Systems Center (NOSC)* studies on ceramic housings for deep submergence vehicles:

a. Is it feasible to significantly extend the cyclic fatigue life of 20-inch OD by 30-inch L by 0.685-inch t monocoque 94-percent alumina-ceramic cylinders serving as external pressure housings beyond 100 pressure cycles to 9,000 psi design pressure?

b. Can the 20-inch OD by 30-inch L by 0.685-inch t monocoque 94-percent alumina-ceramic cylinders tolerate surface and subsurface imperfections in the shape of chips, surface separations, and inclusions without initiation of cracks when pressurized to 9,000 psi design pressure?

c. Can the 0.5 weight-to-displacement (W/D) ratio of 0.685-inch-thick by 20-inch OD monocoque cylinders from 94-percent alumina ceramic be reduced significantly by decreasing the wall thickness without a corresponding reduction in cyclic fatigue life?

APPROACH

The objectives of the study were met by selecting the following experimental approaches to the problem:

a. A new end cap, NOSC Type Mod 1 (hereafter called Mod 1), was designed, fabricated, and installed on the ends of a 20-inch OD by 30-inch L by 0.685-inch t monocoque 94-percent alumina-ceramic cylinder. This cylinder was, after proof testing to 10,000 psi, pressure cycled to 9,000 psi until implosion. The ends of cylinder were radially supported by titanium hemispheres.

b. A monocoque 94-percent alumina-ceramic cylinder with 20-inch OD by 30-inch L by 0.685-inch t dimensions that included imperfections in the shape of chips, surface separations, and internal inclusions was, after proof testing to 10,000 psi, pressure cycled 100 times to 9,000 psi.

c. The wall thickness of two 20-inch OD by 0.685-inch t monocoque cylinders was reduced by grinding one to 0.586 of an inch and the other to 0.455 of an inch thickness, except for a distance of 2 inches at both ends. These cylinders were, after proof testing to 10,000 psi, pressure cycled to 9,000 psi until failure.

TEST RESULTS

The testing of the 20-inch OD monocoque 94-percent alumina-ceramic cylinders under external pressure generated the following results:

a. The 20-inch OD by 30-inch L by 0.685-inch t cylinder equipped with Mod 1 aluminum end caps failed after two proof tests to 10,000 psi and 453 pressure cycles to 9,000 psi.

b. The 20-inch OD by 30-inch L by 0.685-inch t cylinder with imperfections in the shape of chips, surface separations, and internal inclusions did not crack after two proof tests to 10,000 psi and 100 pressure cycles to 9,000 psi. The ends of the cylinder were equipped with Mod 1 aluminum end caps.

c. The 20-inch OD by 30-inch L by 0.685-inch t cylinder with its wall thickness reduced to 0.455 of an inch along a 13-inch-wide span centered at midbay withstood two proof tests to 10,000 psi and 50 cycles to 9,000 psi prior to initiation of spalling at the ends. The ends of the cylinder were equipped with Mod 1 aluminum end caps.

d. The 20-inch OD by 30-inch L by 0.685-inch t cylinder with its wall thickness reduced to 0.585 of an inch along a 26-inch-wide span centered at midbay failed by buckling during the first proof test at 9,700 psi. The ends of the cylinder were equipped with Mod 1 aluminum end caps.

*NOSC is now Naval Command, Control and Ocean Surveillance Center (NCCOSC), RDT&E Division (NRaD).

FINDINGS

The following conclusions about 20-inch OD monocoque 94-percent alumina-ceramic cylinders have been formed on the basis of the above test results:

a. The cyclic fatigue life of bearing surfaces on 20-inch OD by 30-inch L by 0.685-inch t cylinders have been extended from 100 to 453 cycles at 9,000 psi by replacing the Mod 0 end caps with the redesigned Mod 1 end caps.

b. The 20-inch OD by 30-inch L by 0.685-inch t cylinders can tolerate serious surface and subsurface imperfections, provided that the nominal membrane stresses in hoop and axial direction do not exceed –136,000 and –68,000 psi, respectively, at design depth.

c. The cyclic fatigue life at 9,000 psi design pressure of 20-inch OD cylinders with 0.450-inch wall thickness is 90-percent shorter than the cyclic fatigue life of 20-inch OD cylinders with 0.685-inch wall thickness when both are equipped with Mod 1 end caps.

d. The critical pressure of the 20-inch OD by 30-inch L by 0.585-inch t cylinder when supported by hemispherical bulkheads does not meet the 10,000 psi proof pressure requirement of ceramic housings with 9,000 psi design depth. It imploded at 9,700 psi due to buckling.

CONCLUSIONS

Ceramic with 94-percent alumina composition has been shown to be a structurally reliable, corrosion-resistant, and cost-effective material for construction of large pressure housings for unmanned diving systems. When the nominal membrane design stress is kept below –136,000 psi, the ceramic components can tolerate large surface and subsurface imperfections without initiation of cracking, provided that they are not located on the bearing surfaces.

The 20-inch OD by 30-inch L by 0.685-inch t monocoque cylinders equipped with Mod 1 end caps and mated to titanium hemispheres, or skirted ceramic hemispheres with Mod 1 end caps, have a proven cyclic fatigue life in excess of 400 cycles at 9,000 psi design pressure, provided that an epoxy layer of 0.01- to 0.015-inch thickness separates the mating bearing surfaces of ceramic components and metallic end caps. The 0.5 W/D ratio of the 94-percent alumina-ceramic cylinders with $t/D_o = 0.034$ provides them with a payload-carrying ability that is approximately four times larger than that of rib-stiffened titanium cylinders with the same pressure rating.

RECOMMENDATIONS

1. The external pressure housings assembled from 20-inch OD by 30-inch L by 0.685-inch t monocoque 94-percent alumina-ceramic cylinders and mating-skirted hemispherical bulkheads equipped with Mod 1 metallic end caps should be replaced during underwater vehicle overhauls scheduled after 200 dive intervals to a 20,000-foot design depth. Such an arrangement will provide a 100-percent safety margin against potential catastrophic failure initiated by cyclic fatigue of the bearing surfaces on the ceramic components.

2. The Mod 1 end caps can be fabricated from steel, titanium, or aluminum, with a compressive yield of >65,000 psi. The titanium Ti-6Al-4V alloy appears to be the best choice for this application.

CONTENTS

FIGURES

TABLES

INTRODUCTION

The Navy, among other organizations and institutions, is vitally interested in acquiring the most operationally effective and cost-efficient vehicles for deep submergence operations. Three factors determine if such vehicles meet mission standards: payload, operational range, and speed. Each of these factors is a direct function of the buoyancy provided by the pressure hull. Clearly, buoyancy of the pressure hull is the critical issue. Maximum buoyancy is provided by a competent design of the pressure hull and the application of premium structural material to its construction. When both are present, it is feasible to attain a pressure hull with a low weight-to-displacement (W/D) ratio. The reason for seeking the low W/D ratio is to maximize payload, while minimizing the size of the hull. This, in turn, reduces the hydrodynamic drag, and, thus, permits the vehicle to achieve maximum range and speed.

A W/D ratio less than, or equal to, 0.5 has been found by operational experience to be desirable for the pressure housing assembly. A 0.5 W/D ratio provides the vehicle, in most cases, with adequate buoyancy for its propulsion, guidance, and work subsystems. Ceramics not only possess the required structural properties for construction of external pressure housings with <0.5 W/D ratio for service to 20,000 feet (table 1, figure 1),[1] but also are impermeable, corrosion resistant, and good conductors of heat. Their sole shortcoming in comparison to titanium is low fracture toughness, which may cause improperly designed pressure housings to fail unexpectedly in service (table 2).

To arrive at an operationally usable external pressure housing of ceramic material, several fabrication and design problems need to be solved that have, in the past, worked against the acceptance of such housings by the ocean engineering community. These problems were economical fabrication of large ceramic cylinders, reliable mechanical joining of several ceramic cylinders into a cylindrical pressure housing of desired length, elimination of stress risers on the ceramic bearing surfaces between individual housing assembly components, secure mounting of payload components inside the ceramic housing, and protection against impact.

Since the potential payoffs for deep-submergence unmanned vehicles in terms of size reduction and drag decrease are very substantial, the Navy has a keen interest in developing this technology for application to its vehicles. As a result of the Navy's interest in more efficient pressure hulls for deep submergence vehicles, the Naval Command, Control and Ocean Surveillance Center (NCCOSC) RDT&E Division (NRaD)[2] has set out to demonstrate that the problems can be addressed and solved to a degree that will make the ceramic housings acceptable for practical applications.

As a result of NRaD engineering efforts, it was shown conclusively that cylindrical external pressure housings of up to 20 inches in diameter can be economically fabricated from 94-percent alumina ceramic for a 20,000-foot design depth. The 0.5 W/D ratio of these cylinders represents a significant improvement in weight over titanium housings of identical size with only a 0.87 W/D ratio. Because of the significantly lower W/D ratio, the ceramic housings provide more than three times the buoyancy of titanium housings with the same design depth.

This report describes additional work performed by NRaD since the completion in 1990 of the 20-inch-diameter ceramic housing exploratory development program (reference 1). The objectives of this work were to provide further improvement in payload capability and cyclic fatigue life of the 20-inch-diameter cylindrical alumina-ceramic housings with a design depth of 20,000 feet. This work resulted in increasing by 300 percent the cyclic fatigue life of alumina-ceramic cylinders with 0.5 W/D ratio. It also demonstrated that the W/D ratio of alumina-ceramic cylinders can be decreased from 0.5 to 0.4, provided that the underwater vehicle can tolerate a decrease in fatigue life from 450 to less than 50 dives to 9,000 psi design depth.

1. Figures and tables are placed at the end of the text.

2. NRaD was previously Naval Ocean Systems Center (NOSC).

SUMMARY OF PAST INVESTIGATIONS ON 20-INCH HOUSINGS

OBJECTIVE

The objective of the NRaD pressure housing development program was to develop a design for a 20-inch-diameter cylindrical ceramic housing with a low W/D ratio for operational service to a depth of 20,000 feet. The housing was to consist of an assembly of cylindrical and spherical ceramic sections secured together by mechanical joints that provide for rapid disassembly and access to their interiors for servicing of the payload.

APPROACH

The external pressure housing was designed (reference 1) to be assembled from one or more 20-inch OD by 0.685-inch-thick by 30-inch-long ceramic monocoque cylindrical sections, capped at their ends with titanium rings that facilitated mating them with similar ring caps bonded to ceramic hemispheres (figures 2, 3, 4, and 5).

If the payload requirement could not be satisfied with a single cylindrical section radially supported by titanium or ceramic hemispherical bulkheads (figure 6), two cylinders could be joined by a titanium ring stiffener to provide greater payload capability (figure 7). The titanium ring stiffener, besides serving to align the two cylindrical sections, provided additional radial support against buckling of the cylindrical sections.

The ceramic hemispheres were provided with circular penetrations into which metallic penetrators with electrical connectors could be threaded (figure 8). The penetrators rested on glass fiber-reinforced plastic pads to eliminate any point loading between the penetrator and the ceramic hemisphere (figure 9).

FABRICATION

A total of three 20-inch OD by 18.64-inch ID by 30-inch L cylinders (figure 2) and two 19.66-inch OD by 18.98-inch ID hemispheres (figure 4) were fabricated by Coors Ceramics. The associated metallic components including joint rings, stiffeners, and penetration inserts were machined from Ti-6Al-4V alloy. In addition, a series of handling and test fixtures were fabricated in aluminum for the handling of the individual ceramic components and the assembled housings during pressure testing. Polyurethane jackets protected the ceramic components of the housings against point impacts during assembly and handling.

TESTING

The testing of the 20-inch housings took place in the 30-inch-diameter by 120-inch-long pressure vessel of the Southwest Research Institute. Testing was first performed on individual cylinders capped with hemispheres (figure 6) and, subsequently, on assemblies made up of two cylinders joined by a ring stiffener and closed off at the ends with hemispheres (figure 7). Testing consisted of pressurizing each individual cylinder test assembly once to the proof-test pressure of 10,000 psi, followed by 10 pressurizations to design pressure of 9,000 psi. The two-cylinder test assembly was subjected once to test pressure, followed by 100 pressurizations to design pressure. Strains were recorded during the testing.

TEST RESULTS

The 94-percent alumina, 20-inch-diameter ceramic pressure housings performed structurally under external pressure in the same manner as the 4-, 6-, and 12-inch pressure housings tested at NRaD in prior years (references 2 and 3). At 9.000 psi hydrostatic pressure loading, the maximum recorded stress at midbay on the internal surface of the cylinders was –136,000 psi in hoop and –68,000 psi axial directions. In the hemisphere, both hoop and meridional stresses were –134,000 psi on the internal surface. The axial bearing stress on plane ends of the cylinders was –68,000 psi and on hemispheres, –134,700 psi. This indicates that small alumina-ceramic housings can be scaled-up to large dimensions without a noticeable decrease in physical properties. Based on this finding, one can expect that even a very large alumina-ceramic pressure housing will provide unmanned vehicles with a 0.5 W/D ratio.

The titanium NOSC Type Mod 0 (hereafter called Mod 0) end caps on 20-inch-diameter ceramic

housing components, using 0.010-inch-thick epoxy adhesive as a bearing gasket, withstood successfully two tests to 10,000 psi, and 100 pressure cycles to 9,000 psi. Implosion occurred after the assembly was subjected to an additional 10 cycles to 9,000 psi.

The implosion of the housing was initiated by the cracking of ceramic material on the plane-bearing surfaces of the cylinders and hemispheres. At those locations, residual microcracks from grinding grew progressively with each pressurization under the action of local tensile radial stress component into large, circumferentially oriented vertical-fracture planes that ultimately weakened the walls of the ceramic housing components to such a degree that catastrophic failure took place. The cracks appeared first on the plane-bearing surfaces of the ceramic hemispheres and were the source of severe spalling that resulted in catastrophic failure of the housing assembly after only 109 pressure cycles to 9,000 psi. The cracking on bearing surfaces occurred first on hemispheres due to the fact that the bearing-stress exerted by the thin hemispherical shell on a metallic end cap is twice as high as of the 100-percent-thicker cylindrical shell.

CONCLUSION

The pressure housing development program conducted by NRaD during FY 90 has conclusively shown that 20-inch diameter external pressure housings with a 0.5 W/D ratio, providing payload capability in the range of 237 to 375 pounds, can be successfully fabricated from 94-percent alumina ceramic for operational service to a depth of 20,000 feet.

The cyclic fatigue life of these housings equipped with Mod 0 end caps was shown to be in excess of 100, but less than 150, dives to the design depth of 20,000 feet. For repeated dives to lesser depths, the fatigue life in all probability exceeds several hundred dives.

Since the cyclic fatigue life of ceramic housings is governed by the formation of cracks on the plane-bearing surfaces, steps had to be taken to eliminate, or at least retard, the initiation and propagation of these cracks. This could be accomplished by reducing the bearing stress on hemispheres by increasing wall thickness, redesigning the metallic end caps for both cylinders and spheres, selecting different bearing gasket material, and improving grinding techniques for bearing surfaces.

The redesign of metallic end caps for cylinders was chosen as the first phase for improving the cyclic fatigue life of ceramic pressure housings. The other parameters controlling the fatigue life of housings will be studied and may be modified in following phases of the ceramic housing program. In particular, the shape of the hemisphere will be modified to increase the plane-bearing surface area to match that of cylinders without increasing the thickness of the hemisphere. This will be achieved by having the hemisphere terminate at the equator in a cylindrical skirt of which the thickness matches that of the mating cylinder.

PROGRAM FOR MODIFICATIONS OF 20-INCH HOUSINGS

OBJECTIVE

The modification program for improving 20-inch alumina-ceramic housings developed in prior years by Dr. Stachiw (reference 1) focused on two areas:

1. Cyclic fatigue life of ceramic housing components.
2. Payload capability of the housing assembly.

APPROACH

The first objective, improving cyclic fatigue life, was to be achieved by redesigning metallic end cap rings for the ceramic bearing surfaces on cylinders and hemispheres, rather than modifying the composition of the ceramic or its fabrication process. This course of action was chosen because budget restrictions did not permit pursuing the other more promising, but more costly, approaches.

The second objective, improving payload capability, was to be achieved by raising the magnitude of design stress, rather than changing the ceramic composition (i.e., selecting ceramic compositions with lower density, like beryllium oxide, silicon

carbide, or boron carbide). This course of action also was chosen for economic reasons, as it would require an extensive development program to fabricate successfully 20-inch cylinders and hemispheres from ceramic compositions with higher strength/weight ratios.

SCOPE

The scope of the program encompassed the design, fabrication, and experimental evaluation of three 20-inch-diameter 94-percent alumina-ceramic (table 2) cylinders designed to different sets of criteria (table 3), and a single 20-inch-diameter 94-percent alumina-ceramic cylinder with severe defects including surface separation, internal inclusion, and chipped chamfers on bearing surfaces.

DESIGN CRITERIA

Test Cylinder A

The 20-inch OD by 30-inch L by 0.685-inch t dimensions of test cylinder A (figure 10) were identical to those of the 20-inch-diameter alumina-ceramic cylinders fabricated and tested during the development program of fourth-generation NOSC ceramic housings (reference 1). During that development program, the cylinders (PN 55510–0121758) and associated hemispheres (PN 55910–0121705 and PN 55910–0121954) imploded during pressure cycling to 9,000 psi design pressure on the 109th cycle, even though their design was considered to be fairly conservative (i.e., 1.5 stress factor [S.F.] for buckling and 2.2 S.F. for material failure).

The most direct and sure way of extending the cyclic fatigue life of these components would have been to lower the compressive axial-design stress by increasing the thickness of the ceramic components, as it has been experimentally shown that the magnitude of radial tensile stress on the bearing surface and the cracks that it initiates with repeated pressurization are directly related to the compressive loading on the bearing surface (reference 3). Since the bearing stresses on the edge of the sphere are twice as high as they are on the end of the cylinder, the proper course of action would be to double the sphere's shell thickness so that its fatigue life matches that of the cylinder. This approach, unfortunately, would (1) increase the mismatch in radial displacement between the cylinder and hemisphere resulting in higher bending stresses at the joint, and (2) raise the W/D ratio of the housing beyond the 0.5 limit considered acceptable for high-performance pressure hulls on undersea vehicles with 9,000 psi design pressure.

A unique approach to matching the bearing stresses on the hemisphere's equator to those on cylinder ends without a significant increase in housing weight is to provide the hemisphere with a short cylindrical rim of the same wall thickness as the cylinder. One further advantage of this design modification to the classical hemisphere shape is that the metal end cap would fit both the hemisphere and the cylinder.

It was decided to focus this study on end cap design in view of the fact that after the proposed approach to reduction-in-bearing stresses on the edges of hemispheres there still remained the question of whether the existing Mod 0 end caps for 20-inch cylinders and hemispheres provided an optimized design for reduction of tensile radial stresses on the plane-bearing surfaces. The reasons for choosing end caps for cylinders as the primary objective of investigation were of an economic nature; cylinders and their end caps were cheaper to manufacture than hemispheres and their end caps.

Since it was known from other studies on ceramic external pressure housings (reference 3) that the magnitude of maximum radial stress on the plane-bearing surface of a ceramic cylinder with a given wall thickness is an inverse function of the flange height on the metallic end cap enclosing the ends of the cylinder, a decision was made to increase significantly the height of the flanges on the end cap ring. This approach would result in an insignificant increase of cylinder assembly weight, but a significant reduction in tensile radial stress on the plane-bearing surfaces of the cylinder.

The height of the flanges on the Mod 0 end cap rings used in the fourth-generation 20-inch ceramic housing development program (reference 1) was 1.45 inches on the interior, and 0.65 of an inch on the exterior of the cap (figures 11 and 12). Since the finite-element calculations showed a potential decrease in tensile stresses on the ceramic bearing surfaces only if the height of both flanges was increased beyond 0.65 of an inch, the end cap ring was redesigned to accept longer flanges.

The new height selected for end cap flanges was 1.9 inches (figure 13). This dimension was verified by pressure cycling 12-inch OD by 18-inch L by 0.412-inch-thick 94-percent alumina-ceramic cylinders in an independent exploratory development (IED) ceramic housing program at NRaD (reference 3). In that program, 12-inch OD ceramic cylinders equipped with 1.05-inch-deep end caps successfully withstood 500 pressure cycles to 9,000 psi without visible spalling of bearing surfaces. The 1.9-inch overall height of flanges on NOSC type Mod 1 (hereafter called Mod 1) end caps for 20-inch OD cylinders was obtained by multiplying the 1.05-inch net height of the flange (1.3-inch overall height minus the 0.250-inch seal bevel) on the 12-inch cylinder by a 20/12 scaling ratio of diameters. The resulting value of 1.75 inches for net height was then increased by the depth of the seal bevel to 2.07 inches for overall height. Since significant cost savings can be realized by machining the end caps from standard 2-inch plate, the overall height of the flange was reduced to 1.9 inches.

The new Mod 1 end cap ring for 20-inch ceramic cylinders (figures 13 and 14) has integral 1.9-inch-high flanges on both the exterior and interior surfaces of the ring, except that a 0.320-inch-deep bevel is incorporated into the exterior flange to serve as the seat for an elastomeric seal. The end cap ring for the hemispheres was redesigned in a similar manner.

Test cylinder A (figure 10) with two redesigned titanium Mod 1 end cap rings (figure 15) was calculated to weigh 176 pounds and provide 176 pounds of lift (positive buoyancy), giving this housing component a 0.5 W/D ratio. Because of its conservative structural characteristics, this cylindrical housing section with Mod 1 end cap rings is considered to be the standard of comparison for all other large-diameter alumina-ceramic cylindrical pressure housing designs under design for 9,000 psi operational pressure.

To reduce cost of the test program, all 20-inch cylinders were equipped for test purposes with Mod 1 end caps machined from 2-inch plates of 7075-T6 aluminum alloy instead of Ti-6Al-4V alloy, although it was known that the magnitude of tensile radial stress in ceramic cylinder ends is higher when supported by aluminum, rather than titanium end caps. This was not considered a disadvantage in the test program, as the cyclic fatigue-life data generated by a cylinder equipped with aluminum end caps would be considered conservative for future operational units equipped with titanium end caps of the same dimensions.

Test Cylinder B

The dimensions of test cylinder B (figure 16) were identical to test cylinder A, except for the reduced wall thickness at midbay (figure 10). The thickness was reduced from 0.685 to 0.585 inch to increase the nominal hoop stress level from –136,000 to –158,600 psi, thus reducing the material failure safety factor from 2.2 to 1.9. The ends of the cylinder retained the same thickness as test cylinder A to keep the magnitude of axial bearing stresses on all cylinders the same.

Because of the reduced wall thickness, test cylinder B weighs less (157 versus 176 pounds) and, therefore, provides more positive lift (195 versus 176 pounds) than standard test cylinder A. The W/D ratio of the cylinder B assembly is 0.45.

The reduced wall thickness causes the critical buckling pressure of test cylinder B, when tested with hemispherical bulkheads, to decrease from 13,500 to 9,600 psi, resulting in a safety factor of only 1.07. A low safety factor like this is not acceptable for operational housings, because of uncertainties where computational methods are used for prediction of critical pressures by buckling. In this case, however, it would serve as a test specimen for experimental verification of the BOSOR4 computer program utilized for predicting buckling. If the experimental critical pressure of

test cylinder B validates the critical pressure calculated by BOSOR4, it will be used to size the length of the cylinder needed to provide a 1.5 safety factor for 9,000 psi design pressure against buckling when the wall thickness is reduced to 0.585 inch to provide 24-percent more lift than cylinder A (figure 10) with 0.685-inch wall thickness.

Test Cylinder C

Test cylinder C was conceived to represent the lightest design feasible for 20-inch OD cylinders of 94-percent alumina ceramic for 9,000-psi design pressure (figure 19). Its design was based on an S.F. of 1.5 for both material strength of 300,000 psi and elastic instability at 13,500 psi. To achieve these objectives, the thickness at midbay was reduced to 0.455 inch and the length of the cylinder reduced to 17 inches. The ends of the cylinder (similar to cylinder B) were provided with internal stiffeners of 2-inch width and 0.685-inch thickness. With this arrangement, the compressive loading on the plane-ceramic surfaces was only –68,000 psi at 9,000 psi design pressure even though the hoop membrane stress at midbay was 202,500 psi. Thus, the compressive loading on the plane-bearing surfaces on the ends of cylinder C was identical to the compressive loadings found on cylinders A and B. Because of the reduced wall thickness at midbay, the W/D ratio for cylinder C is only 0.41.

Test Cylinder D

The 20-inch OD by 30-inch L by 0.686-inch t dimensions of test cylinder D (figure 18) were identical to those of test cylinder A. The only differences were a large-surface discontinuity on the internal surface at midbay, several large chips on the bearing surfaces, and an internal void of < 0.05-inch magnitude.

The surface discontinuity was originally in the shape of an oblong cylindrical void (0.187 inch long by 0.062 inch in diameter) of which the major axis was oriented in the hoop direction of the cylinder. During grinding of the interior surface of the cylinder, sufficient material was removed to expose the 0.03-inch-deep by 0.150-inch-long by 0.02-inch-wide cross section of the void (figure 19).

One of the chips was located on end A, and another on end B. The largest chip was on end B. Its dimensions were 0.375-inch long by 0.187-inch wide by 0.25-inch deep (figure 20). The chip on end A was only 0.2-inch long by 0.06-inch wide by 0.187-inch deep. Both chips were the result of carelessness during handling by the fabricator (i.e., placing the cylinder on edge during handling).

The objective of testing test cylinder D was to determine experimentally whether the presence of (1) a large discontinuity on the interior surface, (2) a void in the shell wall, and (3) chips on the edges of bearing surfaces of the alumina-ceramic cylinder would initiate a crack when the surface is stressed to –151,000 psi in the hoop and –76,000 psi in the axial direction at 10,000 psi proof loading. Following the proof test, the cylinder would be cycled 100 times to 9,000-psi design pressure which generates a stress field with –136,000 psi in hoop and –68,000 psi in axial orientation. If the cylinder successfully withstands such testing, this will indicate that ceramic housing components (cylinders and hemispheres) can tolerate large surface and internal discontinuities, provided they are located in areas of compressive stress.

FABRICATION

All test cylinders (figures 10, 16, 17, and 18) were fabricated for this program by Coors Ceramics from AD 94 composition containing 94-percent aluminum oxide. Mod 1 end cap rings for test cylinders (figure 15) were machined from 7075-T6 aluminum instead of titanium for two reasons. During testing, they would not be exposed to seawater, and the compressive bearing stresses at the joint were below the yield strength of this aluminum alloy.

In addition to end cap rings, a set of titanium and steel hemispheres and aluminum wedge clamps were machined to mate with the end cap rings on 20-inch ceramic cylinders (figures 21, 22, and 23). The titanium and steel bulkheads of identical dimensions were designed to serve as bulkheads for the ceramic test cylinders during pressure testing. To preclude failure during pressure testing, the hemisphere wall thickness was sized for design

pressure of 9,000 psi with a 1.5 safety factor on plastic buckling. A single penetration was dimensioned in the hemisphere to receive either threaded instrumentation cable bulkhead penetrators, or plugs (figure 24).

An aluminum ring also was machined to serve as a spacer (figure 25) between the titanium hemispheres when they were assembled and proof tested to 10,000 psi prior to mating them with the test cylinder for cyclic testing.

NON-DESTRUCTIVE TESTING

After fabrication, all ceramic cylinders were inspected visually by dye penetrant and ultrasonic methods for the presence of inclusions and cracks. Prior to inspections, a grid was penciled on the exterior of each cylinder to aid in the location of structural anomalies detected by these nondestructive evaluation (NDE) inspection techniques (figure 26).

The A, B, C, and D test cylinders were first inspected by the dye penetrant method at Coors Ceramics, followed by ultrasonic NDE methods at Martin Marietta Laboratories (MML). These methods included ultrasonic C Scans for rapid evaluation and defect mapping of the entire cylinder, and Scanning Acoustic Microscopy (SAM) to determine size and shape of some individual flaws detected by the C Scans. The Advanced Ultrasonic Test Bed (AUTB) at MML, employing an automated scanning procedure, was used to produce the C Scans. It can accommodate both planar and cylindrical samples. For cylindrical shapes like the NOSC cylinders, the test article was centered on a 30-inch-diameter turntable. The test parameters were optimized to provide high-enough resolution to detect void size $\geq$0.010 with a scan time that was not excessively long.

The procedure selected to provide this high-resolution screening is based on through-transmission, i.e., a transducer on one side of the cylinder transmits an ultrasonic signal and one on the other side receives it. A patented Martin Marietta design water-jet probe was used to house the unfocused 10 MHz transmit and receive transducers and provide a quiet and uniform 0.187-inch-diameter water column to couple the ultrasound to the ceramic cylinders. The through transmission approach, when implemented with an unfocused transducer, provides sensitivity to defects through the entire wall thickness.

Single-sided pulse-echo methods suffer from a near "dead zone" where defects cannot be readily detected. If focused transducers are used, detection can be improved somewhat, but sensitivity to deeper defects suffers considerably. The main advantages of using a water jet rather than conventional full immersion are (1) more-rapid scanning speeds, and (2) a small aperture which can only receive transmitted sound from a small region on the surface, thereby reducing the effective probe diameter and increasing lateral resolution.

A test frequency of 10 MHz was the highest frequency that could provide penetration and adequate signal levels. A scan is created from individual pixels which represent the amplitude of the signal transmitted through the cylinder at a particular location. Each pixel represented an area measuring 0.020 inch by 0.020 inch or 0.010 inch by 0.010 inch and an amplitude value anywhere within 256 discrete levels. This scanning procedure was previously developed and proven on 1- and 2-inch-thick ceramic blocks of similar composition. In that study, simulated cylindrical (1-dimensional) voids on the order of 100 micron (0.004 inch) in diameter were detected in the 1-inch-thick block. In addition, both horizontally and vertically oriented cracks were imaged in the 2-inch-thick block. With this technique, defects measuring smaller than the 0.187-inch probe size can be detected, but will not be sized accurately.

SAM is a high-resolution, defect-imaging technique based on higher frequencies than those used for conventional ultrasonics. The correlation between the size and shape predicted by SAM to the actual size and shape is excellent. For the inspection of 20-inch-diameter cylinders, a 30-MHz frequency was selected to provide the desired resolution and was able to penetrate most of the 0.45- to 0.68-inch-thick walls of the cylinders. The probe used had a spherical focus, with a focal length of 1.25 inches from the probe end when measured in water. Since the speed of sound in alumina is

almost six times greater than it is in water, the actual focal distance in the cylinder is greatly foreshortened. As a general procedure, a first scan covering a 0.4-inch by 0.4-inch square was performed at 0.0015-inch pixel resolution in a suspect area and was followed up by a 0.0005-inch "zoom" scan (0.2-inch by 0.2-inch square) if a void was detected. After the SAM analysis was performed, the cylinders were returned to NRaD for mating with titanium end cap rings.

Neither the dye penetrant, nor the sonic NDE detected any internal inclusion larger than 0.010 inch in A, B, and C cylinders. In cylinder D, a single inclusion with a 0.06-inch diameter was detected inside the wall at midbay. In addition, a large surface separation on cylinder D was detected and classified by the dye penetrant method. Prior to the bonding of the titanium end cap rings to the ends of the cylinders, their bearing surfaces were measured with a laser profilometer for surface roughness (figure 27). The surface roughness measurements fell into a range of values from +4 to –8 micrometers (+160 to –320 microinches). This range of roughness values was exceeded at many locations by narrow valleys with a depth of –16 micrometers (–640 microinches), and at few locations with a depth of –30 micrometers (–1,200 microinches).

PRESSURE TESTING

Test Arrangements

Testing of all four cylinders was performed in the 30-inch by 120-inch pressure vessel with a 10,000 psi pressure rating at Southwest Research Institute. Each test assembly (figure 28) consisted of a cylinder mated at both ends to titanium hemispheres (figure 22) that were secured with wedge bands (figure 23).

Before assembling the cylindrical housings, however, the structural integrity of the titanium hemispherical bulkheads (figure 22) was experimentally validated by joining them with a spacer (figure 25) and a wedge band (figure 29) into a sphere and prooftesting this assembly to 10,000 psi pressure.

The housings were assembled in this series of steps:

a. Remove cylinder from shipping case (figure 30).

b. Instrument the interior surface with strain gages.

c. Bond acoustic transducer to the interior surface of the cylinder at midbay (for cylinder D, the transducer was bonded to the exterior of the pressure vessel).

d. Mate the cylinder to a hemispherical bulkhead (figure 30).

e. Insert a wood block for shock mitigation (figure 32).

f. Close off the other end of cylinder with hemispherical bulkhead (figure 33).

g. Fasten the hemispheres to ends of cylinders with wedge bands (figure 34).

After assembly was completed, the housing was lowered vertically into the pressure vessel for testing (figure 35).

Pressure Testing Procedure

Pressure testing was performed with tap water at a pressurization rate of approximately 1,000 psi a minute. Strains were recorded at 1,000-psi intervals and acoustic emissions were recorded continuously. Depressurization also took place at 1,000 psi a minute.

The test procedure had two phases:

Proof testing—pressurize the cylinder to 10,000 psi, maintain pressure for 60 minutes, depressurize to 0 psi, pressure again to 10,000 psi, pressure hold for a minute, and relax to 0 psi.

Cyclic testing—pressurize the cylinder to 9,000 psi, maintain pressure for one minute, depressurize to 0 psi, and allow to relax at 0 psi for one minute. Continue cycling until spalling of ceramic at cylinder ends is observed, or catastrophic failure takes place.

TEST RESULTS

Cylinder A

The test assembly (figure 35), consisting of a ceramic cylinder (figure 10) capped at both ends with steel hemispherical bulkheads the same dimensions as the titanium hemisphere (figure 22), successfully withstood the proof test to 10,000 psi, followed by 400 pressure cycles to 9,000 psi without any visible cracking or spalling on the cylinder's exterior and interior surfaces.

When, after inspection at 400 cycles, the pressure cycling of the test assembly was resumed to 9,000 psi, catastrophic failure took place on the 453rd cycle (figure 36). Inspection of ceramic fragments inside the metallic end caps disclosed extensive internal spalling, the result of progressive delamination due to repeated pressure cycling.

The strains on the interior surface of the cylinder were linear from 0 to 10,000 psi. The difference between the magnitudes of hoop strains at midbay and ends ranged from 5 to 7 percent (figure 37), indicating that the radial compliance of the steel hemispheres was well matched to the radial compliance of the ceramic cylinder.

The maximum hoop and axial stresses on the interior midbay surface at 9,000 psi design pressure were calculated to be –136,000 psi in hoop and –68,000 psi in axial orientation (figures 38 and 39). The maximum hoop stress represented only 45 percent of the ceramic's uniaxial compressive strength, providing the cylinder with a 2.2 S.F. based on the material's strength.

The acoustic emissions recorded during the proof test and subsequent pressure cycling of the test assembly displayed a moderate Kaiser effect, masked to a large degree by leakage of the pressure vessel at Southwest Research Institute in which the assembly was tested (figure 40).

Cylinder B

The test assembly (figure 41a), consisting of cylinder B (figure 16) capped at both ends with titanium hemispherical bulkheads of the dimensions shown in figure 22, imploded during the first proof test at 9,700 psi (figure 41b).

The strains recorded during the test were linear to the moment of implosion (figure 42). There was a 20-percent difference between hoop strains at midbay and at the ends, indicating that the radial compliance of the cylinder ends was significantly less than the radial compliance of the 0.585-inch-thick ceramic cylinder at midbay.

The maximum compressive stresses were found on the interior surface at midbay (figure 43) and their magnitude at 9,000 psi was calculated to be –158,000 psi in hoop direction. The highest compressive stress on the interior surface in axial direction was found at the wall-thickness transition zone, and its magnitude ranged from –90,000 to –97,000 psi. The 30-percent difference between axial stresses at the transition zone and the 71,000 psi at midbay indicates significant bending at the ends (figure 44).

The total number of acoustic events detected by two transducers bonded to the interior of the cylinder was 9,800 psi just prior to implosion. Since the signal generated by the two transducers were added together, the actual number of events was only 4,900. The total number of events increased linearly with pressure to the moment of implosion, indicating that the failure was not initiated by material failure, but by elastic instability (figure 45).

Cylinder C

The test assembly (figure 46), consisting of cylinder C (figure 17) capped at both ends with steel hemispherical bulkheads of the same dimensions as the titanium hemispherical bulkheads (figure 22), successfully withstood two proof tests to 10,000 psi, followed by 50 pressure cycles to 9,000 psi. Visual inspection did not discover any cracking or spalling on internal or external surfaces of the cylinder at the end of 50 pressure cycles.

During subsequent pressure cycling, severe spalling occurred on the 53rd cycle (figures 47 and 48) and the cylinder began to leak. All the spalling took place in one location on the end of the cylinder at both internal and external surfaces. It is not known how many more pressure cycles would have to be applied before catastrophic failure would occur.

The strains on the interior surface of the cylinder were linear from 0 to 10,000 psi. The difference between the magnitudes of hoop strains (figure 49) at midbay and ends was in the 25-percent range, indicating that the radial compliance of the steel hemispheres was significantly less than the radial compliance of the 0.450-inch-thick ceramic cylinder.

The maximum compressive stresses were found on the interior surface at midbay (figures 50 and 51), and their magnitude at 9,000 psi loading was calculated to be –202,500 psi in the hoop direction. The hoop stresses at the ends were only –164,000 psi. The highest compressive stress in axial direction was observed (figures 50 and 51) at the end of the cylinder on the transition zone between the wall thicknesses, and its magnitude was –149,000 psi. The 50-percent difference in magnitude between –99,000 psi axial stresses at midbay and the axial stress in the transition zone at the ends, as well as the 25-percent difference in hoop stresses at those locations, indicates a very severe mismatch in radial compliance between the steel hemispheres and the cylinder.

The acoustic emissions recorded during the pressurizations exhibited a classic Kaiser effect (figure 52). The number of events decreased from 1,400 during the first pressurization to 85 during the second and 20 during the third. The number of events generated during subsequent pressure cycles remained constant to the 20th cycle, during which a sudden increase of 320 events occurred. After this sudden jump in number of events, the emissions returned to the previous rate of 20 events per cycle to the 30th cycle, when a second sudden increase of 320 events took place. The emission rate settled down again to 20 events per cycle to the 44th cycle, when a sudden increase of 800 events took place. After this, the emission rate settled down to about 30 events per cycle to the 53rd cycle, when a sudden increase of 2,000 events took place and the vessel began to leak.

The acoustic emission record seems to indicate that the crack initiated during the 20th cycle and increased in size stepwise during the 30th, 44th, and 53rd cycles (i.e., it required approximately 10 cycles to build up sufficient residual tensile stress at the crack tip to propagate it further). The crack's growth was slow and hidden inside the end cap until the 53rd cycle, so it was not detected during the visual inspection after the 50th cycle.

Cylinder D

The test assembly (figure 53), consisting of cylinder D (figure 18) capped at both ends with steel hemispherical bulkheads successfully withstood two proof tests to 10,000 psi, followed by 100 pressure cycles to 9,000 psi. Visual inspection of the cylinder surfaces after pressure testing did not reveal any cracks or spalling. The original surface separation (figure 19) did not enlarge, or show any cracks originating at the edges of the separation.

The magnitude of strains on the interior surface away from the separation was identical to those observed at 9,000 psi pressure loading on cylinder A with the same dimensions. The strains recorded around the separation differed only a small amount from those recorded at the location away from the separation. The hoop strains were approximately three-percent higher, and the axial strains were approximately 18-percent lower. No significant difference was found between strains at the tip of the separation and at a location away from the separation. Since the size of strain gages was 0.125 of an inch, the values of strains recorded by these gages represent an average of strains at a distance of 0.125 to 0.375 of an inch from the edge of the separation. Thus, in reality, the strains along the long edge are estimated to be 100-percent lower in axial, and 10-percent higher in hoop direction.

The maximum stresses calculated on the interior surface, away from the separation, were –136,000 psi in hoop, and –68,000 psi in axial direction. These values of stresses are the same as on test cylinder A of the same dimension, indicating that both cylinder A and D are of identical dimensions and material composition. The stresses measured by strain gages 0.25 of an inch away from the separation were only 3-percent higher in hoop and 10-percent less in axial direction.

The acoustic emissions recorded during pressurization exhibited the classic Kaiser effect: a total of 2,800 events during the first pressurization, decreasing stepwise to 20 events during the 20th cycle, and remaining constant at 20 events per cycle thereafter to the 100th cycle. The absence of increases in the event count during pressure cycling indicated that cracking was not initiated anywhere on the cylinder during the first 100 pressure cycles to 9,000 psi.

DISCUSSION

End Cap Design

The significant improvement in fatigue life (453 versus 109 cycles) of 20-inch OD by 30-inch L by 0.685-inch t 94-percent alumina-ceramic cylinders under identical pressure cycling conditions to 9,000 psi after replacement of Mod 0 with Mod 1 end caps serves as experimental validation of the new end cap design for 20-inch cylinders.

The Mod 1 end cap design was conceived and first applied to 12-inch OD by 18-inch L by 0.412-inch t alumina-ceramic cylinders by Dr. Stachiw in a previous NRaD Independent Experimental Development program (reference 3) where it successfully withstood 500 cycles to 9,000 psi without visible spalling or cracking. By comparison, the same 12-inch cylinders, when equipped with Mod 0 end caps exhibited spalling at the ends after only about 100 cycles. Still, catastrophic failure did not take place even after 150 cycles, although spalling after that was extensive on the exterior surface. In the same program, 6-inch OD by 9-inch L by 0.206-inch-thick 94-percent alumina-ceramic cylinders equipped with Mod 1 end caps successfully withstood 2,000 pressure cycles to 9,000 psi without catastrophic failure.

In all Mod 1 end cap designs for the different cylinder diameters, the height of both flanges on the end cap was equal to or exceeded 2.75 t, where t is the thickness of the ceramic shell. By comparison, in Mod 0 end caps, the height of the exterior flange was only 0.8 t. In all cases, the cylinders were bonded into the end caps with epoxy adhesive compound made up of 100-percent CIBA Geigy 6010 resin and 70-percent CIBA Geigy 283 hardener. The thickness of the adhesive bonds between concave and convex cylinder surfaces and the end cap flanges varied from 0.01 to 0.03 of an inch, while the bond between the plane-bearing surfaces was kept constant at 0.01 inch by means of epoxy-soaked cardboard spacers covering less than 50 percent of the bearing surface.

Based on the data generated by this and previous studies, a conservative postulate can be formulated that the Mod 1 end cap design will provide alumina-ceramic cylinders of any size with a guaranteed cyclic fatigue life in excess of 200 pressurizations generating –136,000 psi maximum hoop stress at midbay. At 90-percent confidence level, the cyclic fatigue life at the same hoop stress level exceeds 400 cycles.

Design Stress Level

The testing of cylinders A, B, and C has shown that the 94-percent alumina ceramic will reliably carry compressive membrane stress of up to 200,000 psi magnitude, and thus provide a very attractive W/D ratio of 0.36 for 9,000-psi design depth. Because of the short ring stiffeners at the ends of the cylinders, spalling occurs much sooner, however (cylinder C-51 versus 453 cycles for cylinder A), even though the compressive bearing stress is the same for all three cylinders.

If the length of these ring stiffeners on the cylinder ends were increased from the present 2 inches to 4 or 5 inches, the fatigue life of the cylinders could, probably, be extended by at least 100 percent at the expense of additional weight of ceramic, thus increasing the W/D ratio. But even with this arrangement, the local high-compressive bending stresses generated by the transition zone from thick- to thin-shell sections will result in high shear stresses inside the shell thickness at this location. These shear stresses also may originate spalling at that location, reducing the fatigue life of the cylinder.

The most direct approach to eliminating the problems generated by the thickness transition zone would be to eliminate the ring stiffeners at the ends of the cylinders. Unfortunately, this would increase the bearing stresses for the 0.455-inch-thick cylinder from –64,000 to –101,000 psi, which, in turn,

would cause cracking to originate on the bearing surfaces after only a few cycles.

Based on these considerations, it appears that the hoop design stress of –136,000 psi, providing cylinder A with a fatigue life in excess of 400 cycles, represents a good trade-off between weight, initial fabrication cost, and life cost (fatigue life) for a 94-percent alumina-ceramic cylinder serving as a component in an external pressure housing with a 9,000-psi design depth. At a design stress of –136,000 psi, the ceramic cylinder is 43-percent lighter and carries at least a three-times larger payload than a titanium cylinder with –90,000-psi design stress for a 9,000-psi depth. Furthermore, the monocoque shell of the ceramic cylinder makes its fabrication significantly less expensive than the titanium shell of identical dimensions incorporating integral ribs.

Surface Discontinuities

The test results generated by cylinder D indicate that the presence of large chips on the edges of the cylinder's bearing surfaces does not lead to initiation of spalling on the external surfaces of the cylinder even after 100 pressure cycles to design pressure.

Similarly, the large surface separation on the internal surface at midbay did not initiate cracks on that surface even though the membrane stress field around the discontinuity consisted of –136,000 psi hoop and –68,000 psi axial stresses at design depth.

These findings have been found very useful in helping to define the magnitude of acceptable surface and internal defects on ceramic components selected for external pressure service that will generate a compressive membrane stress of $\leq$136,000 psi magnitude at design depth. Thus, it appears that chips on the edges of plane-bearing surfaces of cylinders may extend to 0.5 t in length and 0.3 t in width without making the cylinder unacceptable for service as a pressure housing component. Surface separations and internal inclusions do not make the cylinder unacceptable unless their length/width aspect ratio >10, length >0.15 inch, and depth >0.05 t.

Acoustic emissions followed the classic Kaiser effects for all four test cylinders, i.e., the number of acoustic events significantly decreases with each following pressure cycle until a minimum is reached after about 20 cycles. After this, the number of events generated during each cycle remained approximately constant until a fracture was initiated. At that instant, the number of events would significantly increase for that cycle, but the following cycle would exhibit, again, the same low number of events that preceded the crack initiation.

During following cycles, the low number of events would be repeated until either a new crack was initiated, or the prior crack propagated itself stepwise. The jumps in number of events would increase in magnitude, until one of them exceeded 1,000 events. At this instant, a fracture plane, probably, reached sufficient dimensions to result in physical spalling of the external surface. The structural integrity of the cylinder can be considered at this point to have been compromised to such an extent that it should be removed from further service as a pressure housing, although experimental data from the prior test program with 12-inch OD by 18-inch L by 0.412-inch t cylinders has shown that the catastrophic failure of a spalled cylinder is probably still 50 cycles away.

CONCLUSIONS

1. Manufacturing technology for 94-percent alumina ceramic has been found to be mature enough and manufacturing equipment large enough to produce cylinders and hemispheres up to 50 inches in diameter on custom, and 20 inches on a mass-production basis. Both Coors Ceramics and WESGO, Inc. have a proven capability to produce large cylinders and hemispheres from alumina ceramic.
2. Monocoque cylinders fabricated from 94-percent alumina ceramic with 20-inch OD by 30-inch L by 0.685-inch t and 0.48 W/D ratio (0.5 for cylinders equipped with end caps) can serve as reliable components of external pressure housings with guaranteed 200 cycles fatigue life to a 20,000 feet design depth, provided that their ends are

encapsulated in Mod 1 metallic end caps that are radially supported by metallic or ceramic hemispherical bulkheads whose critical pressure exceeds 13,500 psi. If, during lifetime service, the majority of dives does not exceed a depth of 15,000 feet, the guaranteed cyclic fatigue life of the cylinders will exceed 400 cycles.

3. The cyclic fatigue life of the 20-inch OD by 30-inch L by 0.685-inch t 94-percent alumina-ceramic cylinders has been experimentally shown to exceed 400 pressure cycles to 9,000 psi design pressure when their ends are bonded to Mod 1 end caps that also serve as supports for equipment inside the cylinder, and as joints for attachment of hemispherical bulkheads, or additional cylinders with intermediate stiffener rings.

4. The 94-percent alumina ceramic under maximum membrane hoop stress of –136,000 psi and –68,000 axial stress in the 0.685-inch-thick cylinders can tolerate chips on the edges of cylinders, surface separations, and internal voids provided their magnitude does not exceed the following limits based on the experimental data from this and other test programs, and their extrapolation by analytical processes:

Chips on Edges:
Length: <0.5t
Width: <0.3t

Surface Separations (Crevasses)
Length: 0.187 inch
Width: 0.03 inch
Depth: 0.03 inch
Location: >6 inches from edge

Inclusions:
Oblong:
Length: 0.187 inch
Diameter: 0.06 inch
Spherical:
Diameter: 0.06 inch
Location: >3 inches from edge
Depth: >0.1 inch below surface

5. The satisfactory performance of the bearing surfaces on ceramic cylinders during 400 pressure cycles to 9,000 psi design pressure is the result of the following parameters:

a. Bearing pressure: ≤68,000 psi

b. End cap design: Mod 1 with A, B, or C sealing options

Radial clearances: 0.01–0.03 inch
Flange height: 1.9 inches

c. Material, listed in order of preference:

Ti-6Al-4V titanium
7178-T6 aluminum
7075-T6 aluminum

d. Bearing support:

Radial: epoxy compound filling the annular clearances 0.01 to 0.03 inch thick

Axial: epoxy compound of 0.01 inch thickness. Thickness is controlled by segments of 0.01 inch thick cardboard gasket acting as spacers. Thickness of epoxy layer is controlled by one inch long segments of 0.01 inch thick manila stock placed at uniform intervals around the seat in the end cap. Spacing between segments is not to exceed 0.25 inches.

Material: 100 parts of resin CIBA Geigy 610, 70 parts of hardener CIBA Geigy 283

6. Monocoque 94-percent alumina-ceramic cylinders with 20-inch OD by 30-inch L by 0.685-inch t, when equipped with Mod 1 end caps can be joined with ring stiffeners (appendix A) to form long cylindrical housings of up to 120 inches in length and 500 pounds of positive lift, when capped with titanium or ceramic hemispherical bulkheads (reference 1).

REFERENCES

1. Stachiw, J. D. 1990. "Exploratory Evaluation of Alumina Ceramic Housings for Deep Submergence Service—Fourth Generation Housings," NOSC TR 1355 (Jun). Naval Ocean Systems Center, San Diego, CA.

2. Stachiw, J. D., and J. L. Held. 1987. "Exploratory Evaluation of Alumina Ceramic Housings for Deep Submergence Service—The Second Generation NOSC Ceramic Housings," NOSC TR 1176 (Sep). Naval Ocean Systems Center, San Diego, CA.

3. Stachiw, J. D. 1989. "Exploratory Evaluation of Alumina Ceramic Housings for Deep Submergence Service—Third Generation Housings," NOSC TR 1314 (Sep). Naval Ocean Systems Center, San Diego, CA.

GLOSSARY

AUTB	Advanced Ultrasonic Test Bed
FEA	finite element analysis
FEM	finite element model
GFRP	graphite fiber-reinforced peek
ID	inner diameter
IED	independent exploratory development
Kpsi	one thousand psi
L	length
L/D	length/diameter
MEK	methyl ethyl ketone
MOR	Modulus of rupture
ND	nondestructive
NDE	nondestructive evaluation
NDT	nondestructive test
NOSC	Naval Ocean Systems Center
OD	outside diameter
PEEK	poly-ether-ether-ketone
rms	root mean square
SAM	Scanning Acoustic Microscopy
S.F.	stress factor
t	ceramic shell thickness
t/D	thickness diameter
t/Ro	thickness external radius
W	width
W/D	weight-to-displacement

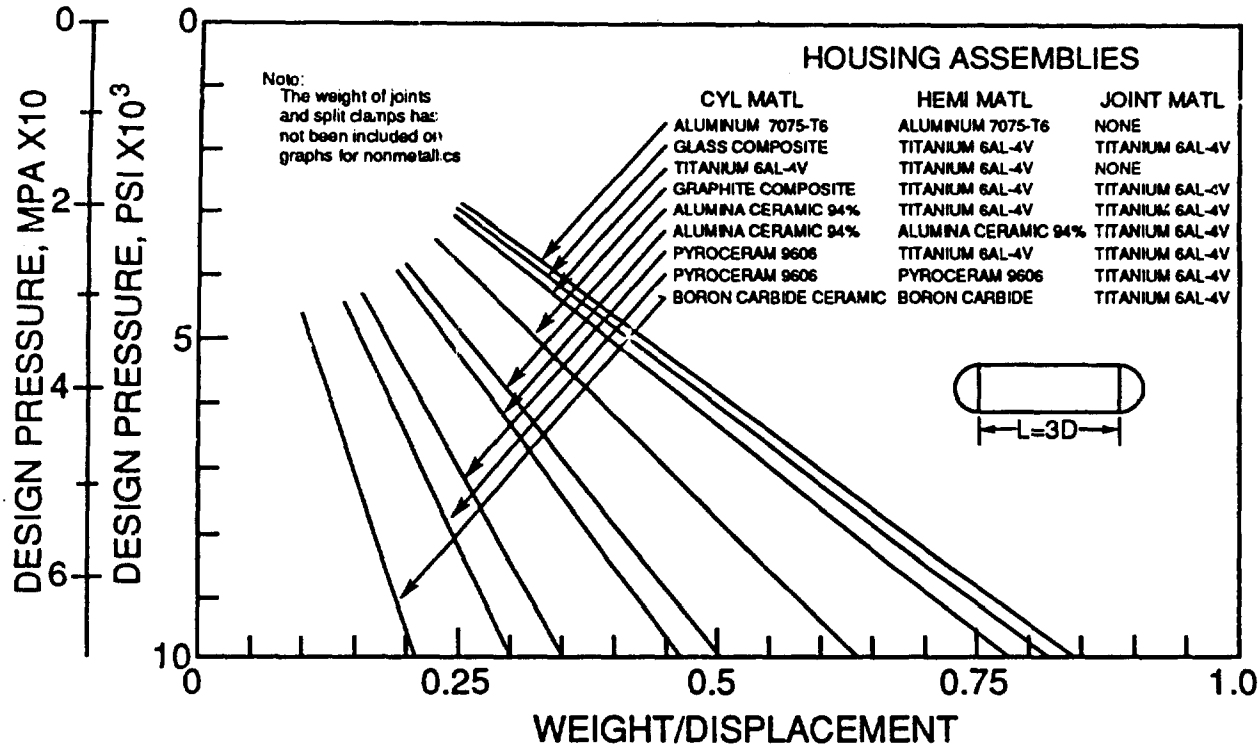

Figure 1. W/D of external pressure housings fabricated from different materials.

Figure 2. Typical 20-inch OD alumina-ceramic cylinder used in the fourth generation of the Navy's ceramic pressure housings.

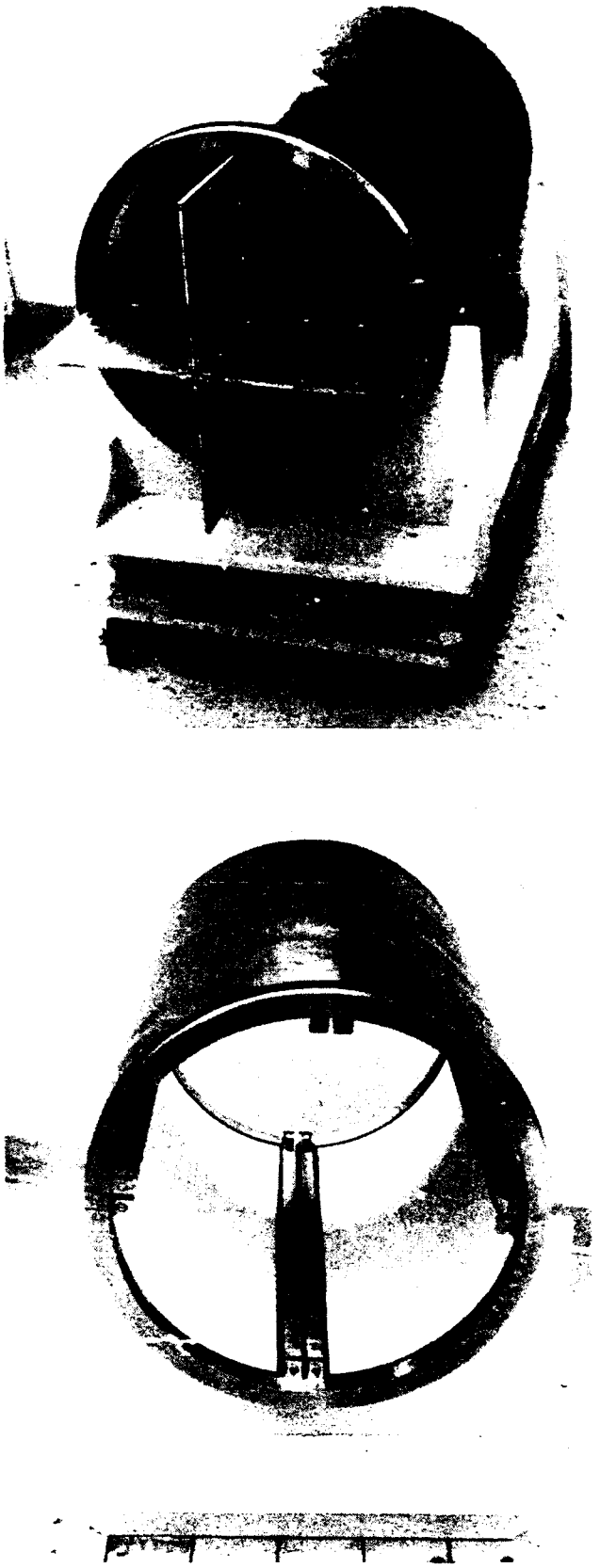

Figure 3. Internal mounts for payload platform inside the 20-inch OD alumina-ceramic cylinders.

Figure 4. Typical 20-inch alumina-ceramic hemisphere used in the fourth generation of the Navy's ceramic pressure housings prior to bonding with the titanium end cap ring and mounting of the penetration insert.

Figure 5. Hemispherical bulkhead assembly for 20-inch OD ceramic pressure housings.

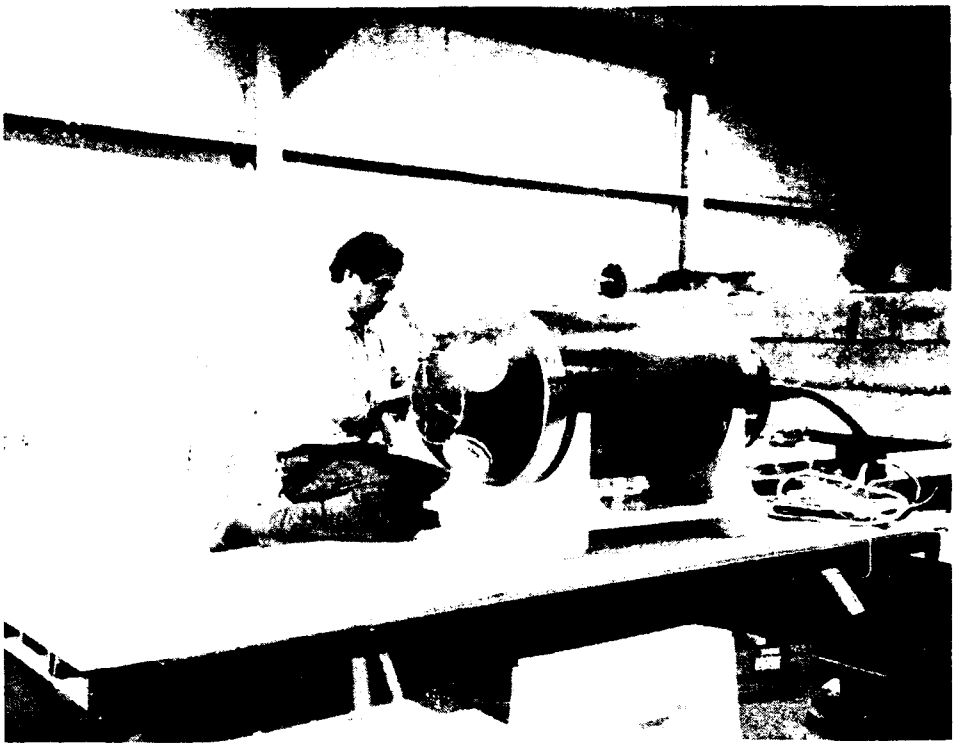

Figure 6. 20-inch OD external pressure housing assembled from a single ceramic cylinder capped at both ends with ceramic hemispheres. Payload rating: 220 pounds at 9,000 psi.

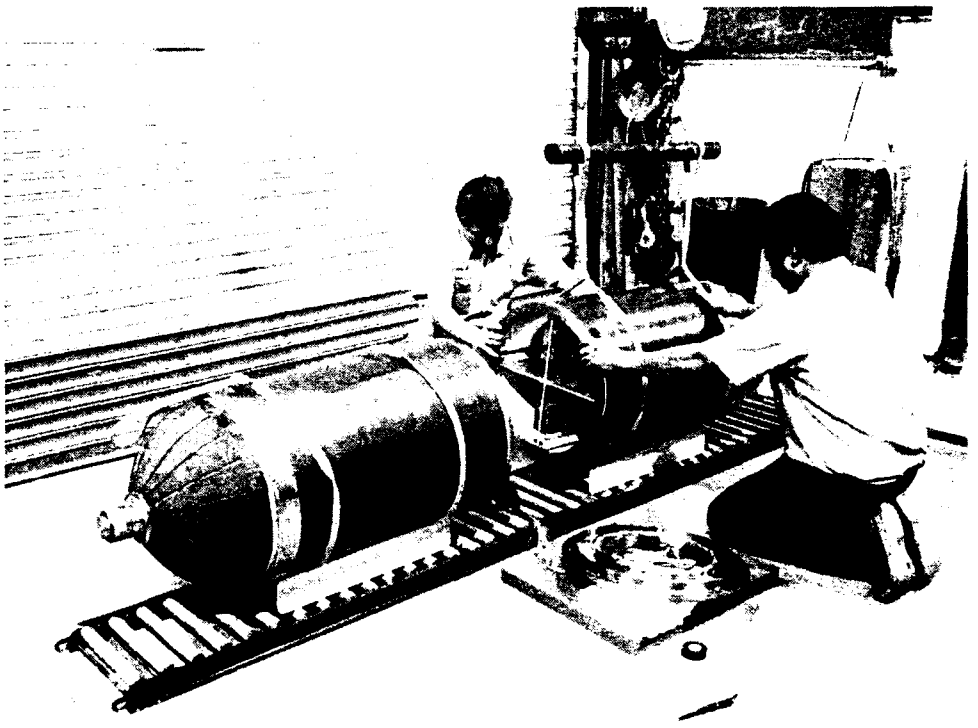

Figure 7. Assembly of a 20-inch OD external pressure housing from two 30-inch-long ceramic cylinders, two ceramic hemispheres, and a single, central joint stiffener. Payload rating: 350 pounds at 9,000 psi.

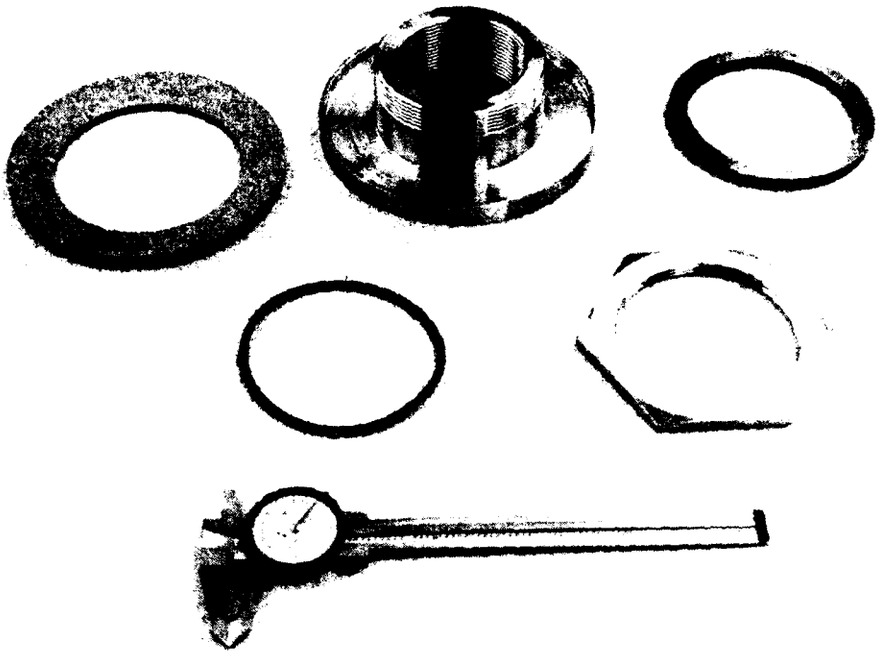

Figure 8. Inserts for penetrations in ceramic hemispheres.

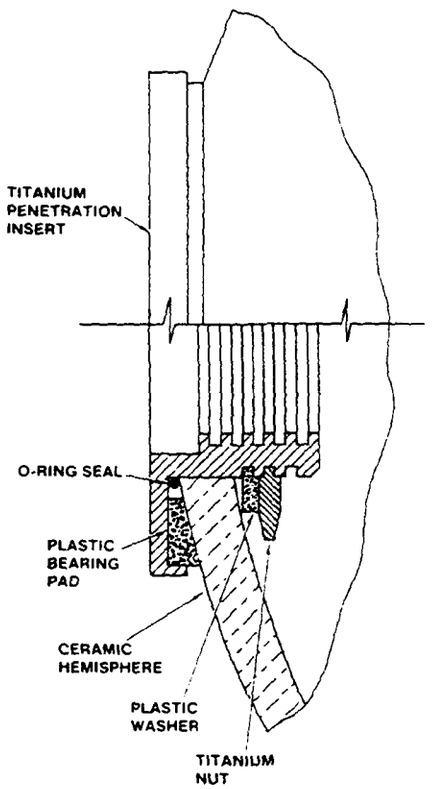

Figure 9. Penetration insert in ceramic hemisphere.

CYLINDER, A
CERAMIC HULL

NOTES:

1. MATERIAL: ALUMINA CERAMIC, COORS AD 94 OR EQUIVALENT
2. MATERIAL REQUIREMENTS:

CERAMIC COMPOSITION	≥ 94% AL_2O_3
© MODULUS OF ELASTICITY	≥ 40 x 10^6 PSI
© COMPRESSIVE STRENGTH	> 300,000 PSI
© MODULUS OF RUPTURE	> 50,000 PSI
POISSON'S RATIO	0.21
SHEAR MODULUS	≥ 7 x 10^6 PSI
BULK MODULUS	≥ 24 x 10^6 PSI
SPECIFIC GRAVITY	3.62
COEFFICIENT OF THERMAL EXPANSION AT 70°F	2 x 10^{-6}/°F

3. WEIGHT/DISPLACEMENT = 0.48
   DESIGN HOOP STRESS = 135,000 PSI
   t/D = 0.034
   L/D = 1.5
   Pcr = 13,500 PSI WITH RADIAL SUPPORT BY TITANIUM HEMISPHERES

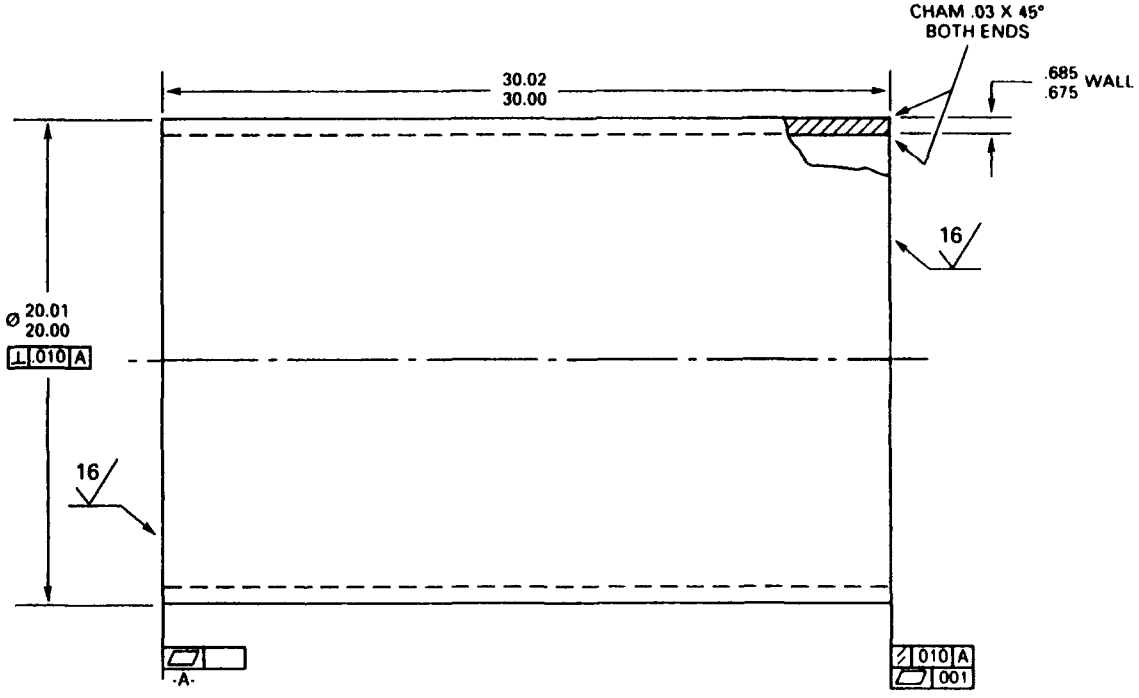

Figure 10. Cylinder A ceramic hull.

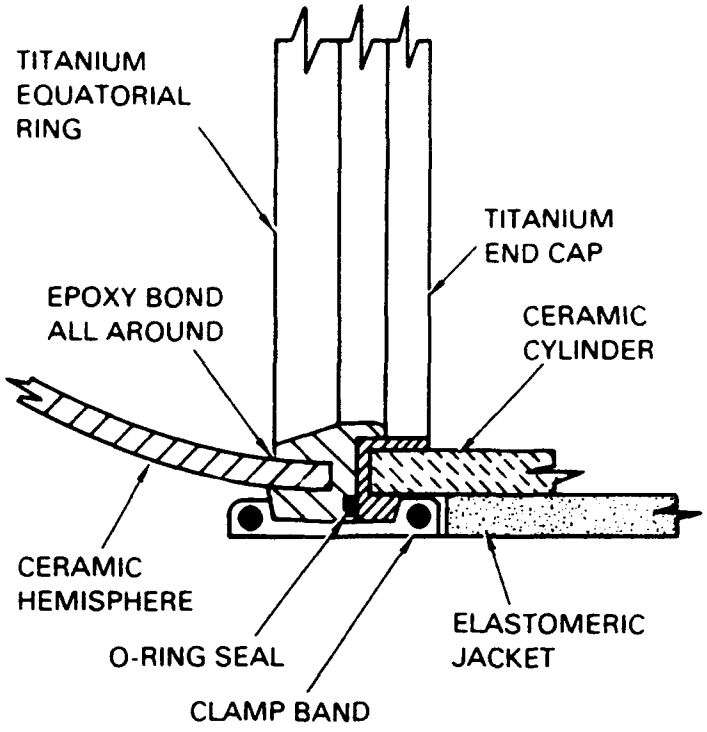

Figure 11. Mod 0 end caps on the ceramic cylinder and hemisphere.

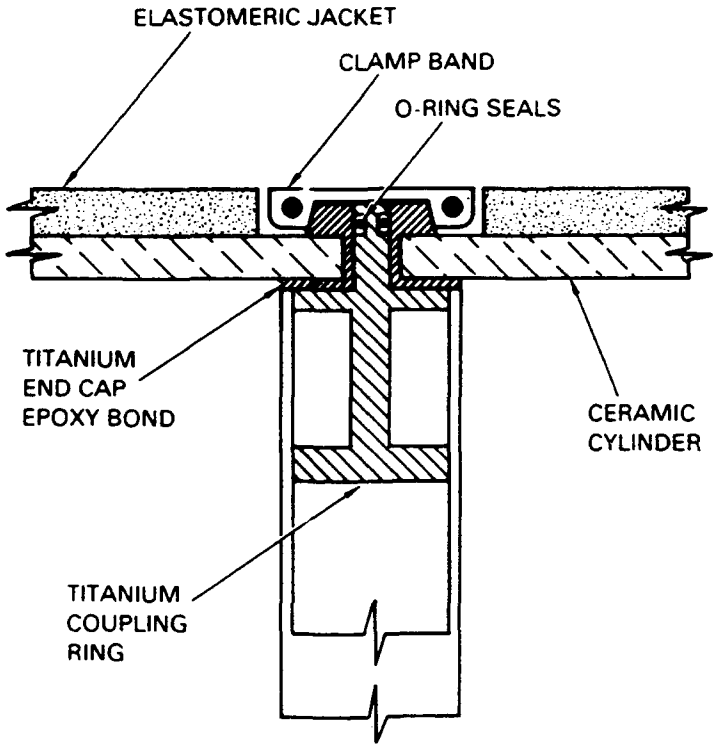

Figure 12. Mod 0 end caps on the ceramic cylinders at housing midbay stiffener.

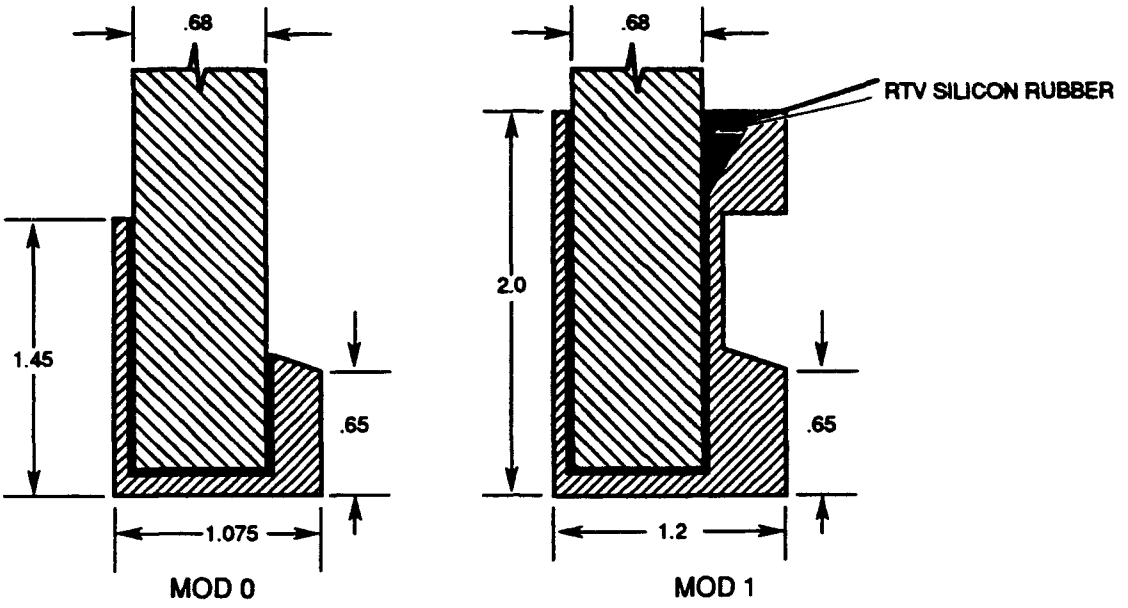

Figure 13. Comparison of Mod 0 and Mod 1 end cap designs.

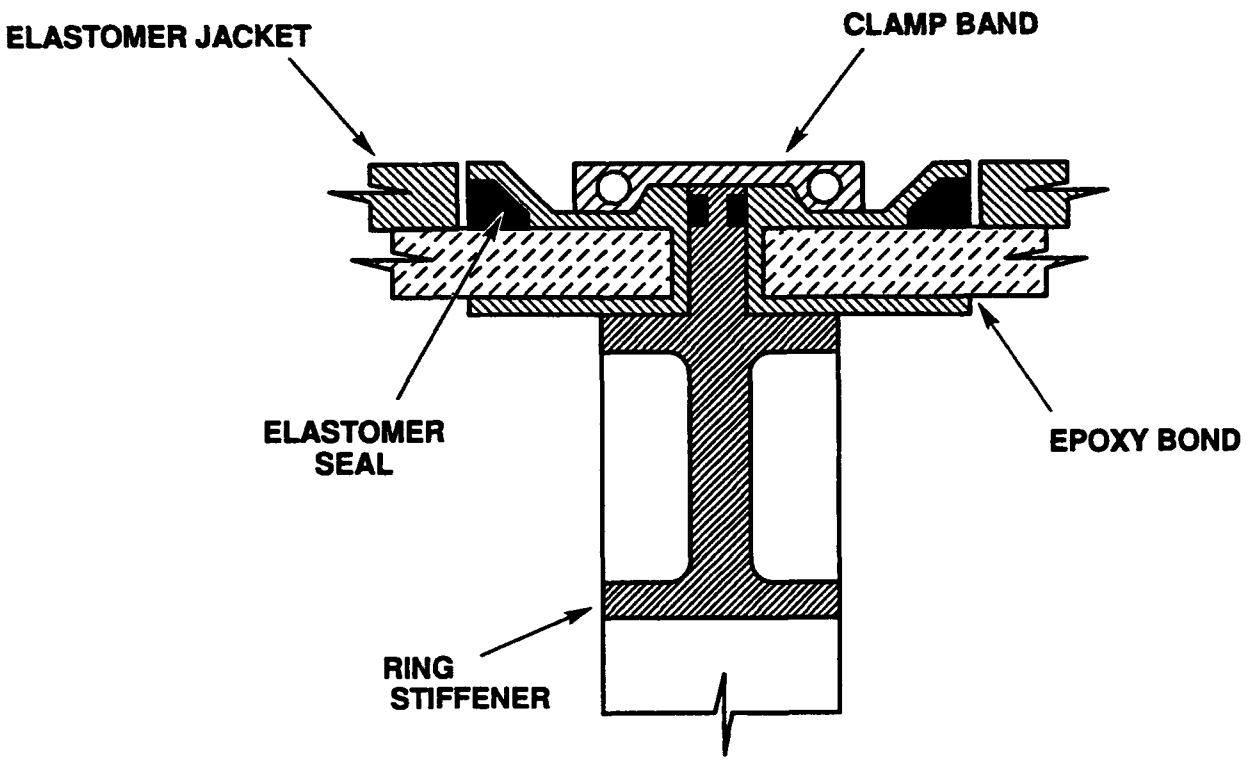

Figure 14. Optimized Mod 1 end caps on cylinder ends at midbay ring stiffener.

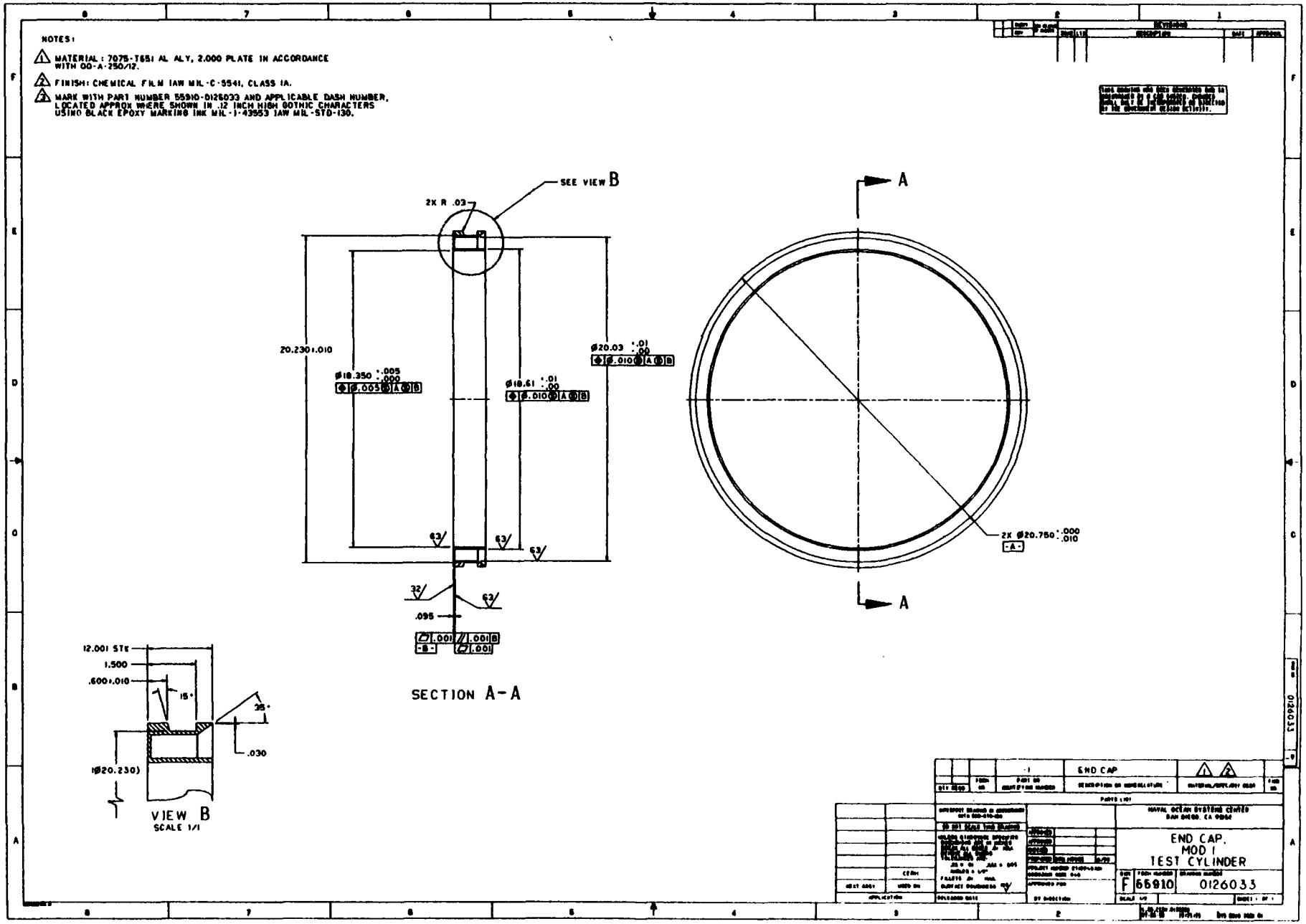

Figure 15. Mod 1 end cap for 20-inch OD ceramic test cylinders.

CYLINDER, B
CERAMIC HULL

NOTES:

1. MATERIAL: ALUMINA CERAMIC, COORS AD 94 OR EQUIVALENT
2. MATERIAL REQUIREMENTS:

CERAMIC COMPOSITION	≥ 94% AL_2O_3
© MODULUS OF ELASTICITY	≥ 40 x 10^6 PSI
© COMPRESSIVE STRENGTH	> 300,000 PSI
© MODULUS OF RUPTURE	> 50,000 PSI
POISSON'S RATIO	0.21
SHEAR MODULUS	≥ 7 x 10^6 PSI
BULK MODULUS	≥ 24 x 10^6 PSI
SPECIFIC GRAVITY	3.62
COEFFICIENT OF THERMAL EXPANSION AT 70°F	2 x 10^{-6}/°F

3. WEIGHT/DISPLACEMENT = 0.42
   DESIGN HOOP STRESS = 156,000 PSI
   t/D = 0.029
   L/D = 1.5
   P_{cr} = 9600 PSI WITH RADIAL SUPPORT BY TITANIUM HEMISPHERES

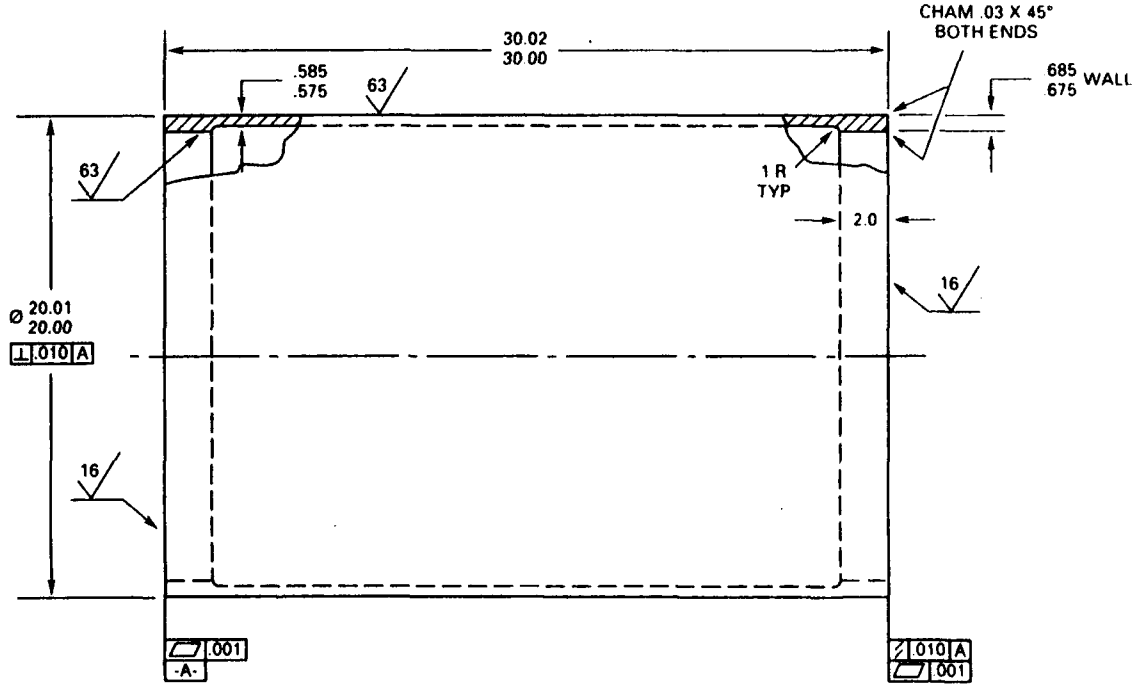

Figure 16. Cylinder B ceramic hull.

NOTES:

1. MATERIAL: ALUMINA CERAMIC, COORS AD 94 OR EQUIVALENT
2. MATERIAL REQUIREMENTS:

CERAMIC COMPOSITION	≥ 94% AL_2O_3
© MODULUS OF ELASTICITY	≥ 40 x 10^6 PSI
© COMPRESSIVE STRENGTH	> 300,000 PSI
© MODULUS OF RUPTURE	> 50,000 PSI
POISSON'S RATIO	0.21
SHEAR MODULUS	≥ 7 x 10^6 PSI
BULK MODULUS	≥ 24 x 10^6 PSI
SPECIFIC GRAVITY	3.62
COEFFICIENT OF THERMAL EXPANSION AT 70°F	2 x 10^{-6}/°F

3. WEIGHT/DISPLACEMENT = 0.36
   DESIGN HOOP STRESS = 200,000 PSI
   t/D = 0.023
   L/D = 0.85
   pcr = 12,000 PSI WITH RADIAL SUPPORT BY TITANIUM HEMISPHERES

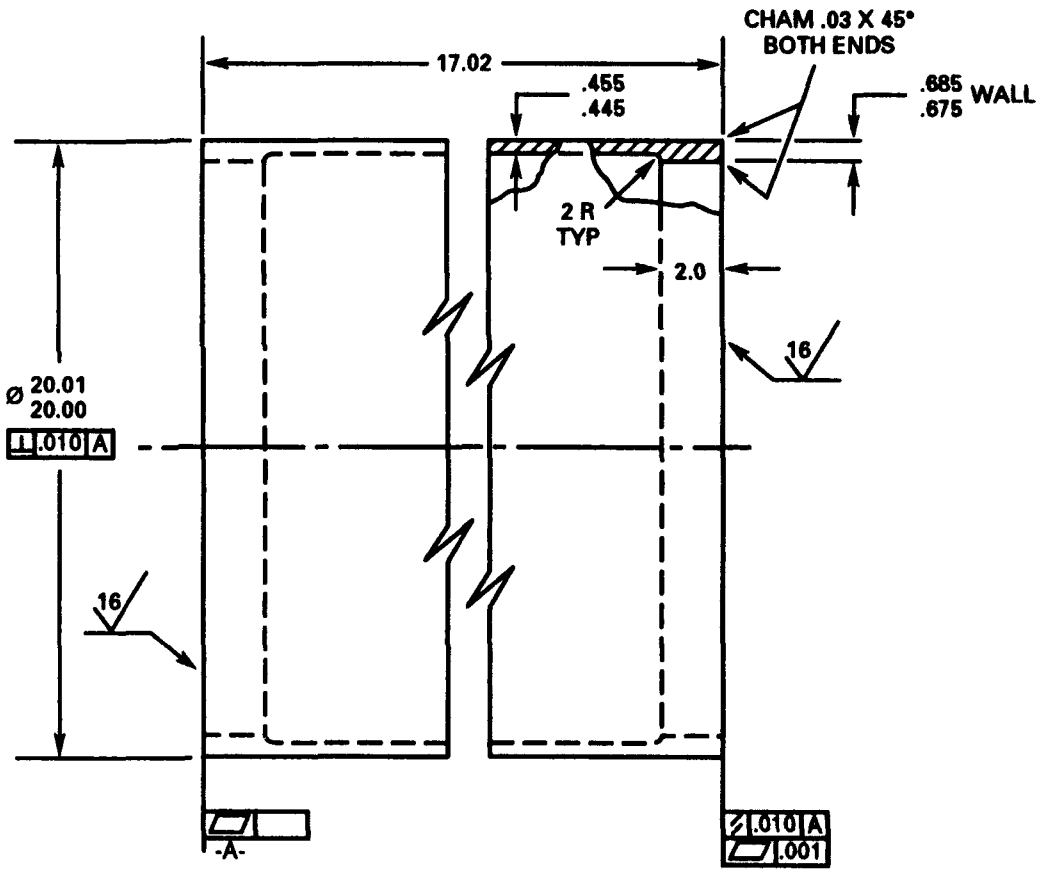

Figure 17. Cylinder C ceramic hull.

NOTES:

1. MATERIAL: ALUMINA CERAMIC, COORS AD 94 OR EQUIVALENT
2. MATERIAL REQUIREMENTS:

CERAMIC COMPOSITION	≥ 94% Al_2O_3
© MODULUS OF ELASTICITY	≥ 40 x 10^6 PSI
© COMPRESSIVE STRENGTH	> 300,000 PSI
© MODULUS OF RUPTURE	> 50,000 PSI
POISSON'S RATIO	0.21
SHEAR MODULUS	≥ 7 x 10^6 PSI
BULK MODULUS	≥ 24 x 10^6 PSI
SPECIFIC GRAVITY	3.62
COEFFICIENT OF THERMAL EXPANSION AT 70°F	2 x 10^{-6}/°F

3. WEIGHT/DISPLACEMENT = 0.48
   DESIGN HOOP STRESS = 135,000 PSI
   t/D = 0.034
   L/D = 1.5
   Pcr = 13,500 PSI WITH RADIAL SUPPORT BY TITANIUM HEMISPHERES

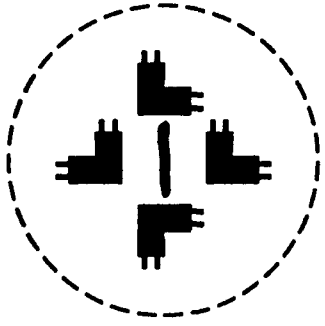

INSTRUMENTATION AT SURFACE SEPARATION

DETAIL A

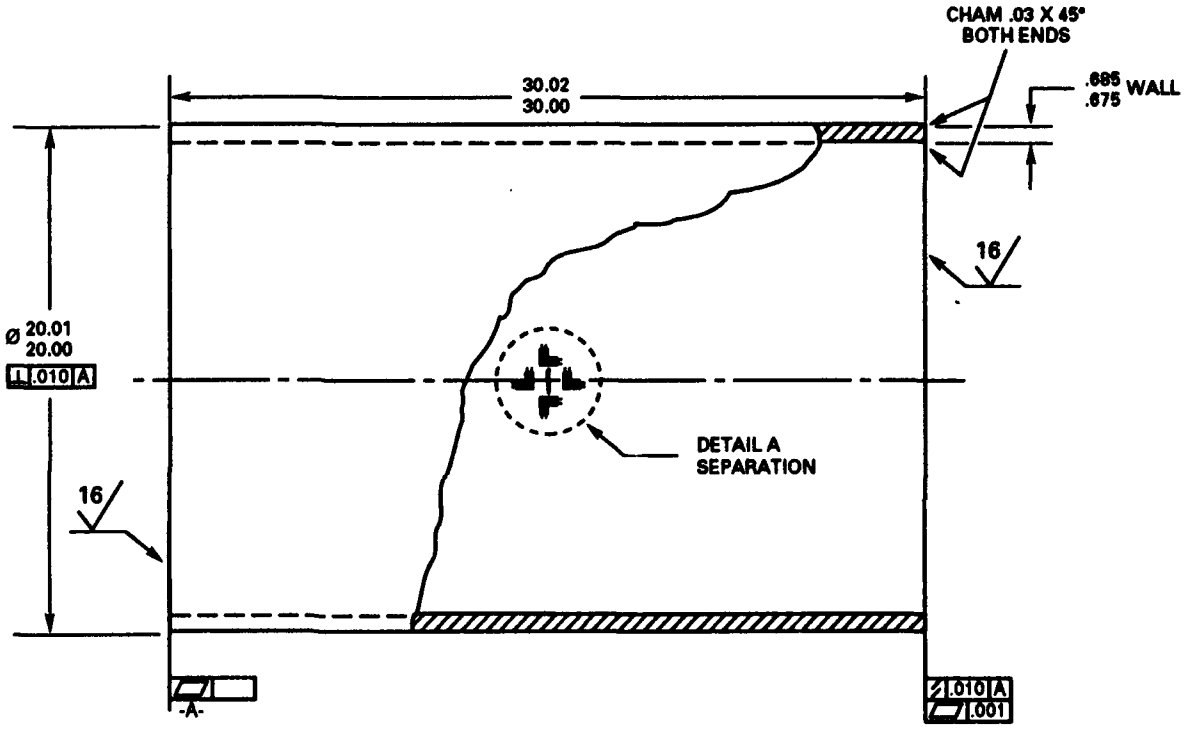

Figure 18. Cylinder D ceramic hull.

Figure 19. Cross-section of a void on the interior surface of cylinder D. The inclusion is approximately 0.03 of an inch deep.

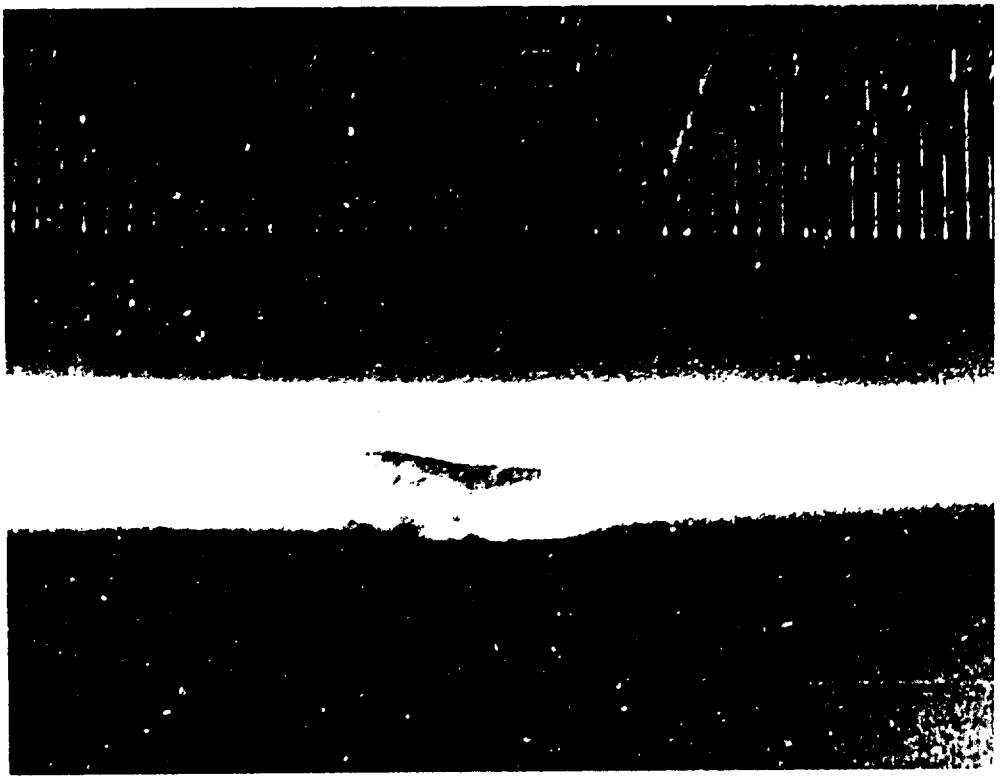

Figure 20. One of the larger chips on the plane-bearing surface of cylinder D.

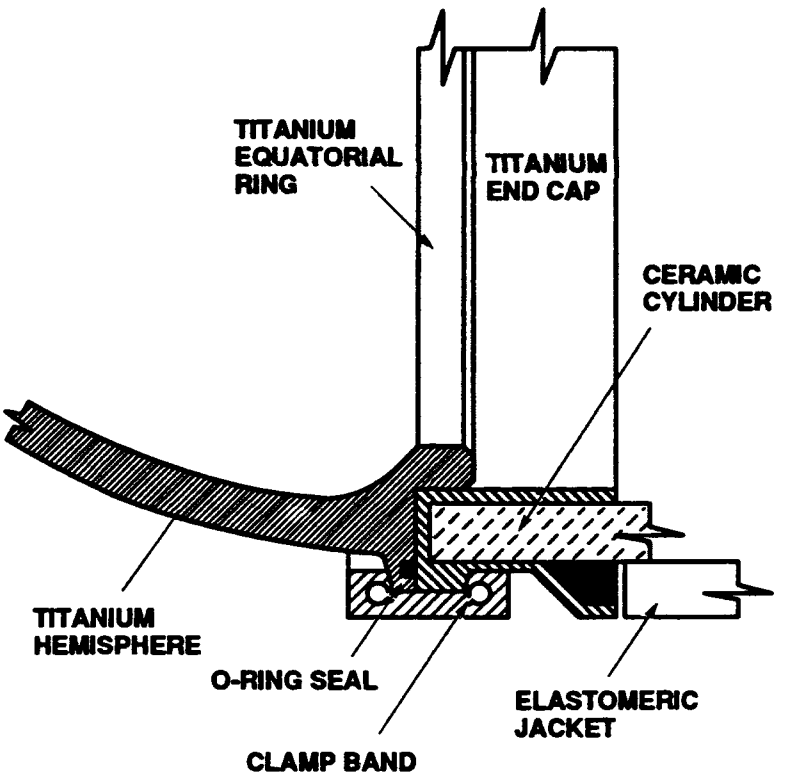

Figure 21. Cylinder with Mod 1 end cap at the interface with the titanium hemisphere.

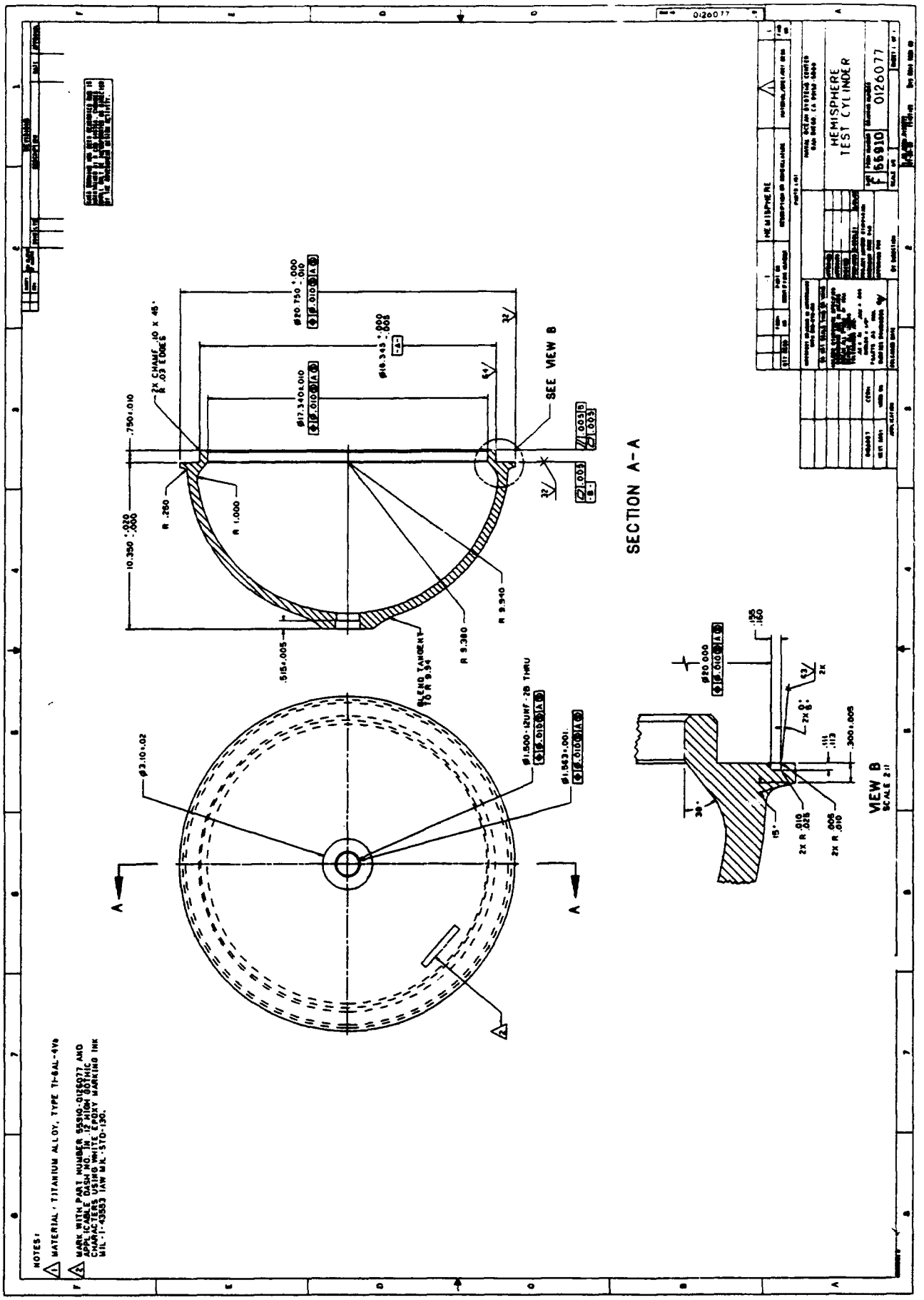

Figure 22. Titanium hemisphere bulkhead for 20-inch OD ceramic test cylinders.

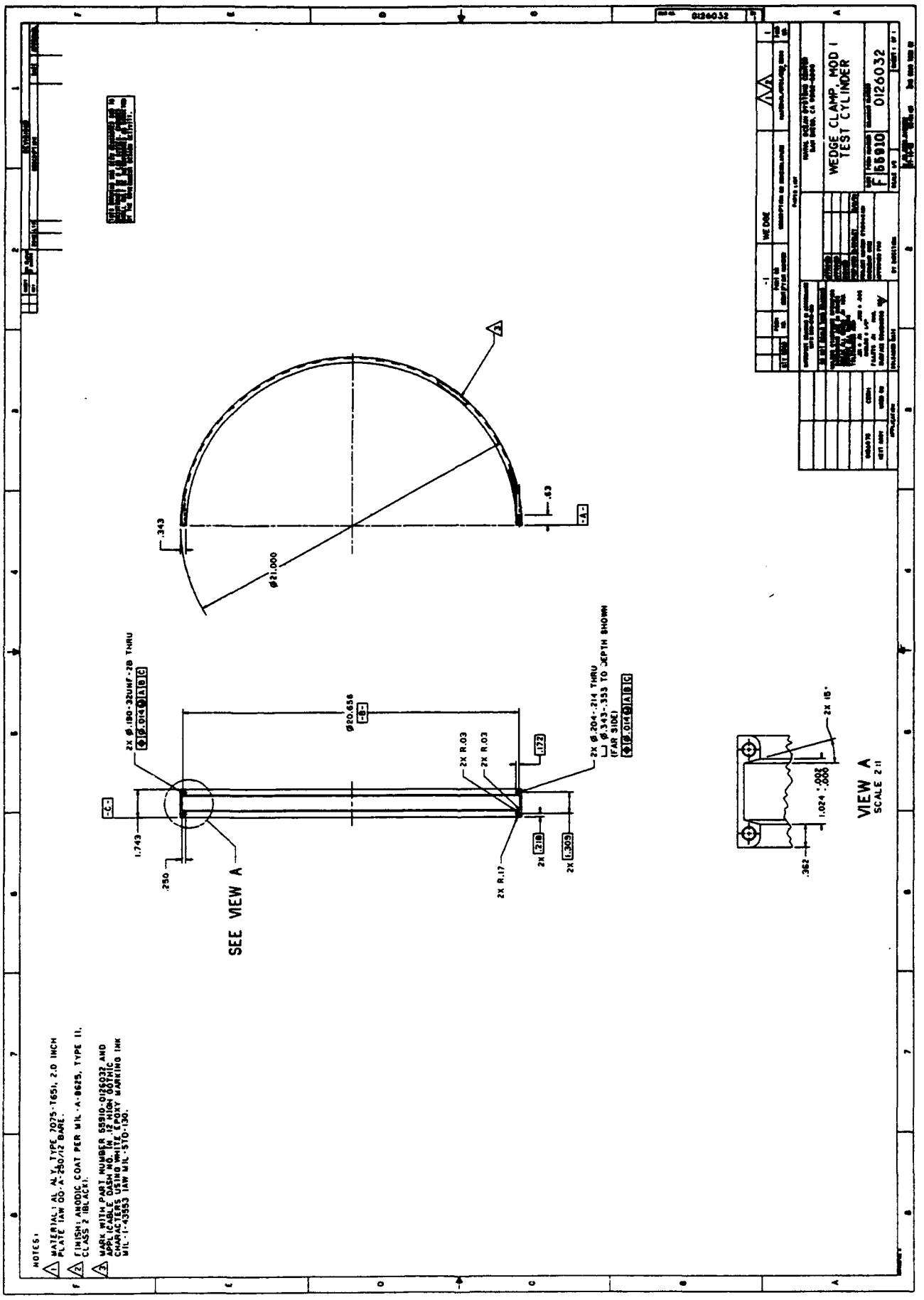

Figure 23. Wedge clamp for fastening metallic hemispherical bulkheads to 20-inch OD ceramic test cylinders.

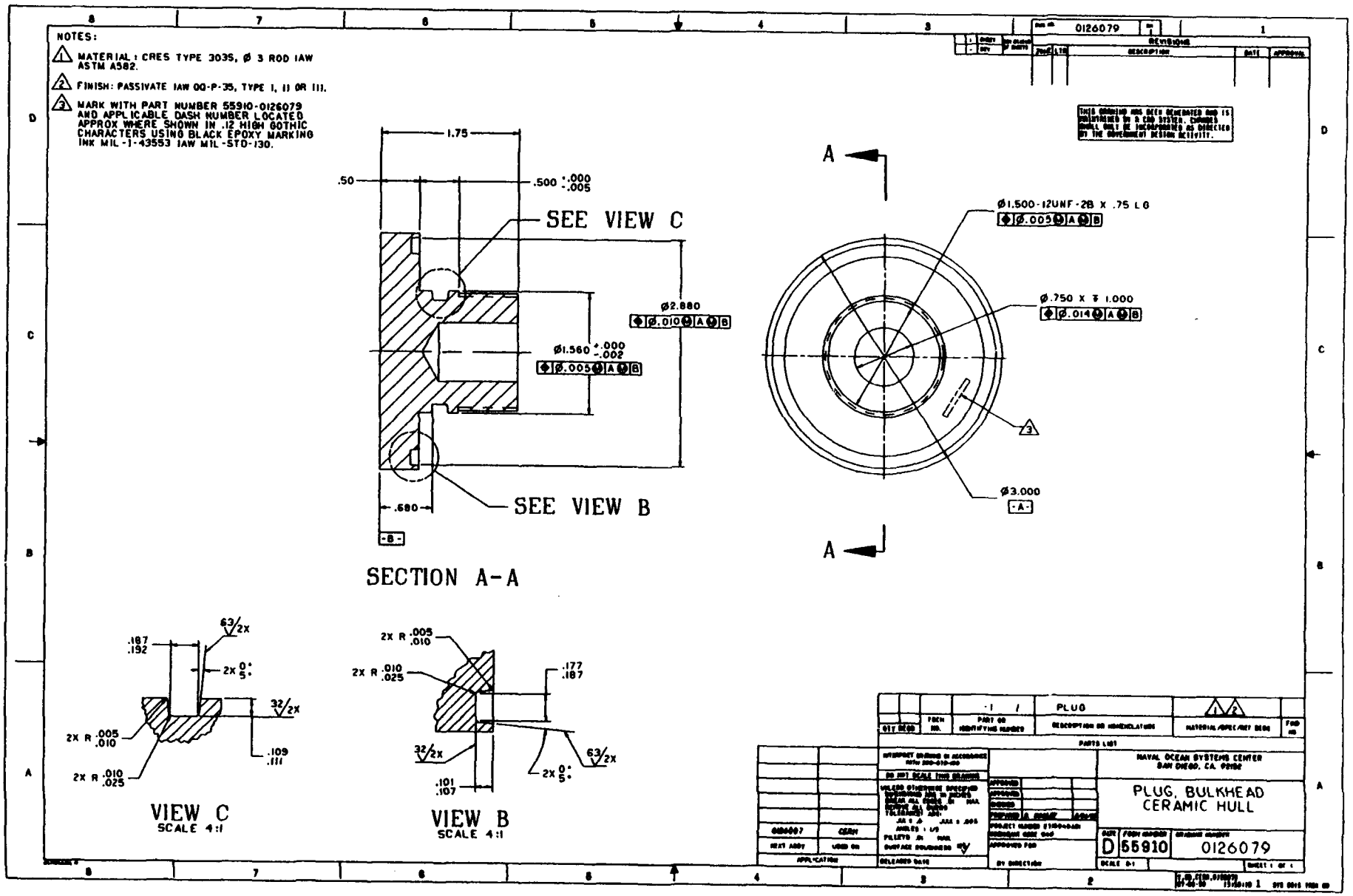

Figure 24. Plug for metallic hemispherical bulkhead.

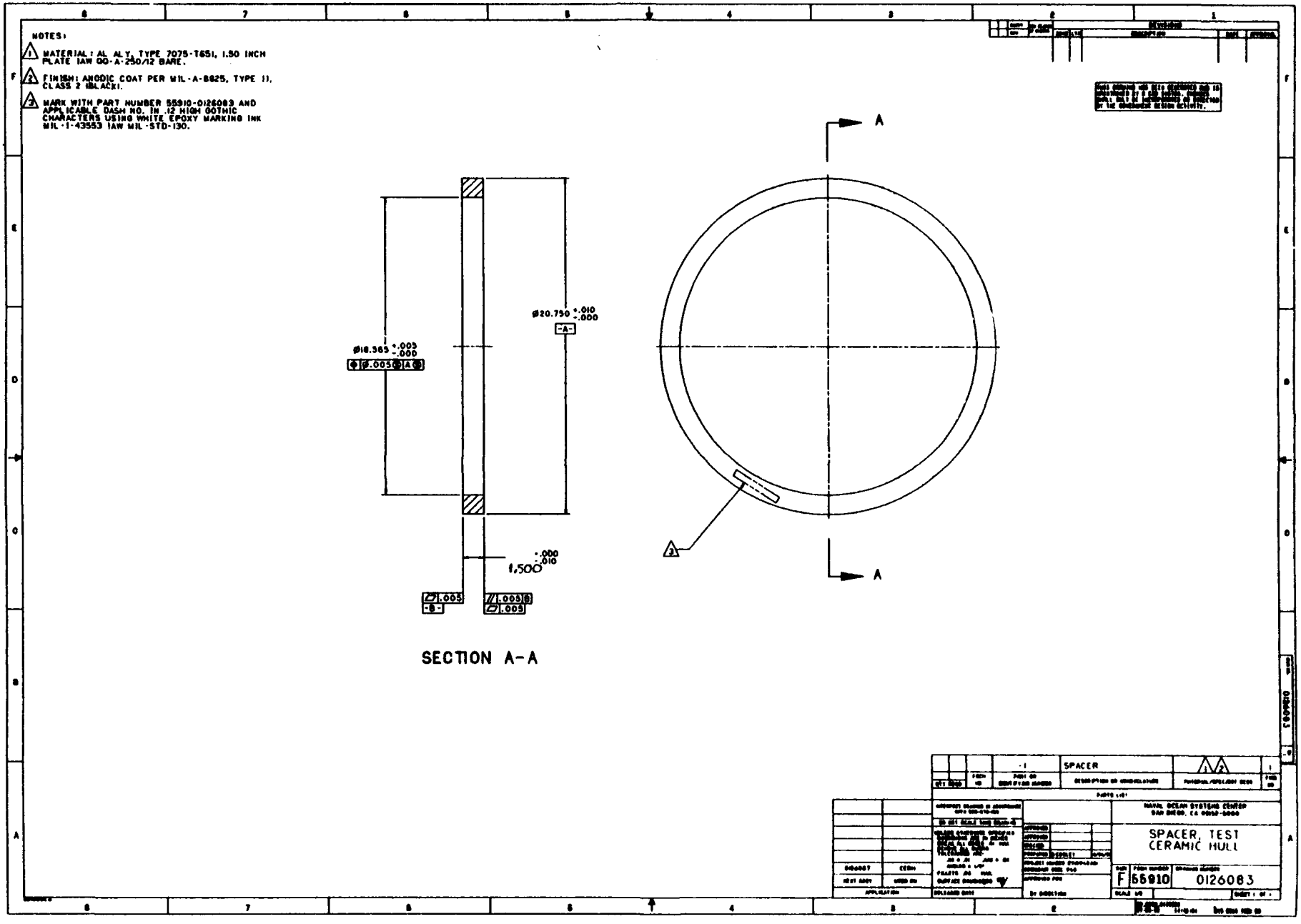

Figure 25. Spacer ring for joining two metallic hemispherical bulkheads into a spherical pressure housing for subsequent prooftesting.

Figure 26. Cylinder A with Mod 1 aluminum end cap rings marked up for ultrasonic NDT.

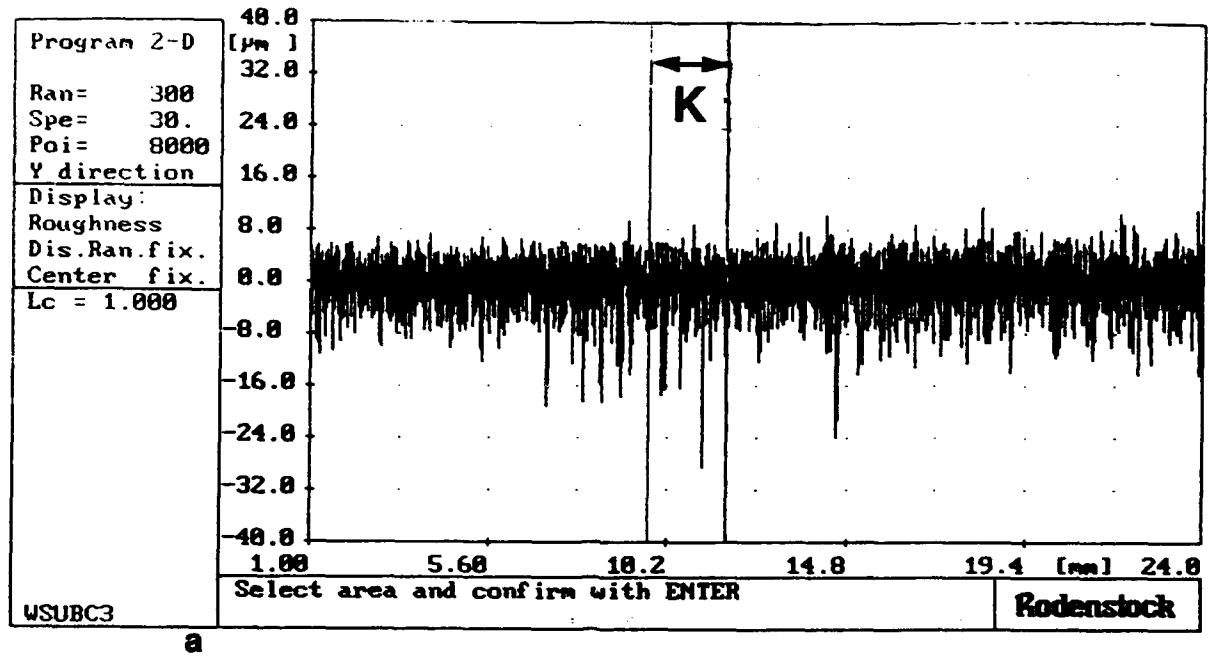

a

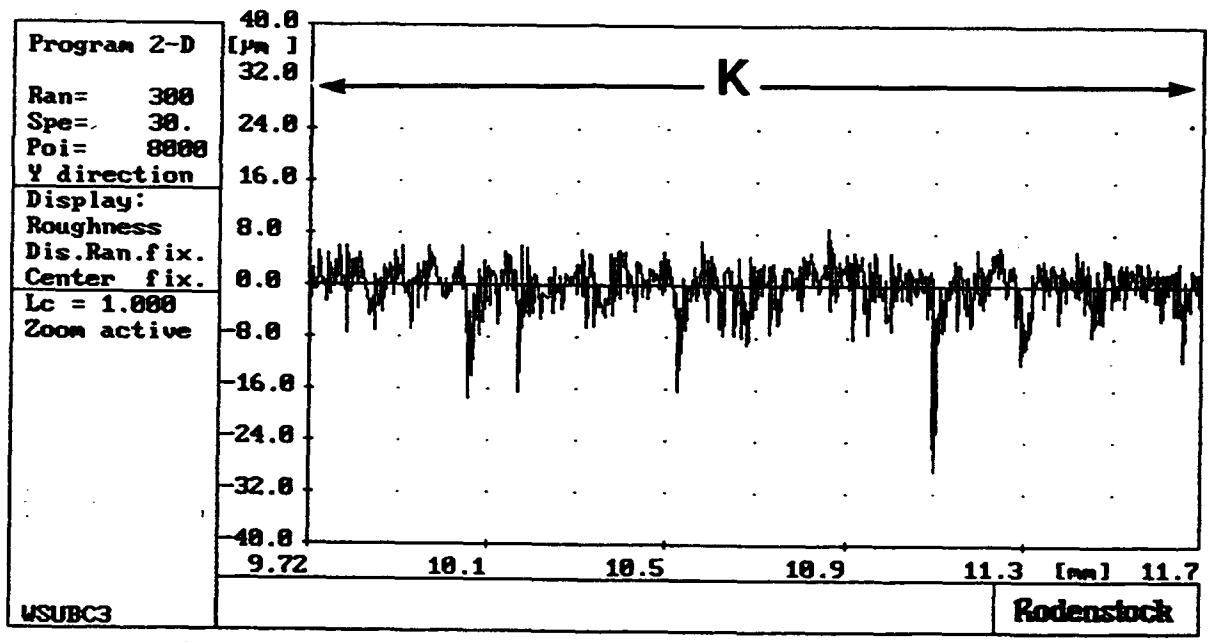

b

Figure 27. Surface roughness profile for the ground plane-bearing surfaces on cylinder A.
a. One-inch profile of bearing surface.
b. Enlargement of profile "a" in the K space.

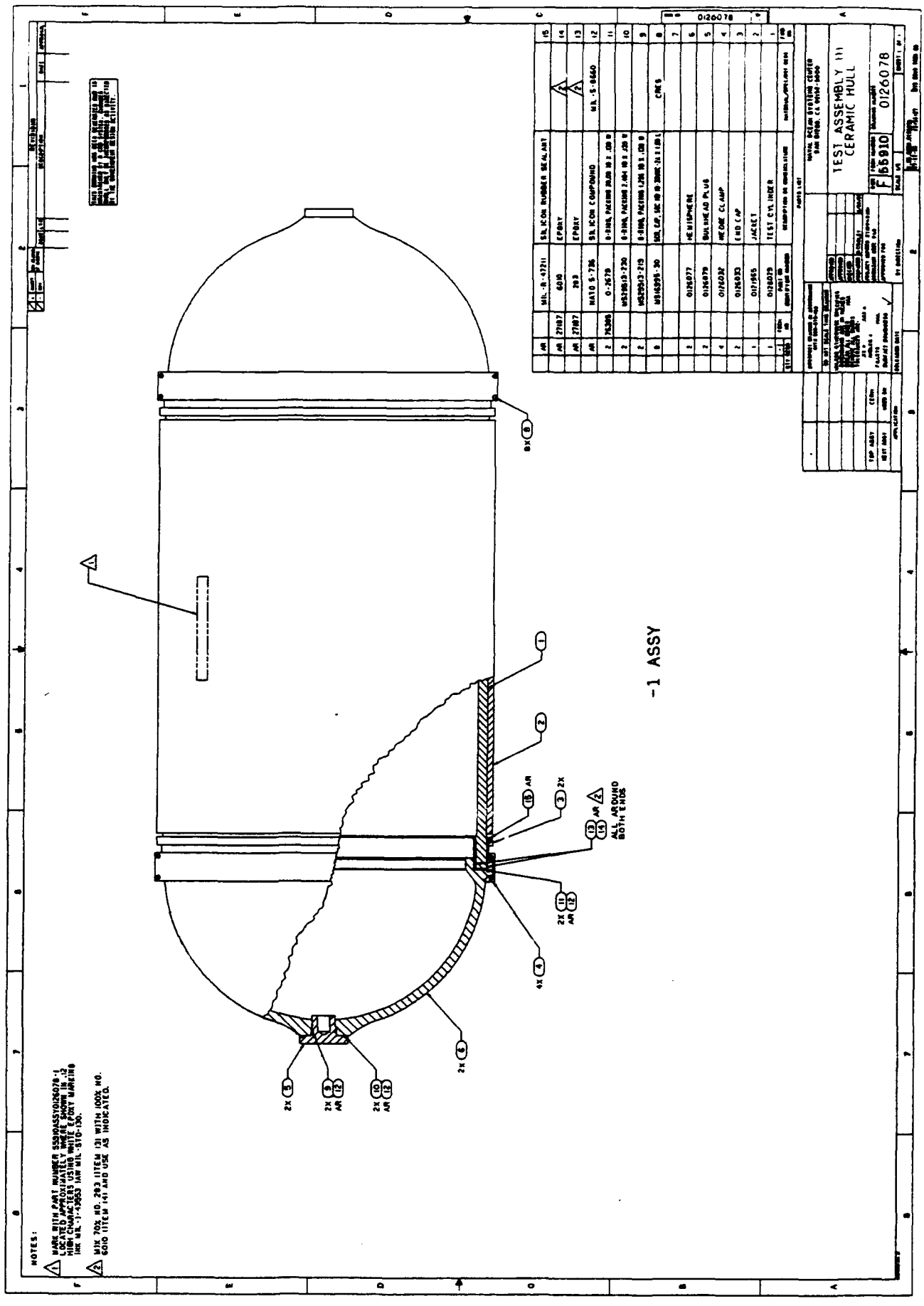

Figure 28. Housing test assembly for pressure testing of 20-inch OD ceramic cylinders.

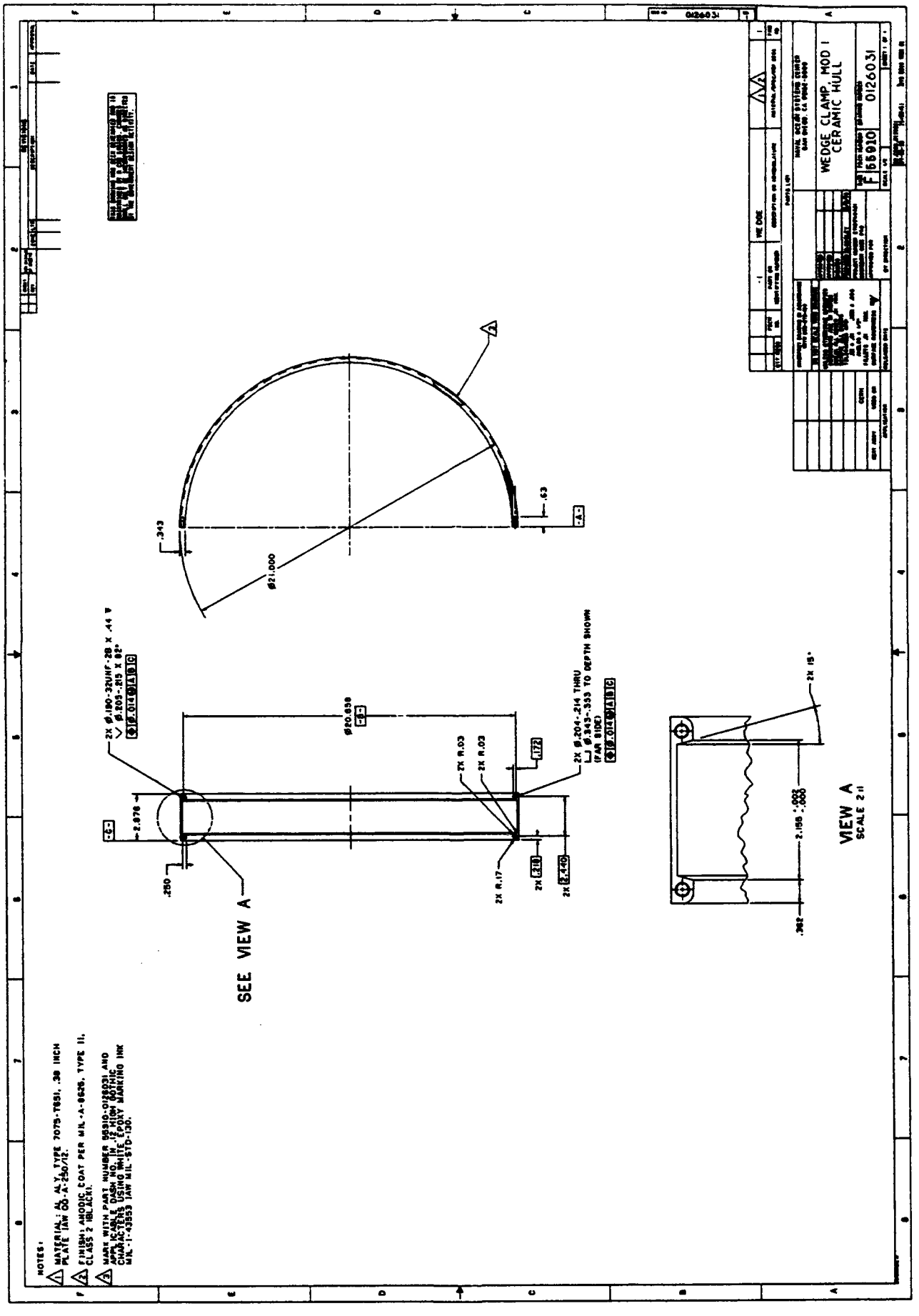

Figure 29. Wedge band for clamping the two metallic bulkheads together over a spacer ring (Figure 25) for their proofteeting.

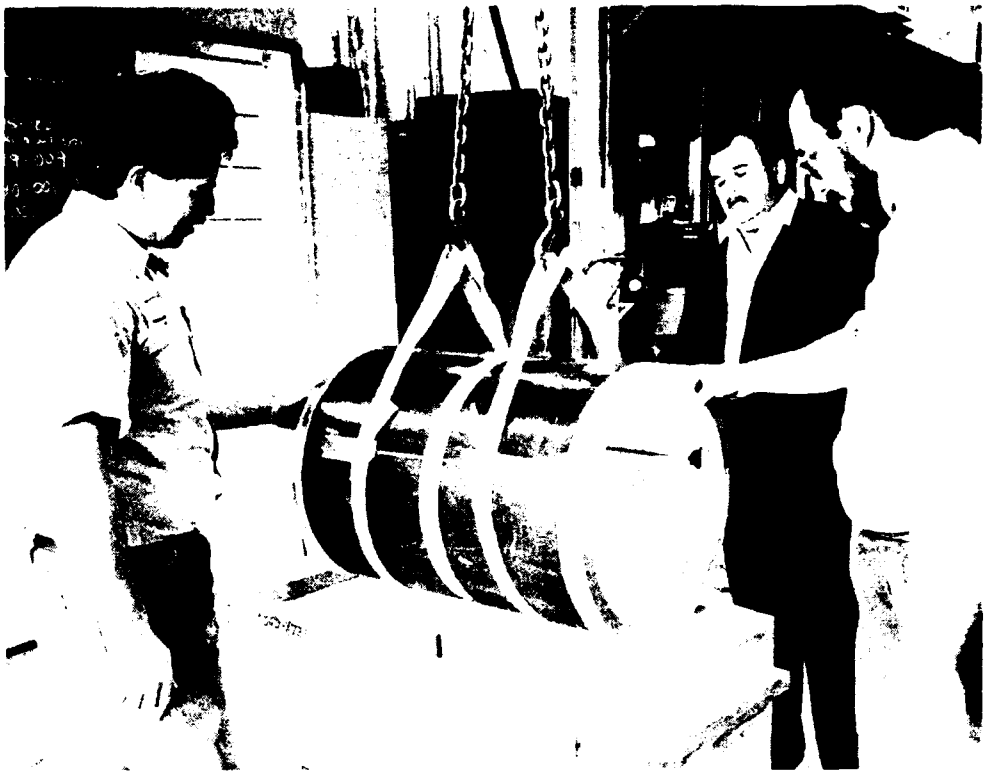

Figure 30. Typical handling arrangement for 20-inch OD test cylinders.

Figure 31. Mounting of the ceramic cylinder to the hemispherical bulkhead.

Figure 32. Insertion of wood block inside the test cylinder for mitigation of implosion shock.

Figure 33. Placement of the other bulkhead on the ceramic test cylinder.

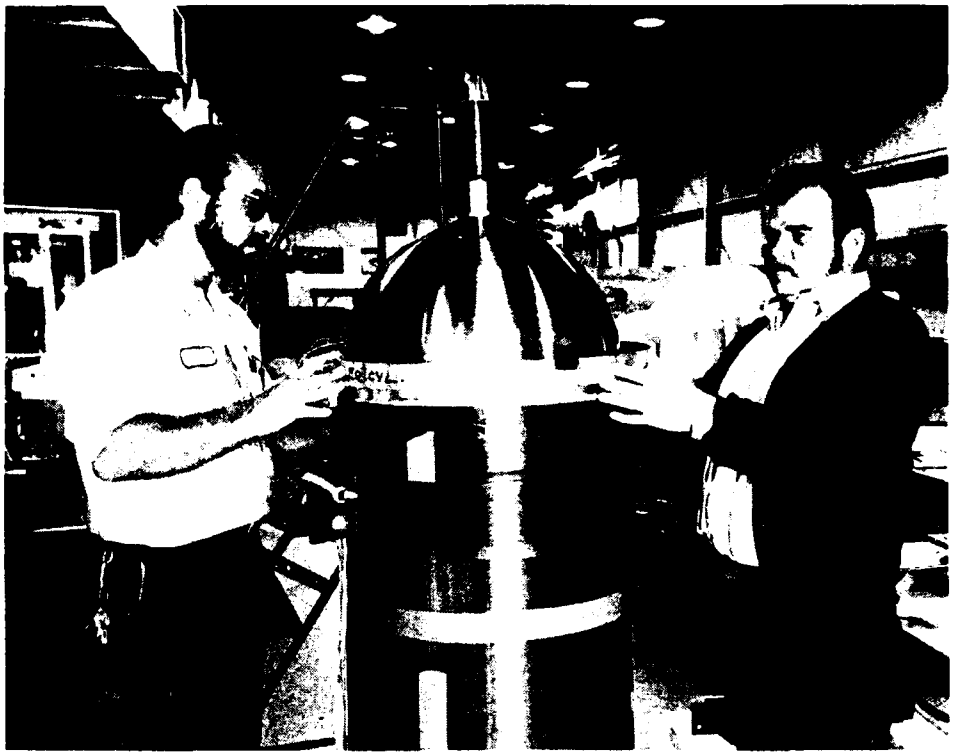

Figure 34. Fastening of the bulkheads to the ceramic test cylinder with wedge band clamps.

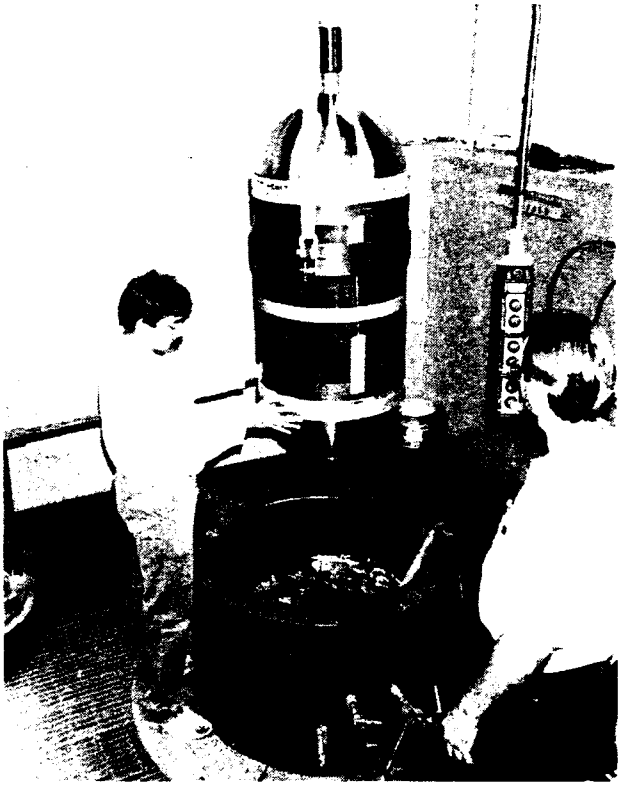

Figure 35. Placement of the 20-inch OD ceramic housing test assembly into the 30-inch ID pressure vessel at the Southwest Research Institute.

Figure 36. Imploded cylinder A with 20-inch OD by 30-inch L by 0.685-inch dimensions. The test assembly withstood sequentially a proof test to 10,000 psi and 452 pressure cycles to 9,000 psi prior to implosion.

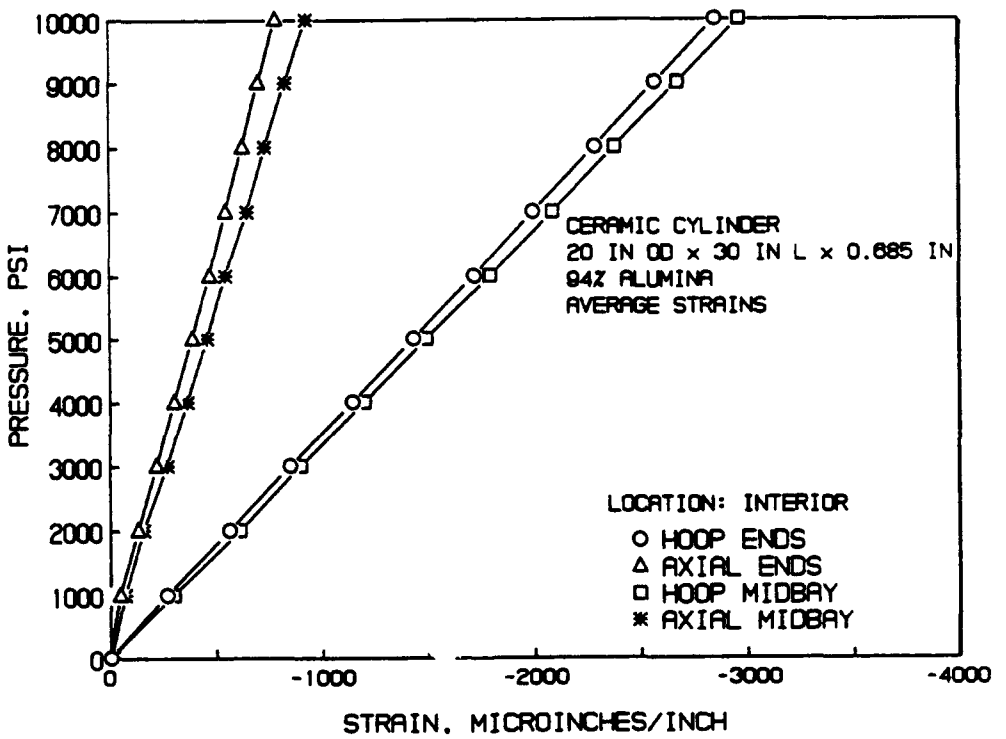

Figure 37. Average strains on the interior surface of cylinder A supported at ends by steel hemispheres.

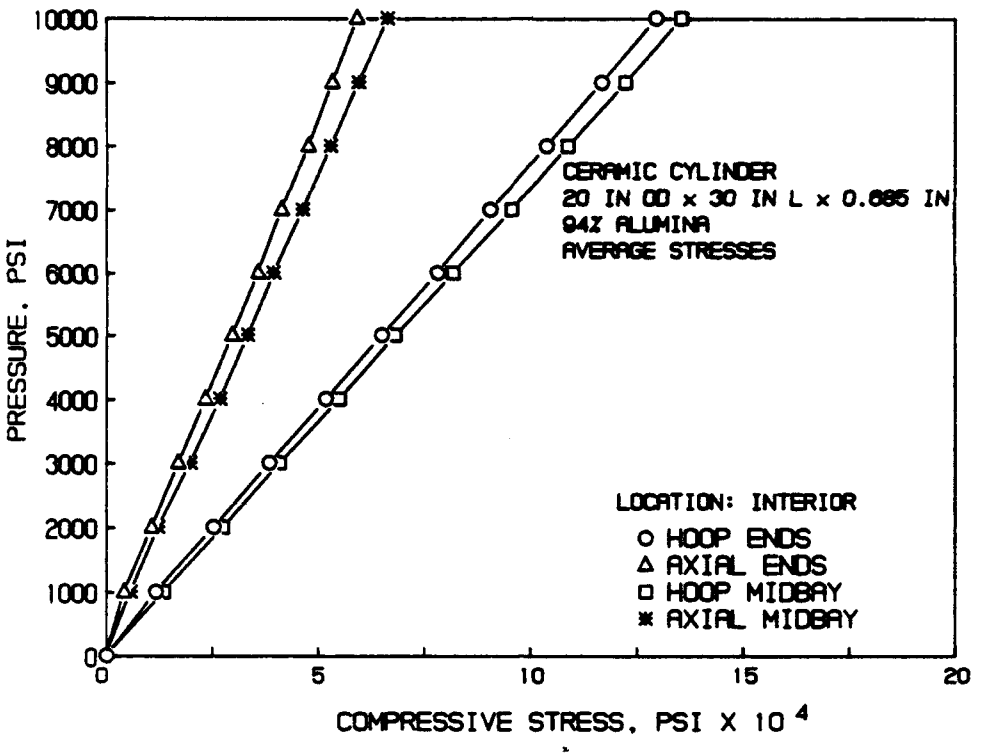

Figure 38. Average stresses on the interior surface of cylinder A supported at the ends by steel hemispheres.

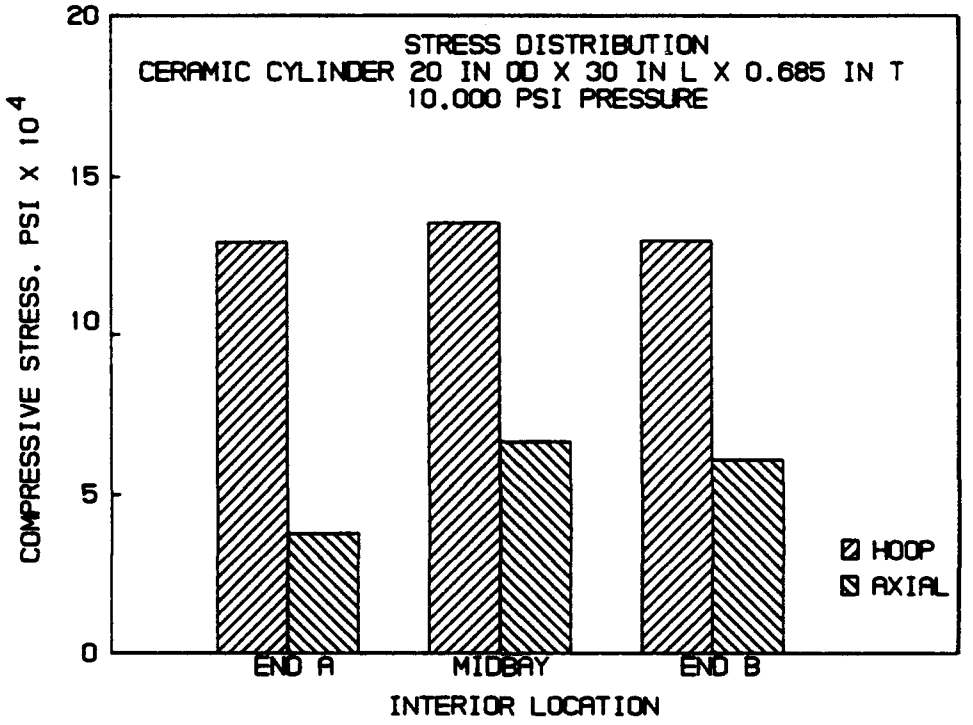

Figure 39. Stress distribution on the interior surface of cylinder A supported at the ends by steel hemispheres.

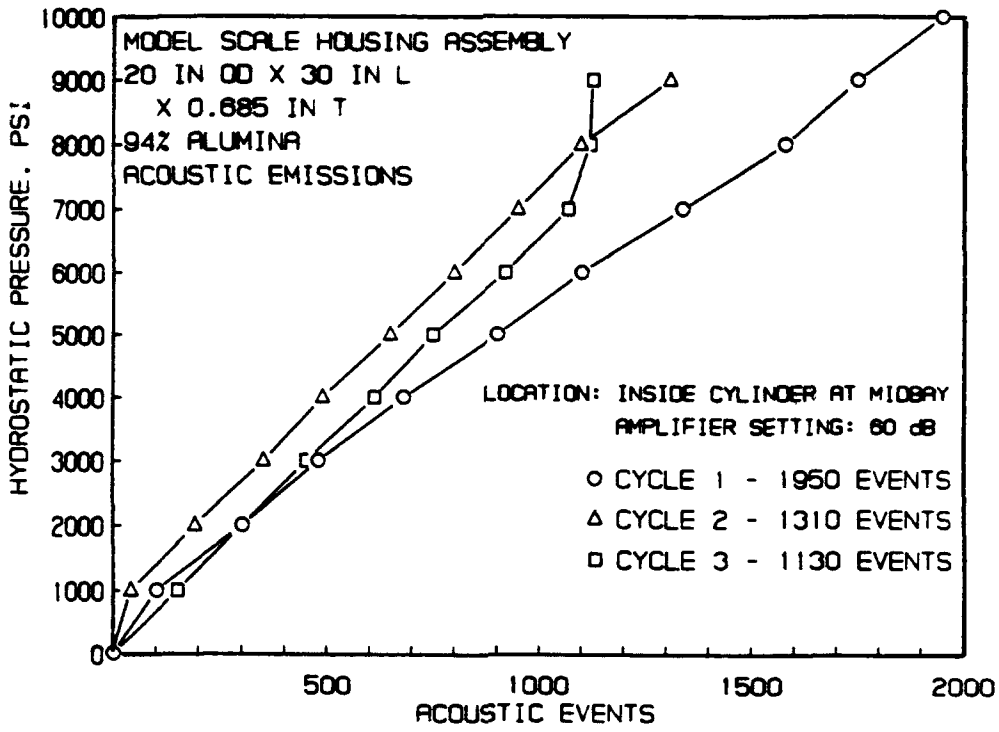

Figure 40. Acoustic emissions generated by cylinder A during pressure testing.

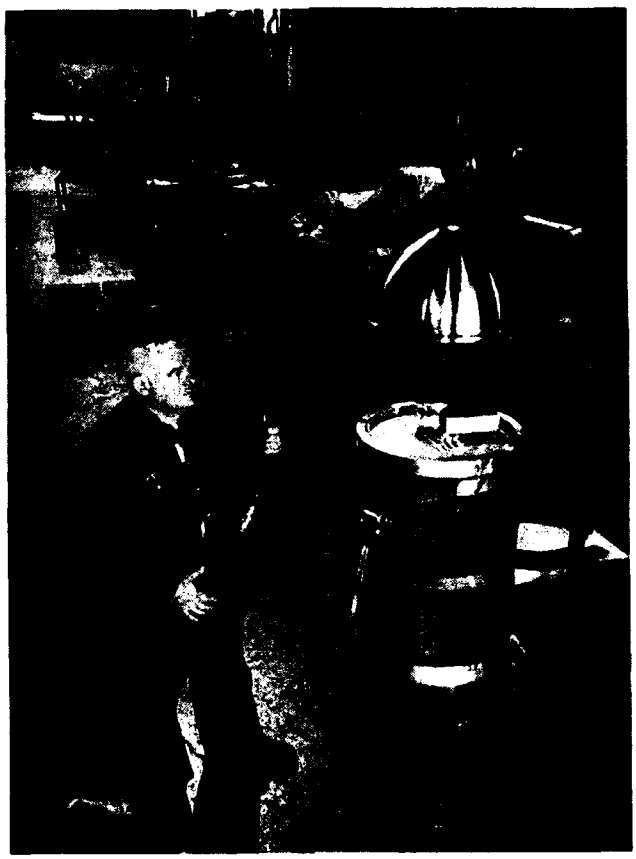

Figure 41a. Cylinder B before pressure testing to 9,700 psi.

Figure 41b. Cylinder B after pressure testing to 9,700 psi.

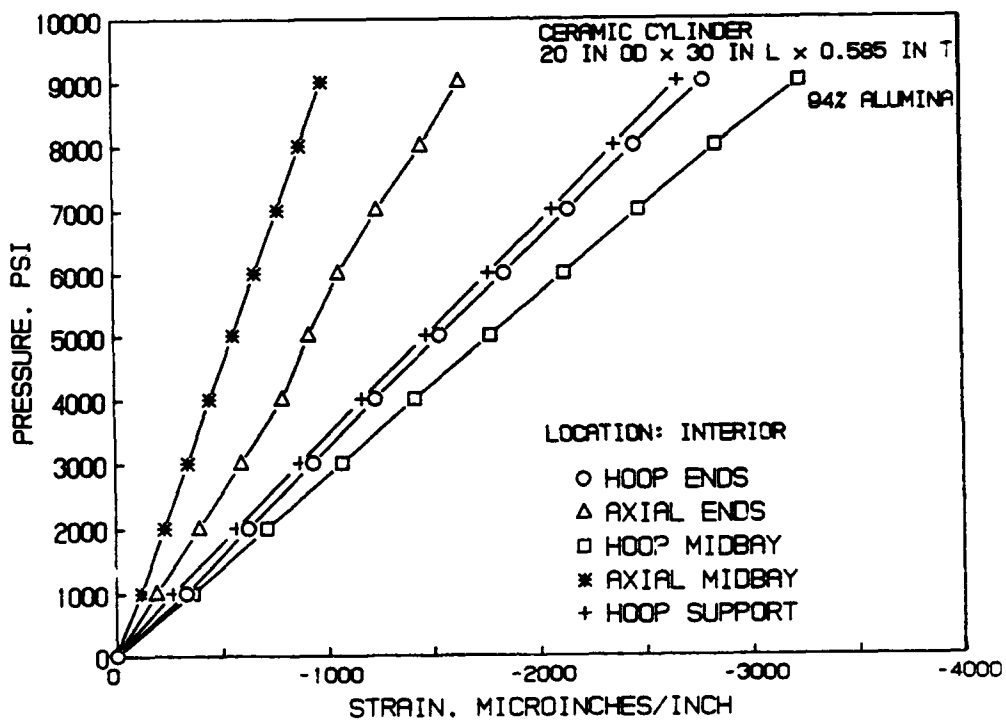

Figure 42. Average strains on the interior surface of cylinder B supported at ends by titanium hemispheres.

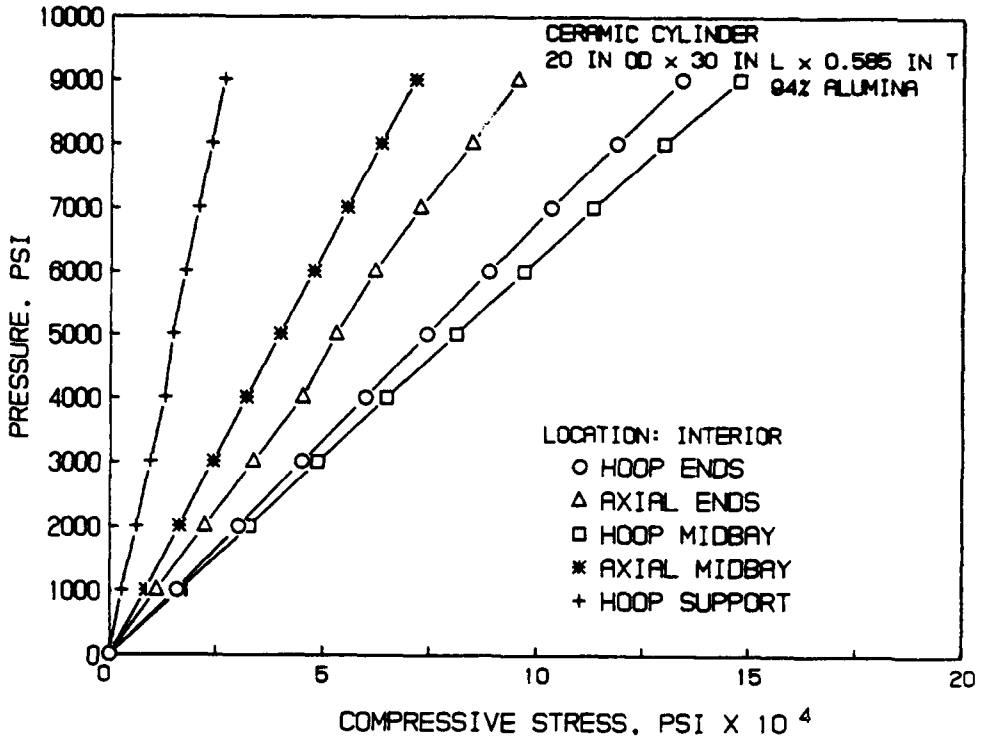

Figure 43. Average stresses on the interior surface of cylinder B supported at ends by titanium hemispheres.

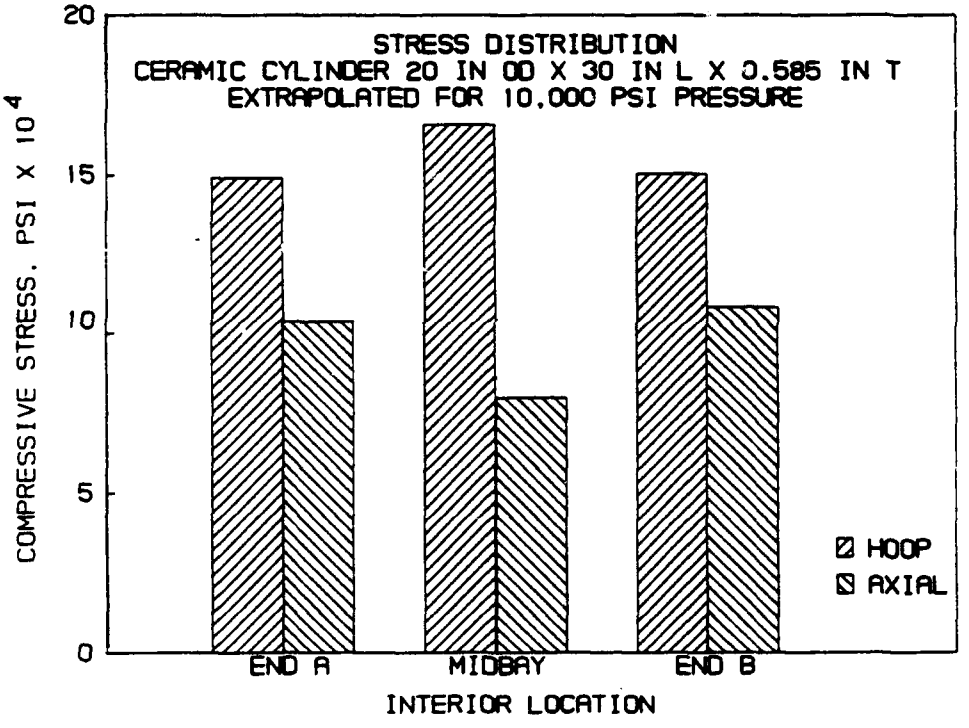

Figure 44. Stress distribution on the interior surface of cylinder B supported at ends by titanium hemispheres.

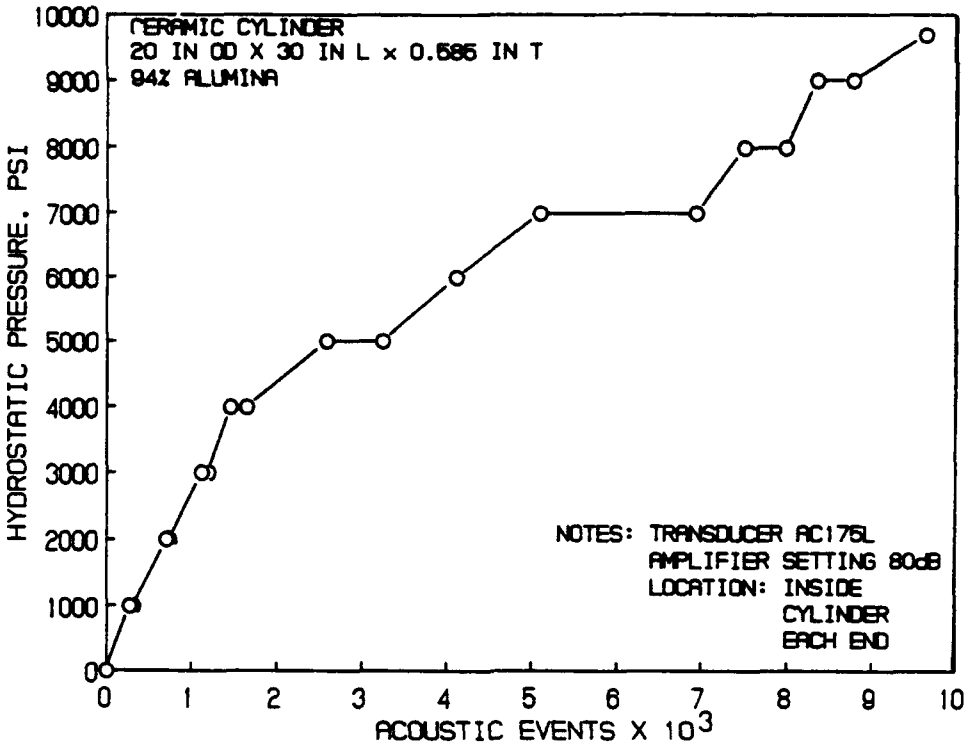

Figure 45. Acoustic emissions generated by cylinder B during pressure testing.

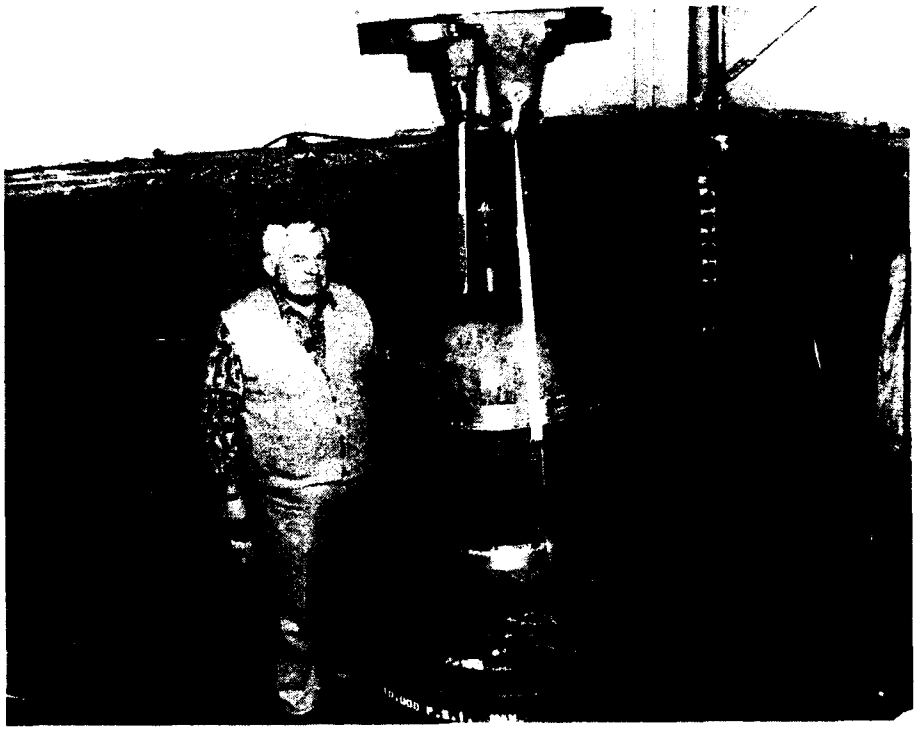

Figure 46. Cylinder C before pressure testing.

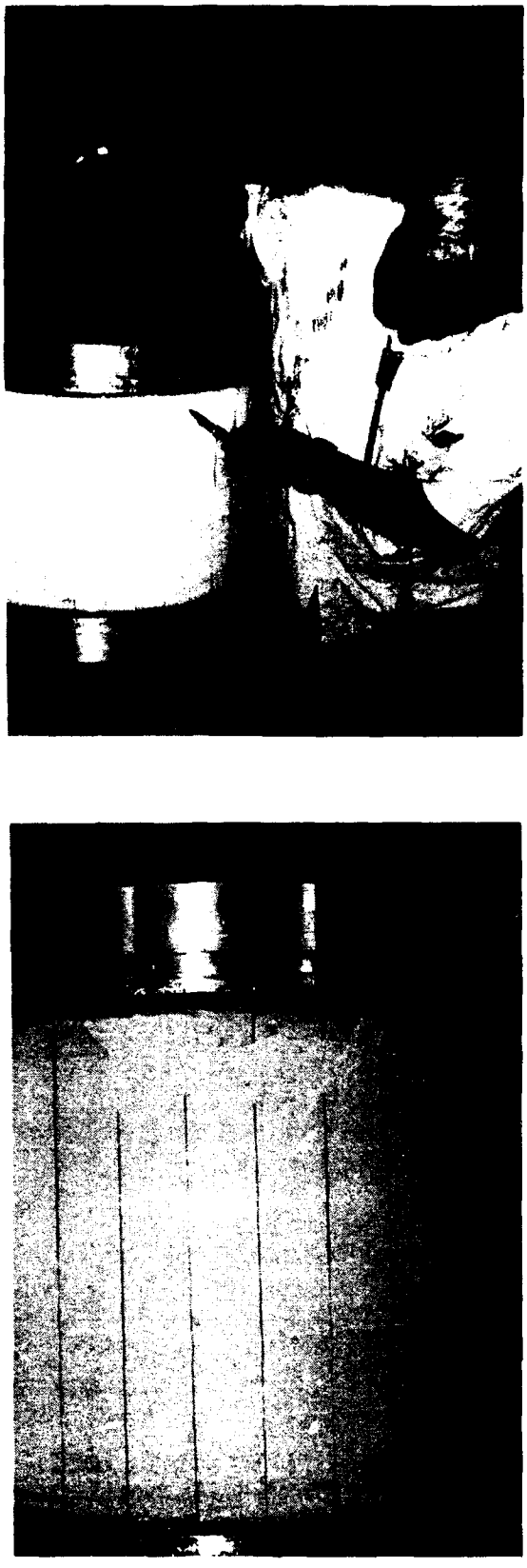

Figure 47. External spalling on cylinder C observed after 53 pressure cycles to 9,000 psi.

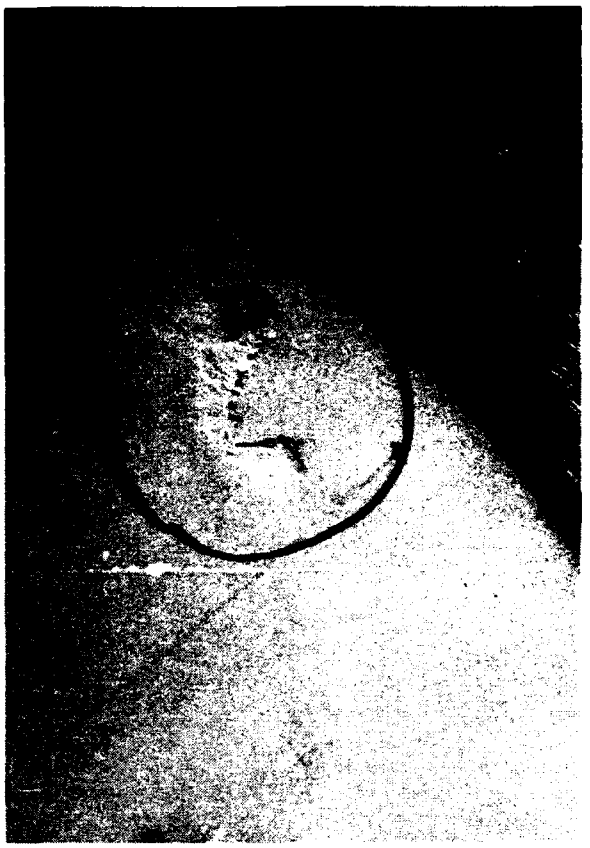

Figure 48. Internal spalling on cylinder C observed after 53 pressure cycles to 9,000 psi.

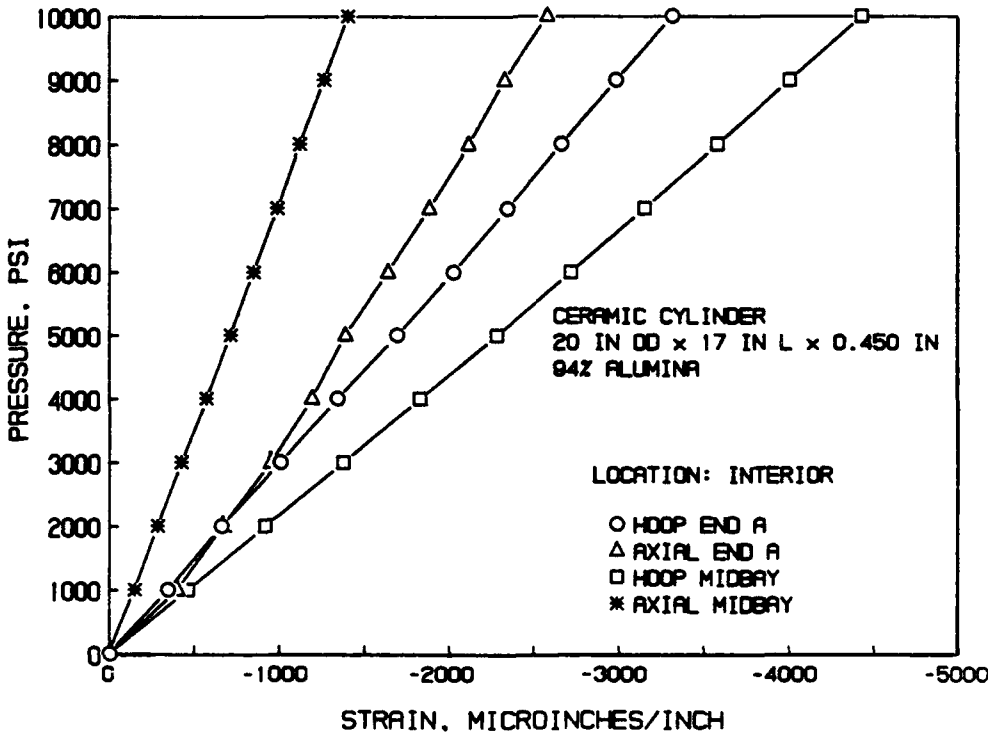

Figure 49. Average strains on the interior surface of cylinder C supported at ends by steel hemispheres.

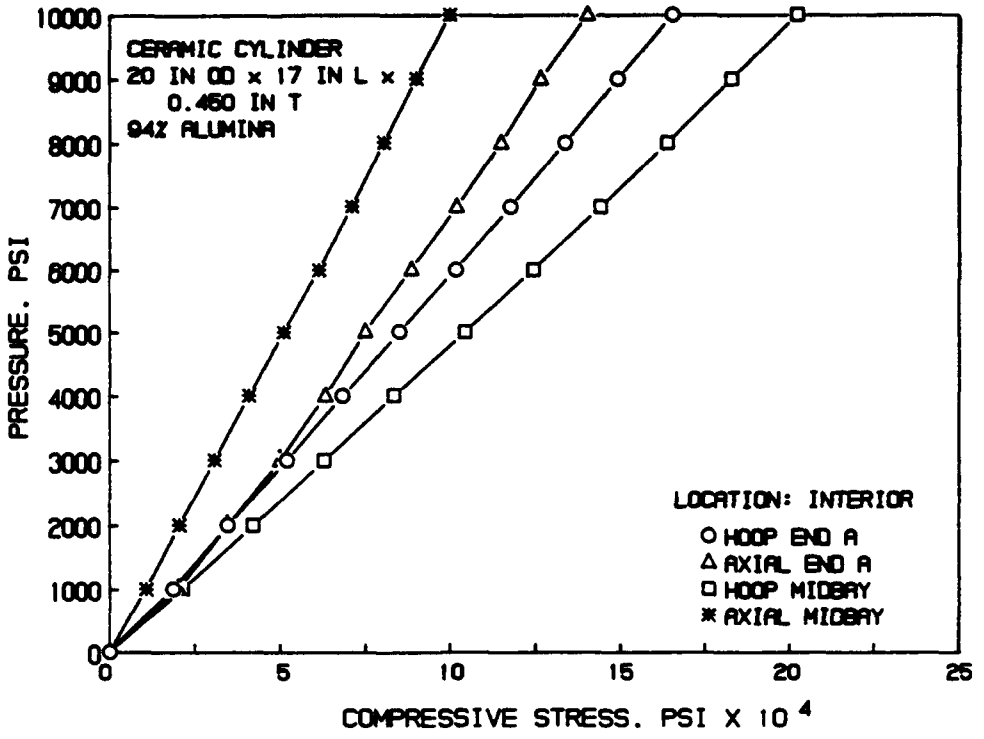

Figure 50. Average stresses on the interior surface of cylinder C supported at ends by steel hemispheres.

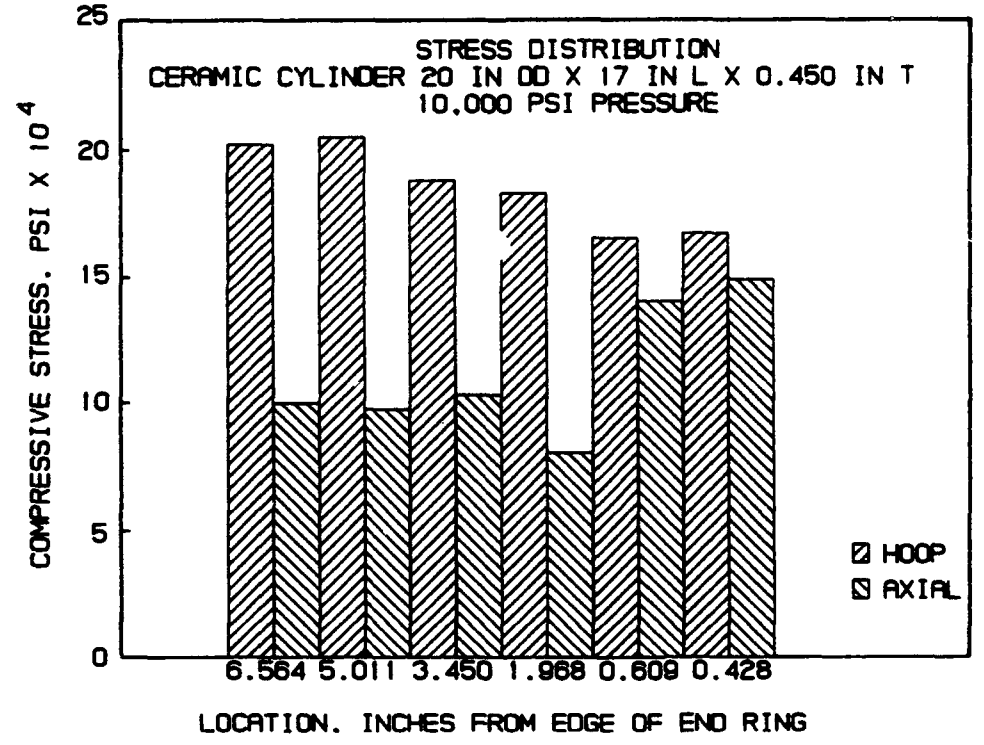

Figure 51. Stress distribution on the interior surface of cylinder C supported at ends by steel hemispheres.

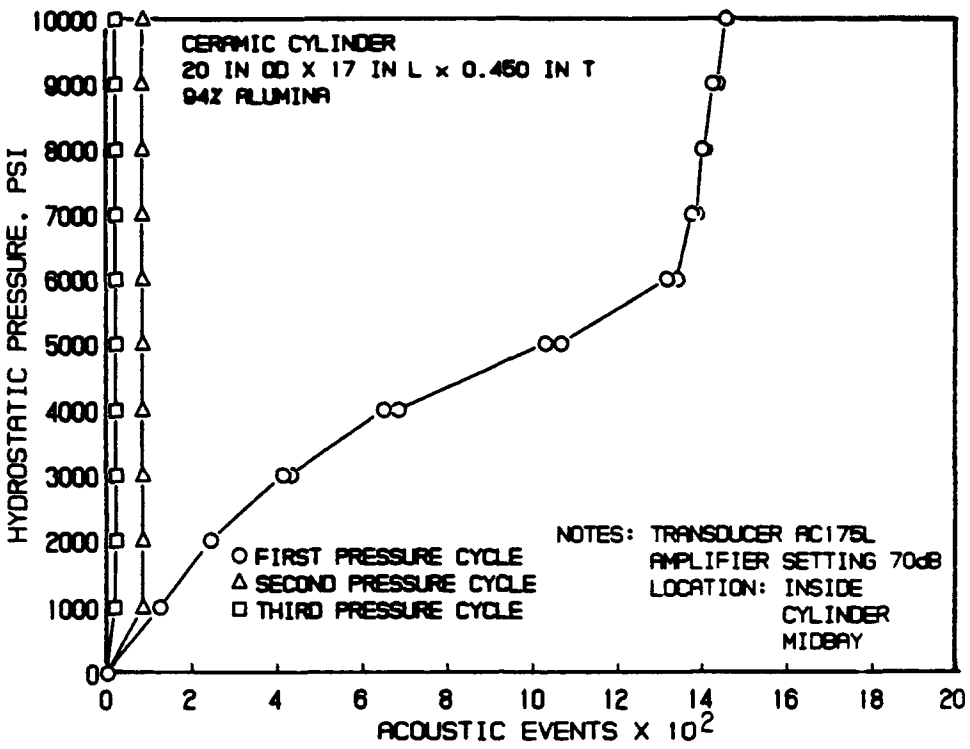

Figure 52. Acoustic emissions generated by cylinder C during pressure testing.

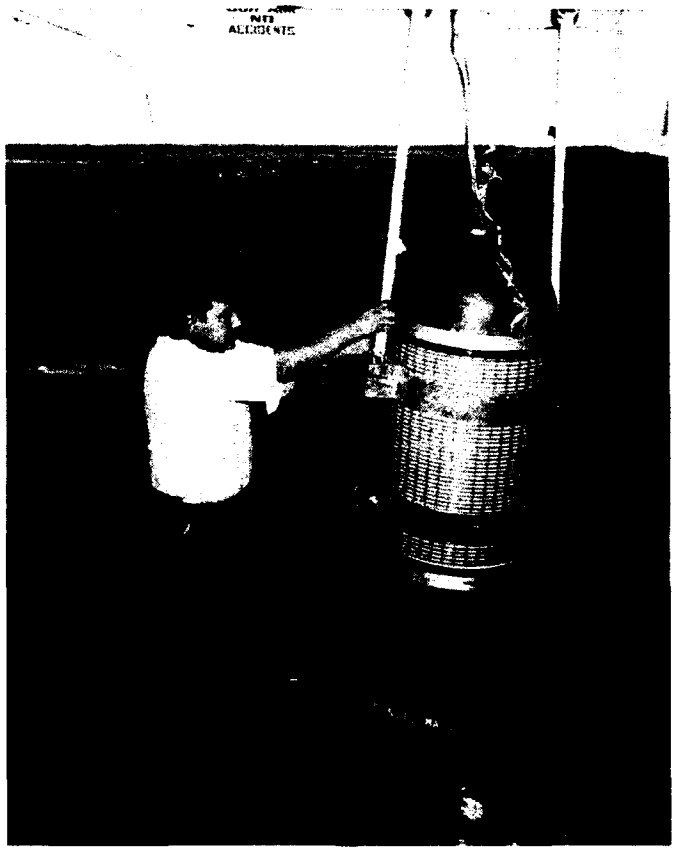

Figure 53. Cylinder D prior to pressure testing.

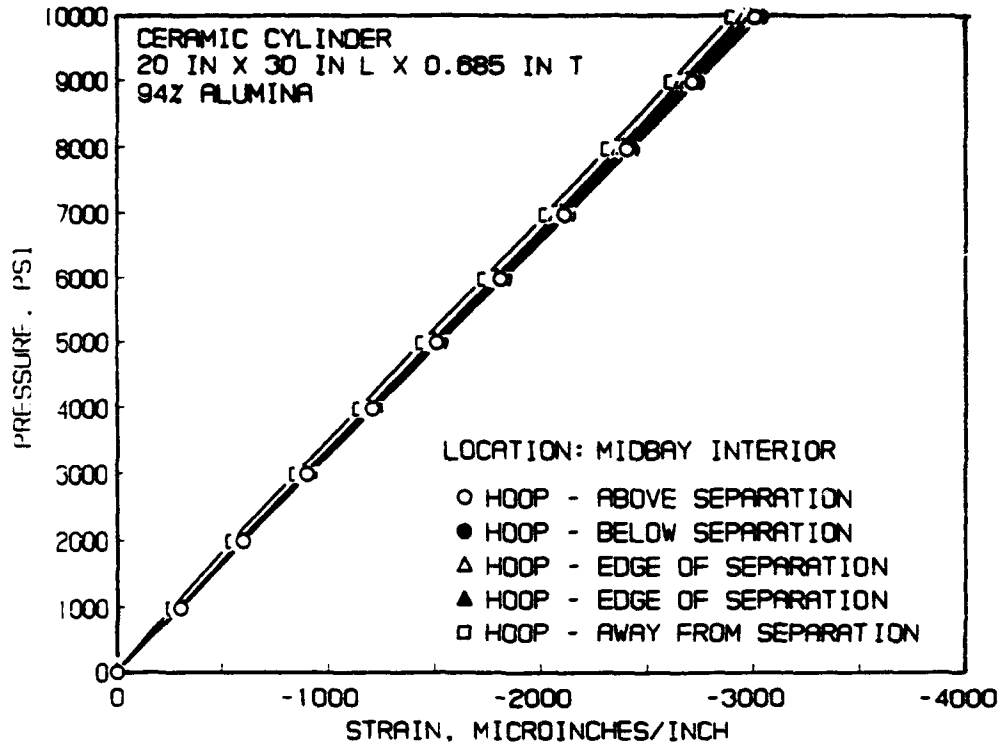

Figure 54. Hoop strains on the interior surface of cylinder D at midbay around surface discontinuity.

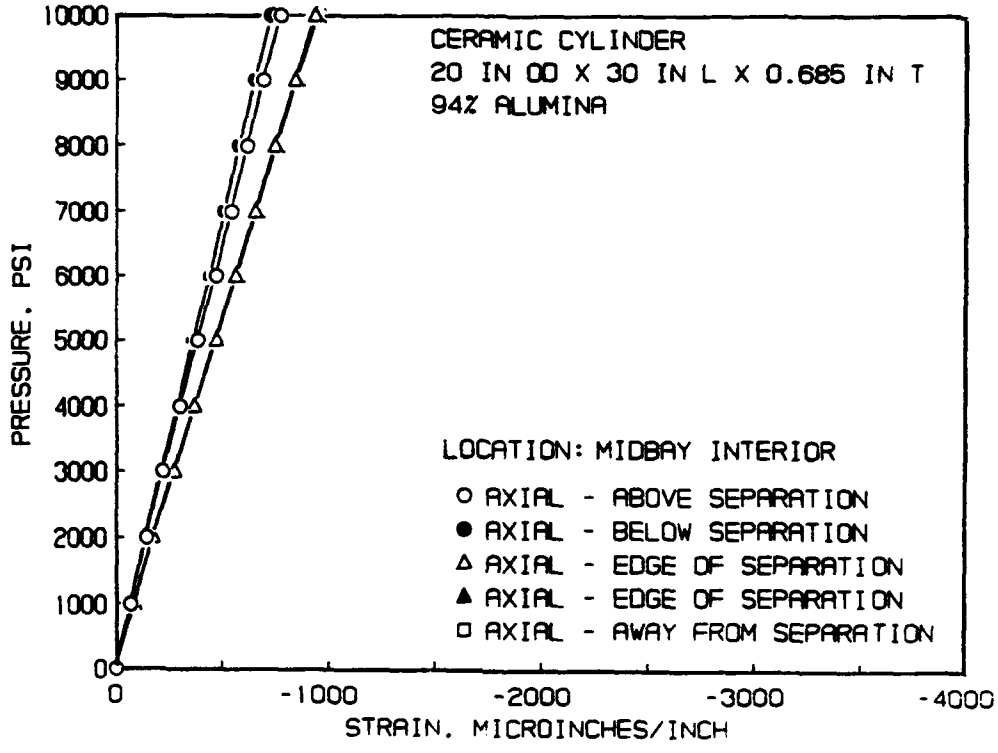

Figure 55. Axial strains on the interior surface of cylinder D at midbay around surface discontinuity.

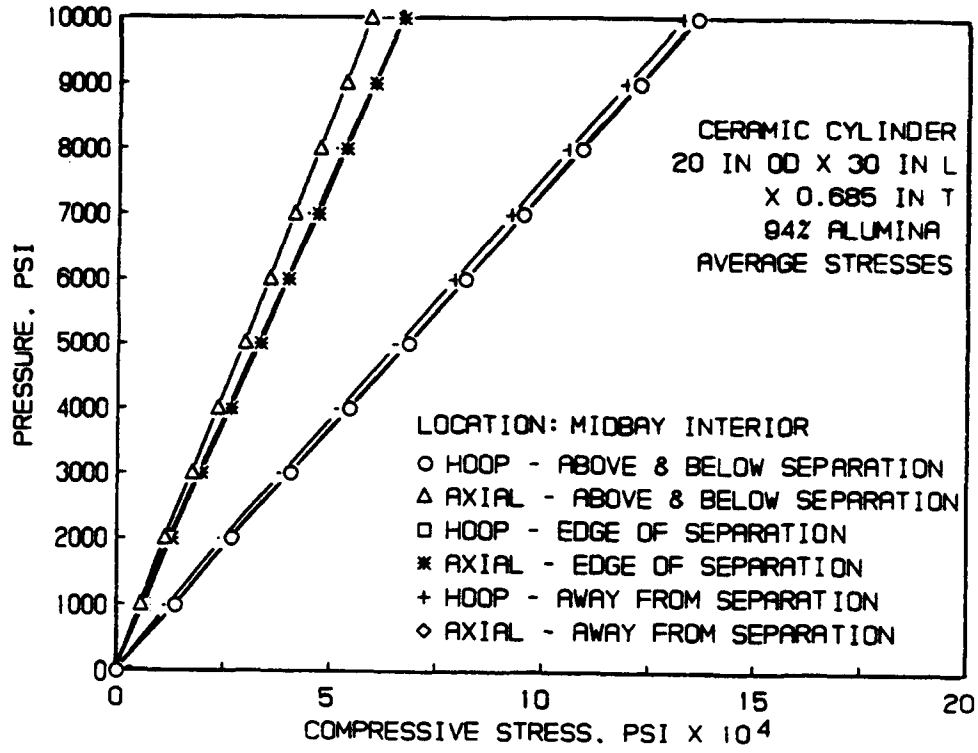

Figure 56. Stresses on the interior surface of cylinder D at midbay around surface discontinuity.

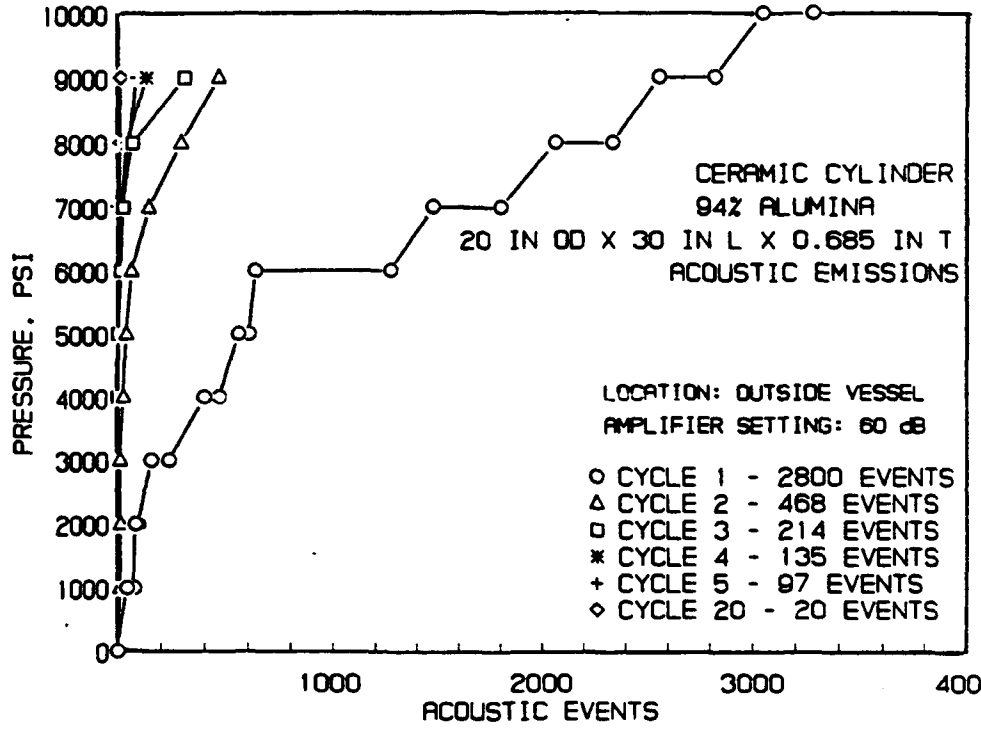

Figure 57. Acoustic emissions generated by cylinder D during pressure testing.

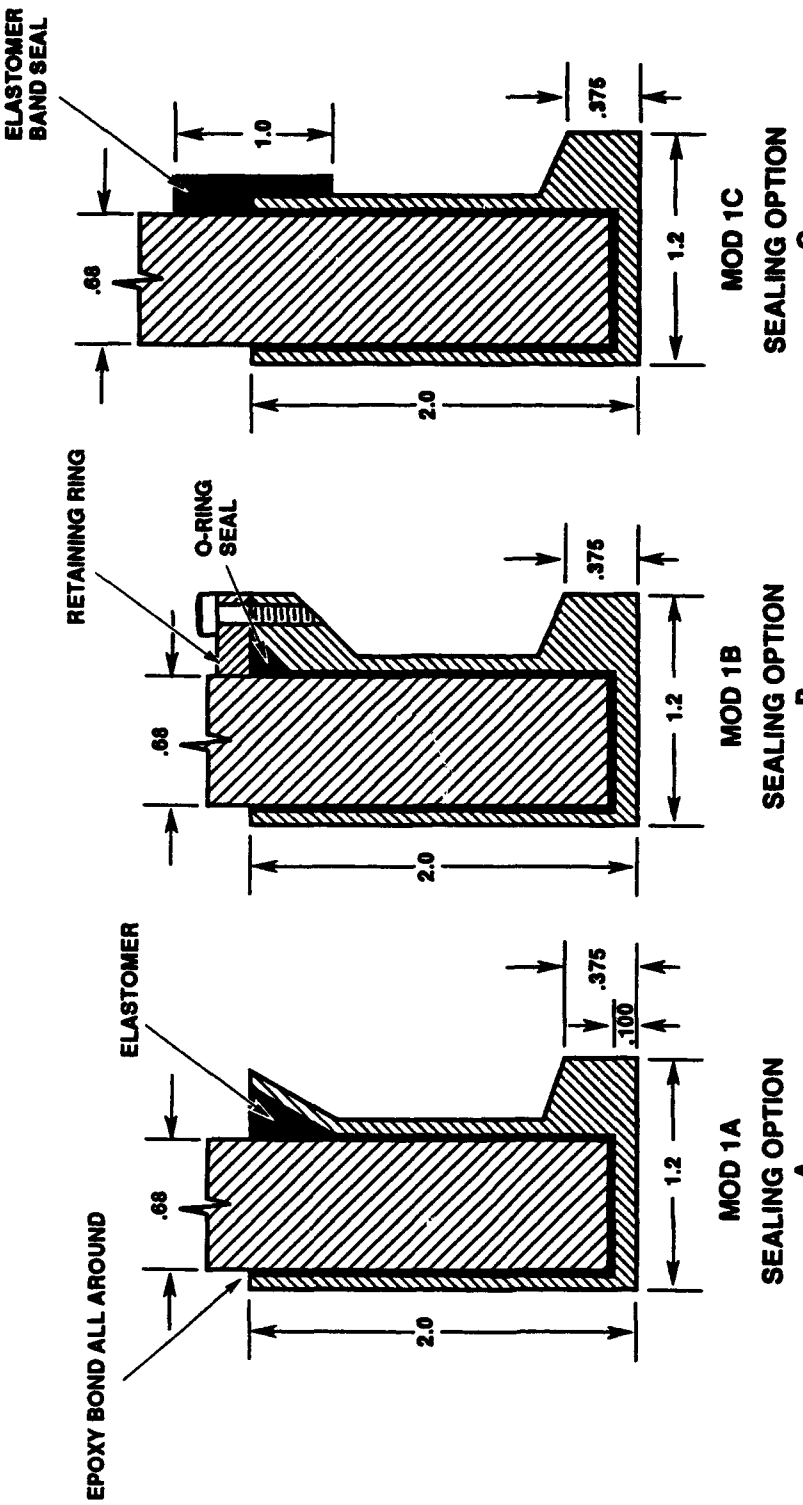

Figure 58. Mod 1 end caps for ceramic cylinders with three different seal options. Same end cap design can be applied to ceramic hemispheres with cylindrical skirts on the equatorial region.

Table 1. Typical materials for construction of deep submergence pressure housings.

Material	Weight (lb/in_3)	Modulus of Elasticity (Mpsi)	Elasticity Weight	Compressive Strength (kpsi)	Strength Weight
Steel (HY80)	0.283	30	106	80	280
Steel (HY 130)	0.283	30	106	130	460
Aluminum (7075-T6)	0.100	10	100	73	730
Titanium (6Al-4V)	0.160	16	100	125	780
Glass (Pyrex)	0.080	9	112	100	1250
Glass Composite	0.075	3.5	47	100	1330
Graphite Composite	0.057	16	280	100	1750
Beryllia Ceramic 99%	0.104	51	490	300	2885
Alumina Ceramic 94%	0.130	44	338	300	2310
Glass Ceramic (Pyroceram 9606)	0.093	17.5	188	350	3760
Silicon Carbide	0.114	59	517	450	3947
Boron Carbide	0.089	63	707	400	4494
Alumina/SiC Composite (Lanxide 90-X-089)	0.124	43	346	300	2419
B_4C/Al Composite (Dow Chemical)	0.093	45	483	350	3763
Silicon Nitride	0.119	44	370	400	3361

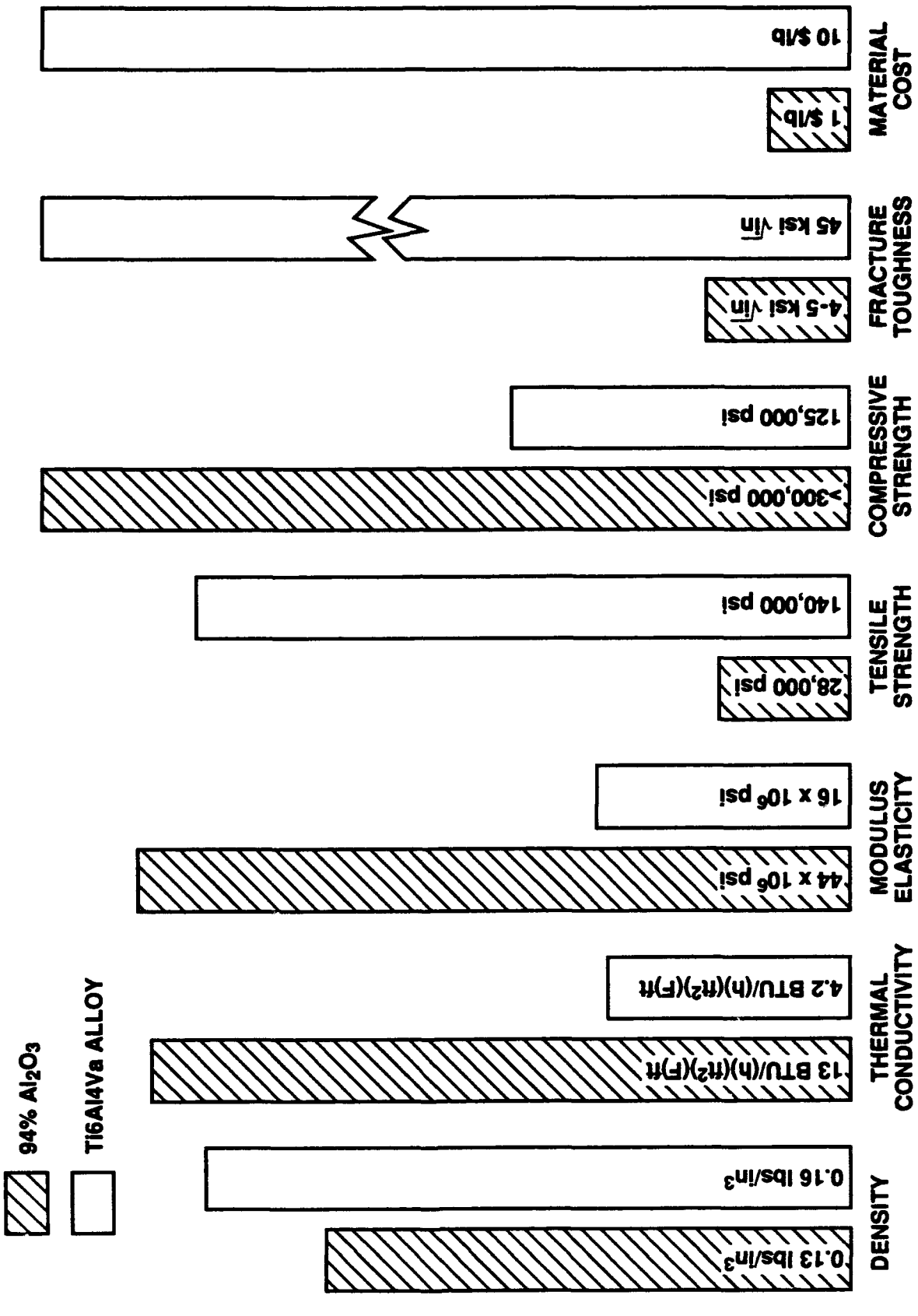

Table 2. Comparison of alumina ceramic to titanium alloy.

Table 3. Design data for test cylinders.

	Test Cylinders			
Material*	**A AD 94**	**B AD 94**	**C AD 94**	**D AD 94**
Hoop design stress, psi	135,000	156,000	200,000	135,000
Critical pressure,** psig	13,500	9,650	12,000	13,500
Outside diameter, in	20	20	20	20
Inside diameter, in	18.630	18.830	19.090	18.630
Wall thickness, in	0.685	0.585	0.455	0.685
Overall length, in	30	30	17	30
Length of ceramic flanges, in	N/A	2	2	N/A
t/D_o	0.034	0.029	0.023	0.034
L/D_o	1.5	1.5	0.85	1.5
Weight of 2 titanium end caps, lb	9	9	9	9
Weight of ceramic cylinder without end caps, lbs	167	148	70	167
Weight to displacement without end caps	0.48	0.42	0.36	0.48
Weight to displacement with end caps	0.50	0.45	0.41	0.50

*AD94 is COORS Ceramics ceramic with 94% alumina composition.
**When radially supported at the ends by titanium hemispheres with $\geq$13,500 psi critical pressure.

APPENDIX A: TEST DATA FROM TESTING PROGRAM

Preceding Page Blank

FIGURES

TABLES

APPENDIX A: TEST DATA FROM TESTING PROGRAM

Appendix A contains all the data generated during external pressure testing of 20-inch OD ceramic cylinders A, B, C, and D. The magnitudes of strains shown on tables and graphs are as recorded by 0.124-inch strain gages bonded to the interior surfaces of ceramic cylinders at locations shown. The stresses shown were calculated on the basis of above strains using a very conservative book value of $E = 41 \times 10^6$ psi for 94-percent alumina ceramic.

Subsequent tests performed on material coupons cut from fragments of failed cylinders have shown that the actual value of E in the 20-inch OD test cylinders was in the range of 44 to 45.5×10^6 psi. For this reason, the magnitude of stresses shown in tables and graphs in this report should be multiplied by a factor of 1.1 to bring them in line with the actual physical properties of 94-percent alumina-ceramic cylinders fabricated by COORS Ceramics.

Average values of strains and stresses shown on some of the graphs have been arrived at by averaging the strain readings from all of the electric resistance strain gages located at different locations around the circumference of the cylinder, but at the same distance from its end. The individual strain readings from such gages may differ from the calculated average value by as much as five percent. This difference in strain readings between individual gages in equivalent stress field locations is considered to be small. It is probably the result of minor deviations in gage axis orientations for the principal stress directions.

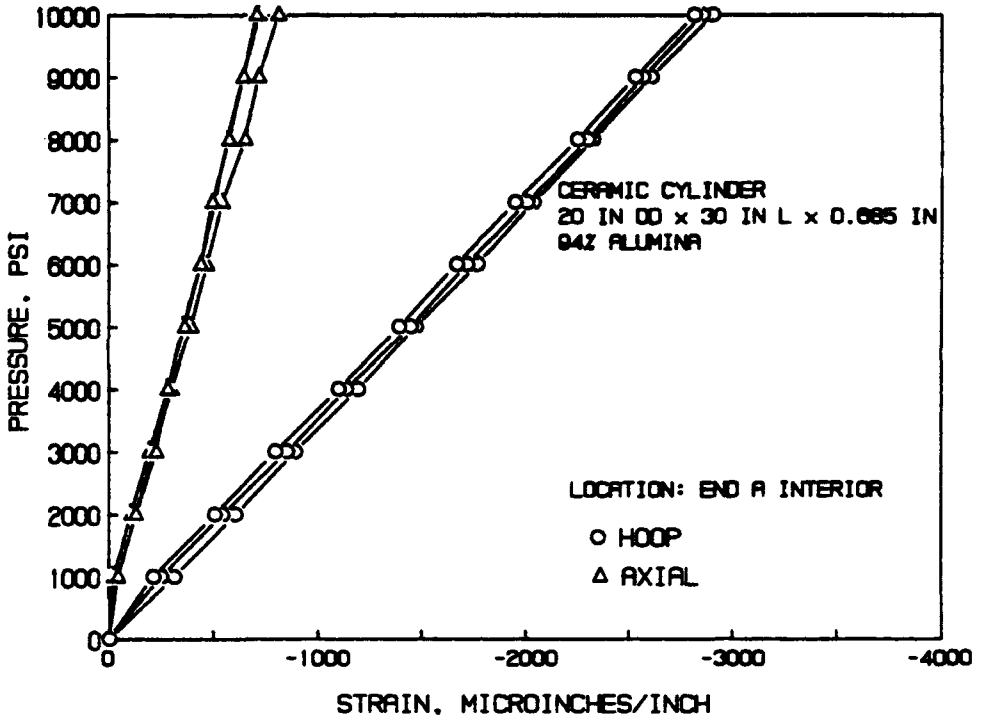

Figure A-1. Strain on cylinder A, end A.

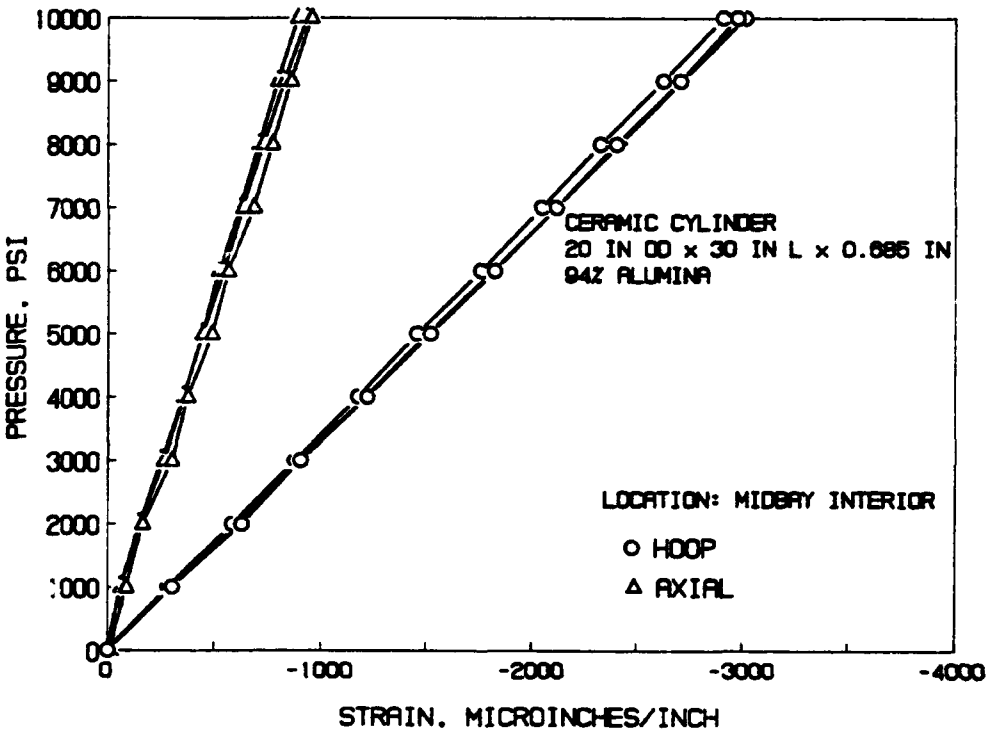

Figure A-2. Strain on cylinder A, midbay.

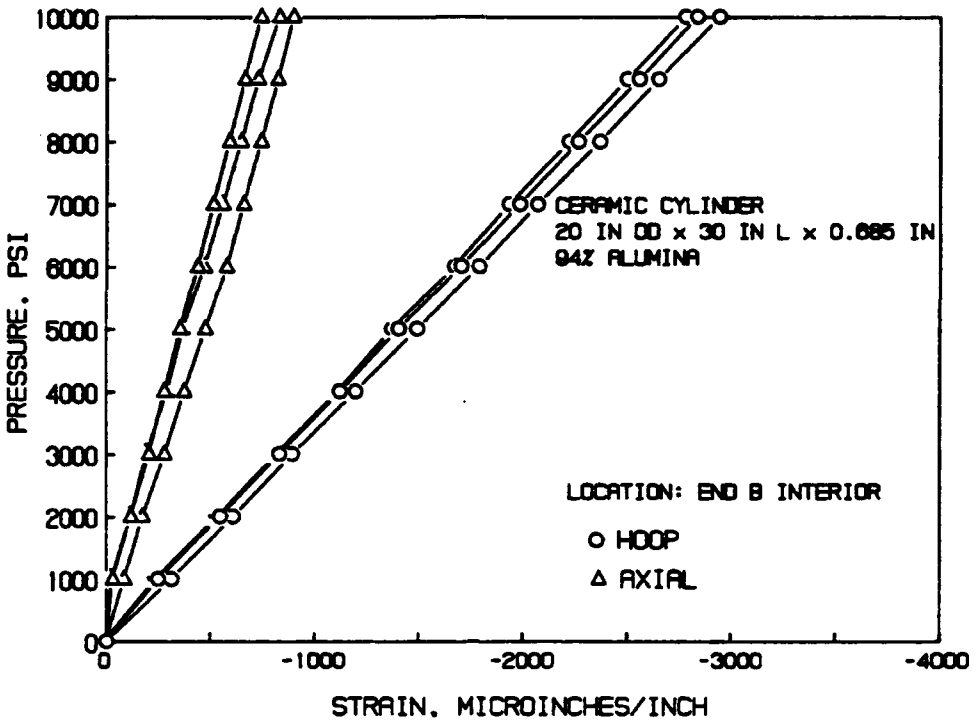

Figure A-3. Strain on cylinder A, end B.

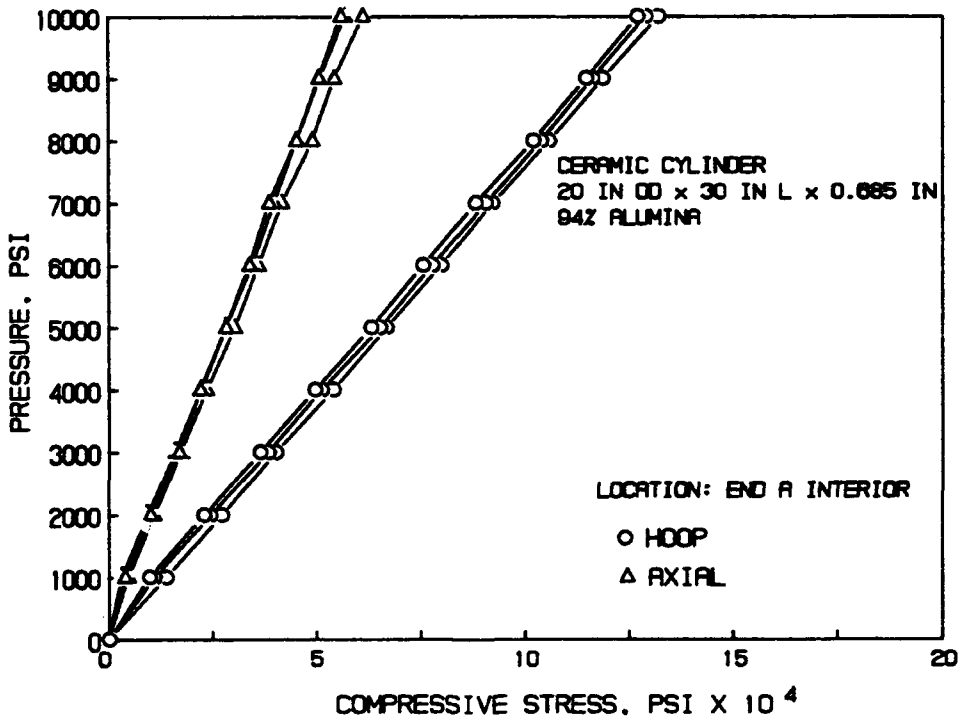

Figure A-4. Compressive stress on cylinder A, end A.

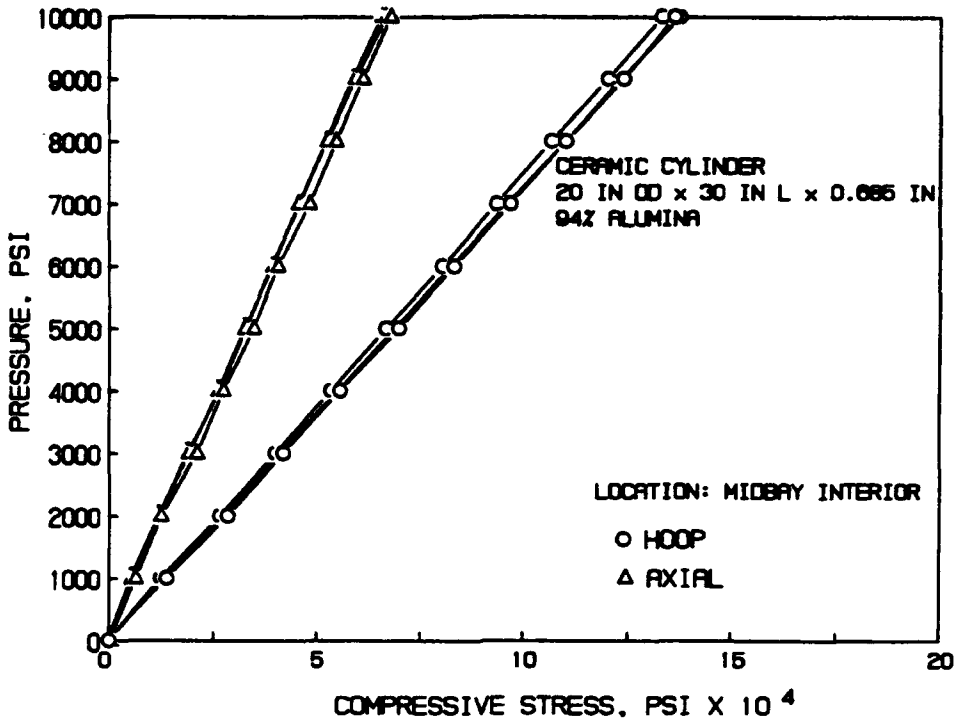

Figure A-5. Compressive stress on cylinder A, midbay.

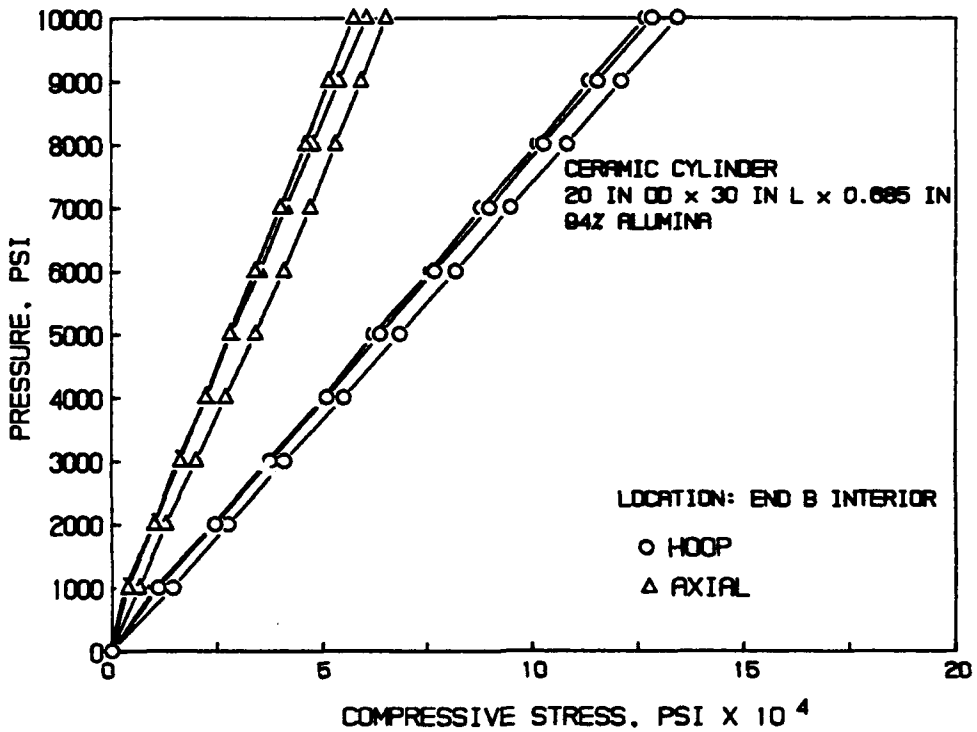

Figure A-6. Compressive stress on cylinder A, end B.

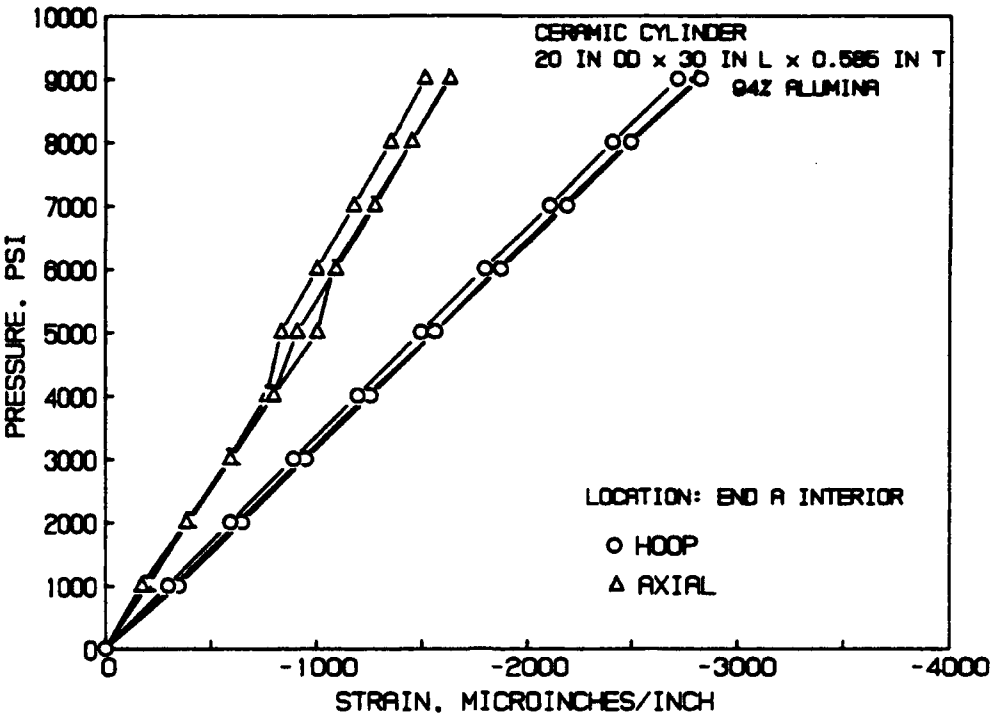

Figure A-7. Strain on cylinder B, end A.

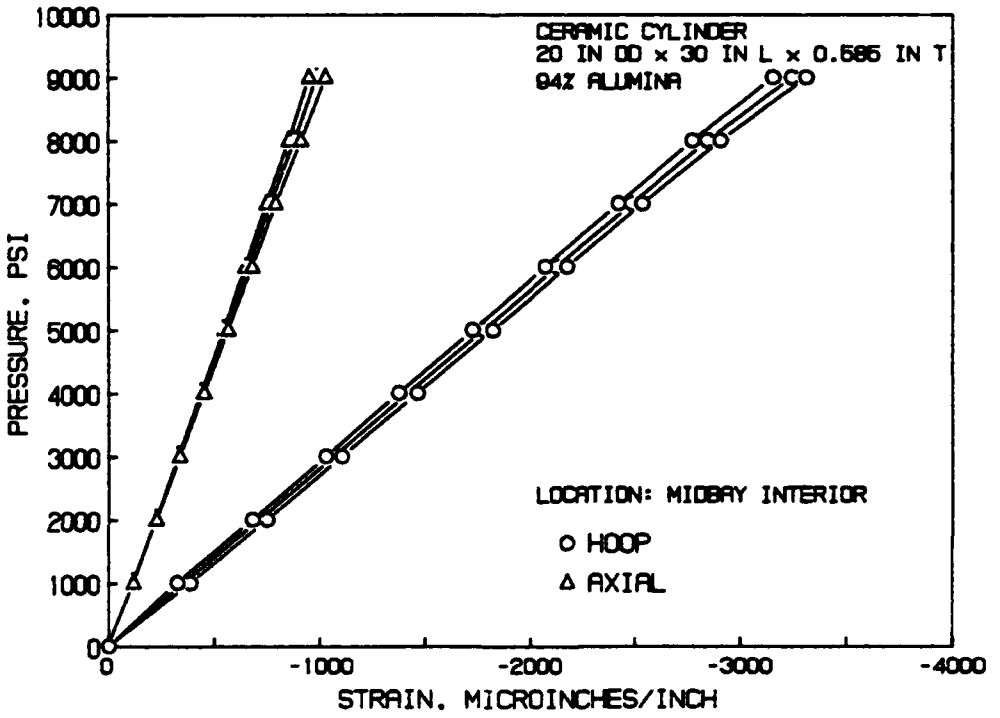

Figure A-8. Strain on cylinder B, midbay.

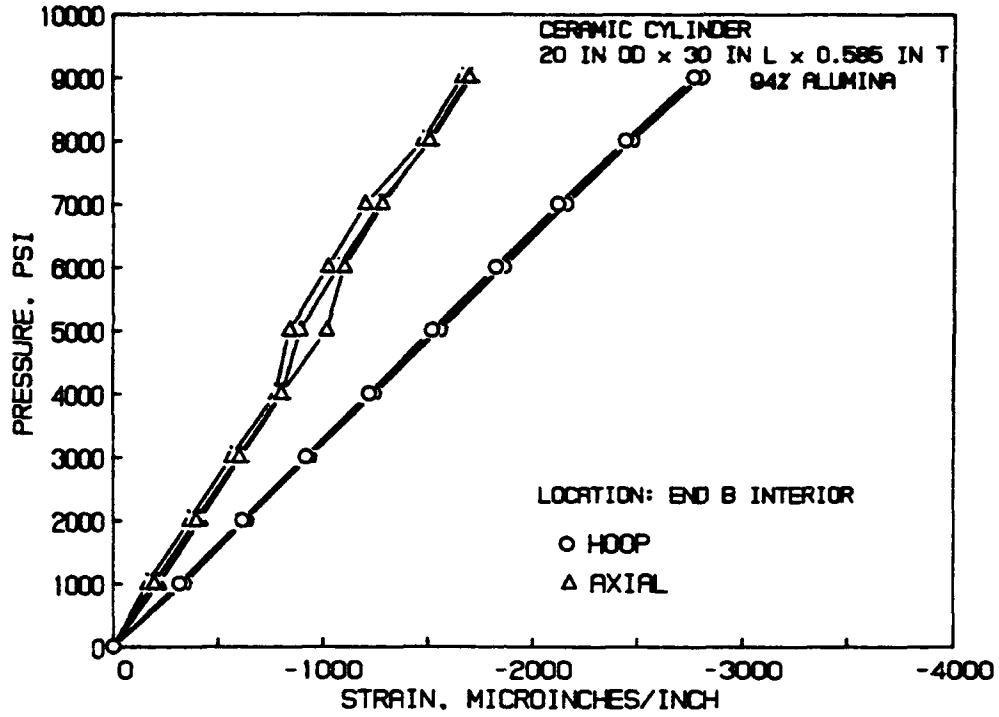

Figure A-9. Strain on cylinder B, end B.

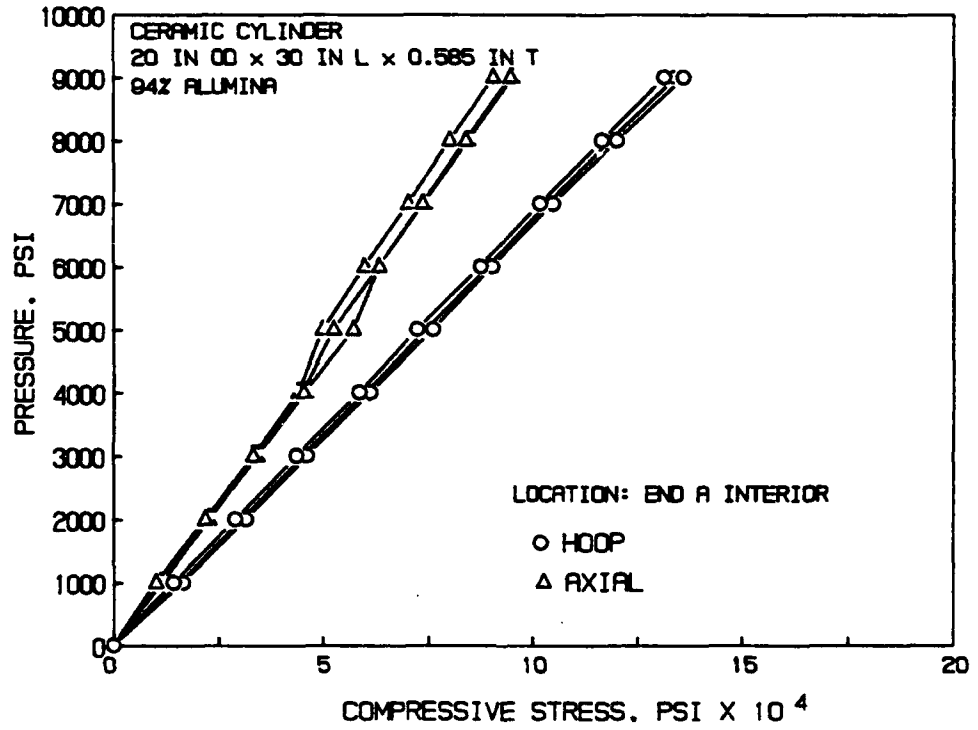

Figure A-10. Compressive stress on cylinder B, end A.

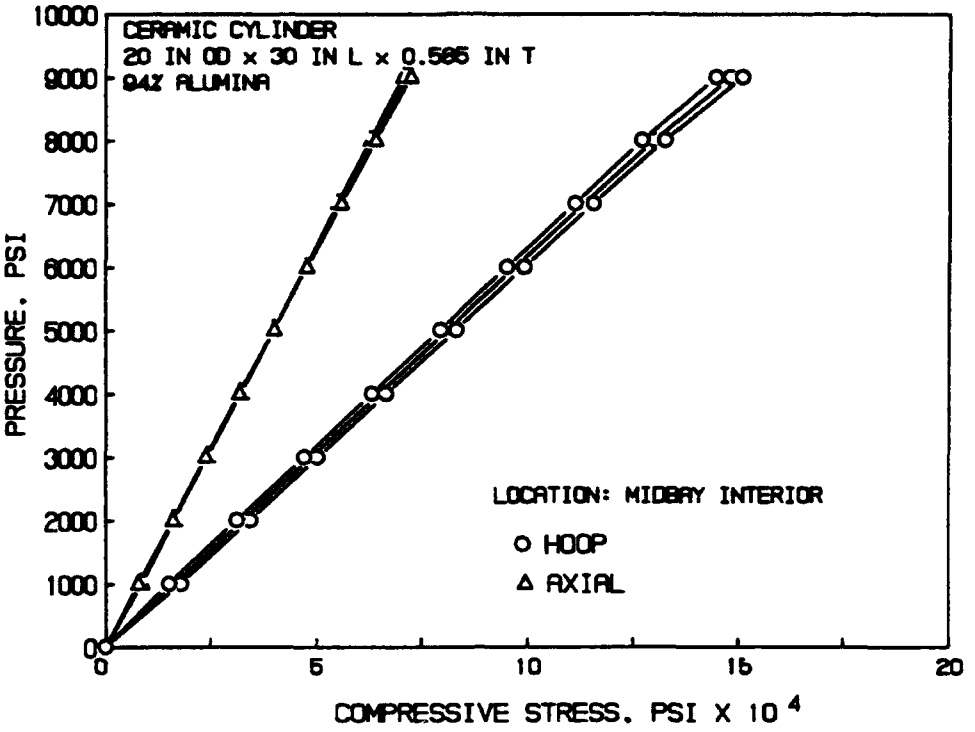

Figure A-11. Compressive stress on cylinder B, midbay.

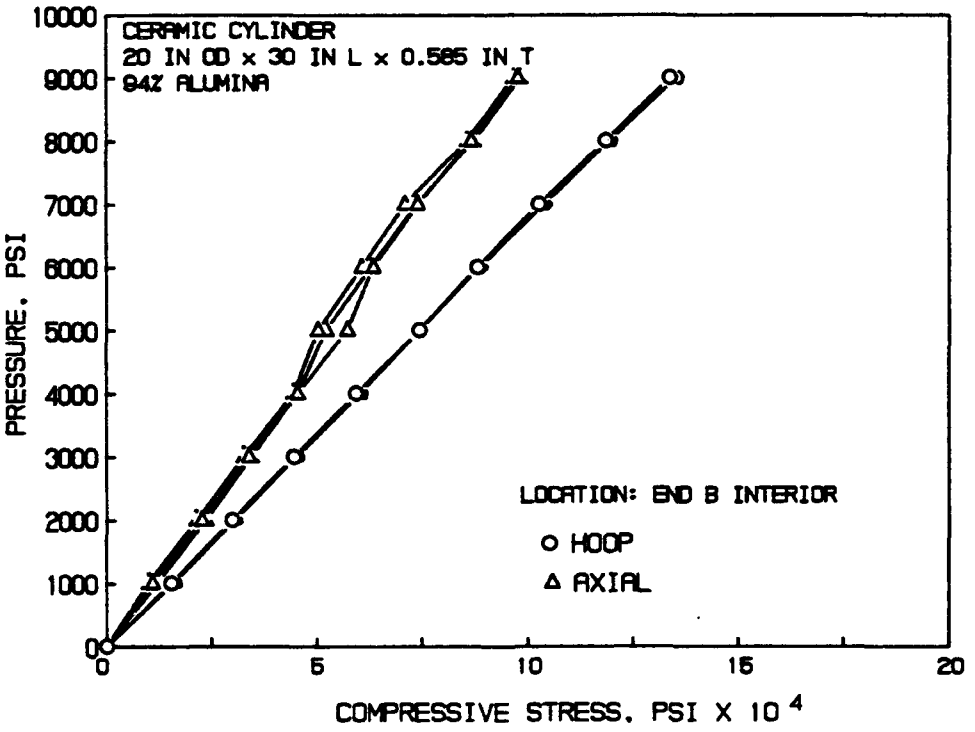

Figure A-12. Compressive stress on cylinder B, end B.

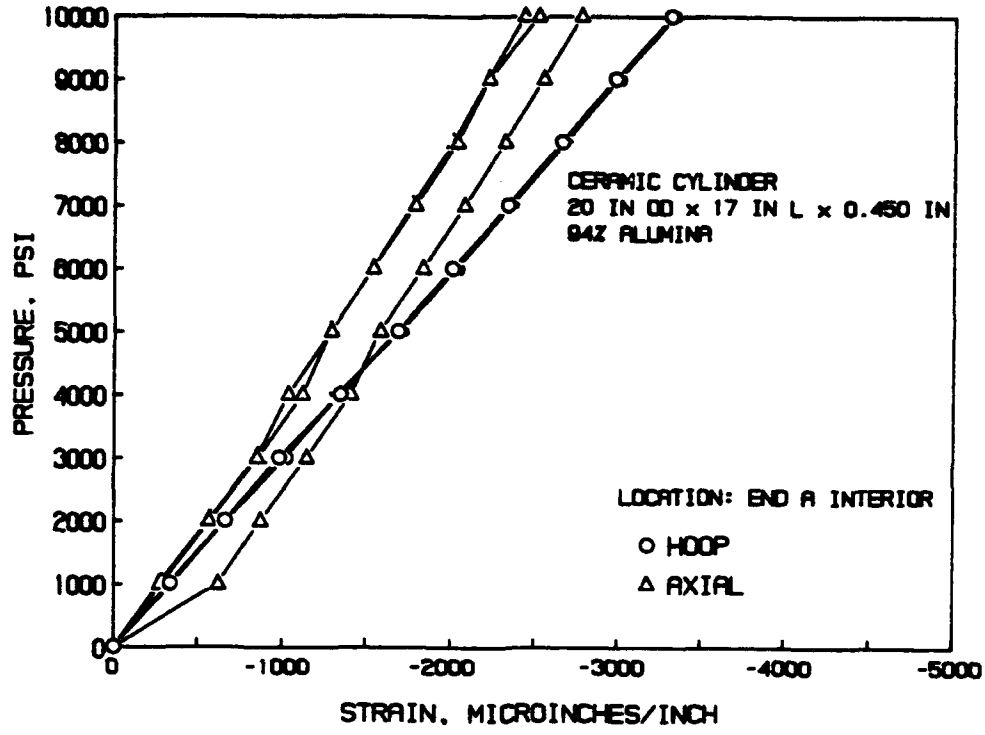

Figure A-13. Strain on cylinder C, end A.

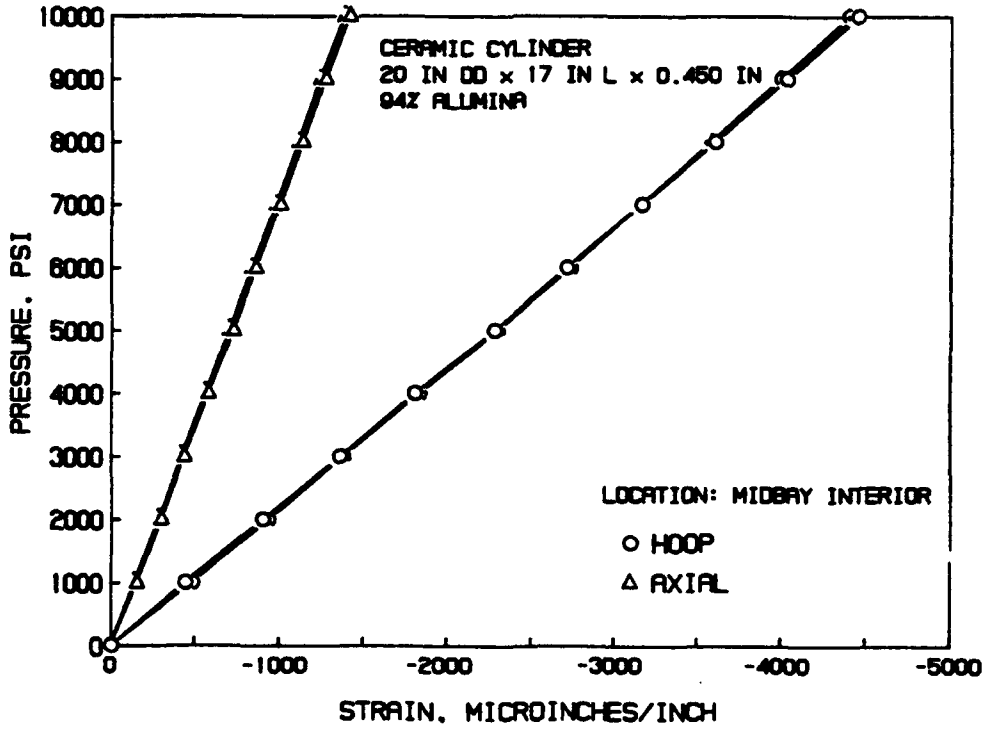

Figure A-14. Strain on cylinder C, midbay.

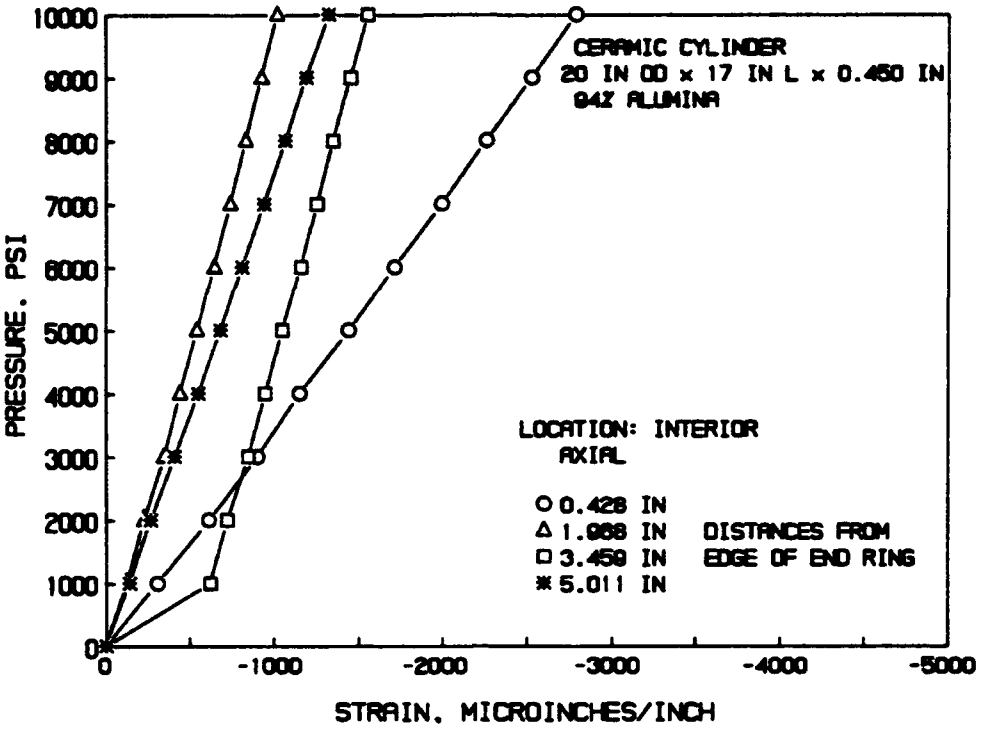

Figure A-15. Strain on cylinder C, axial.

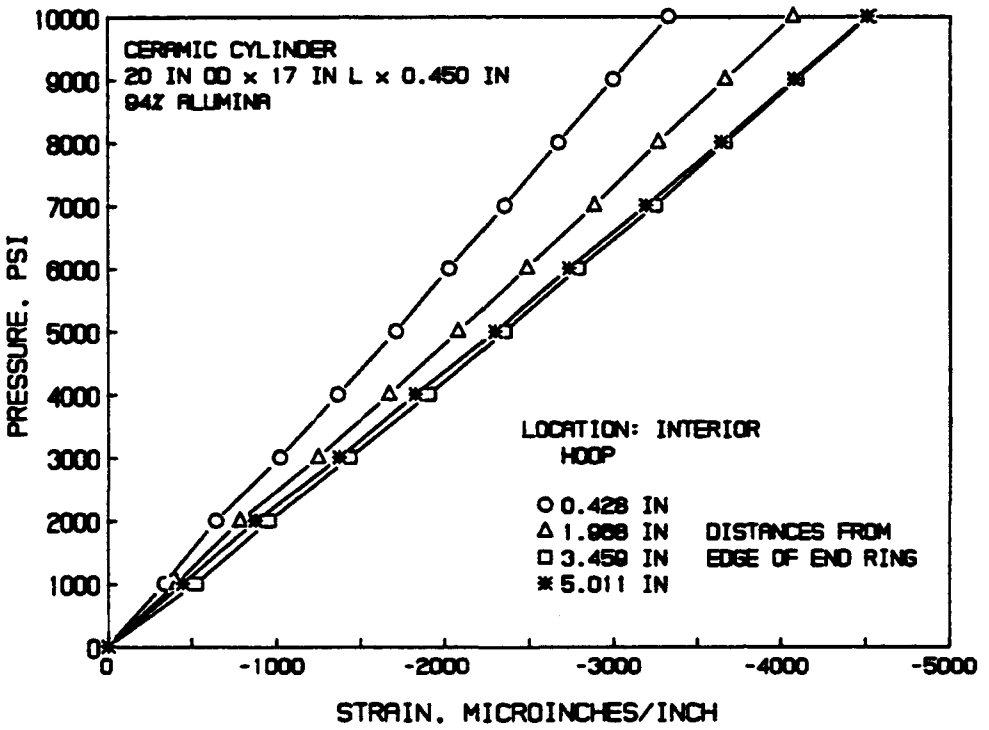

Figure A-16. Strain on cylinder C, hoop.

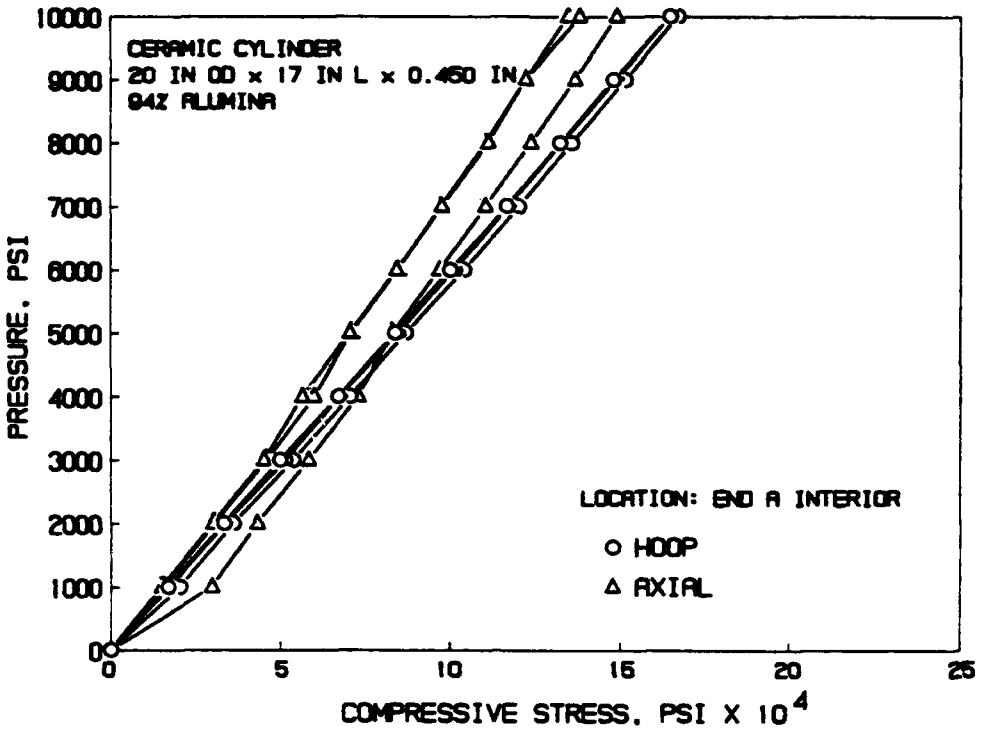

Figure A-17. Compressive stress on cylinder C, end A.

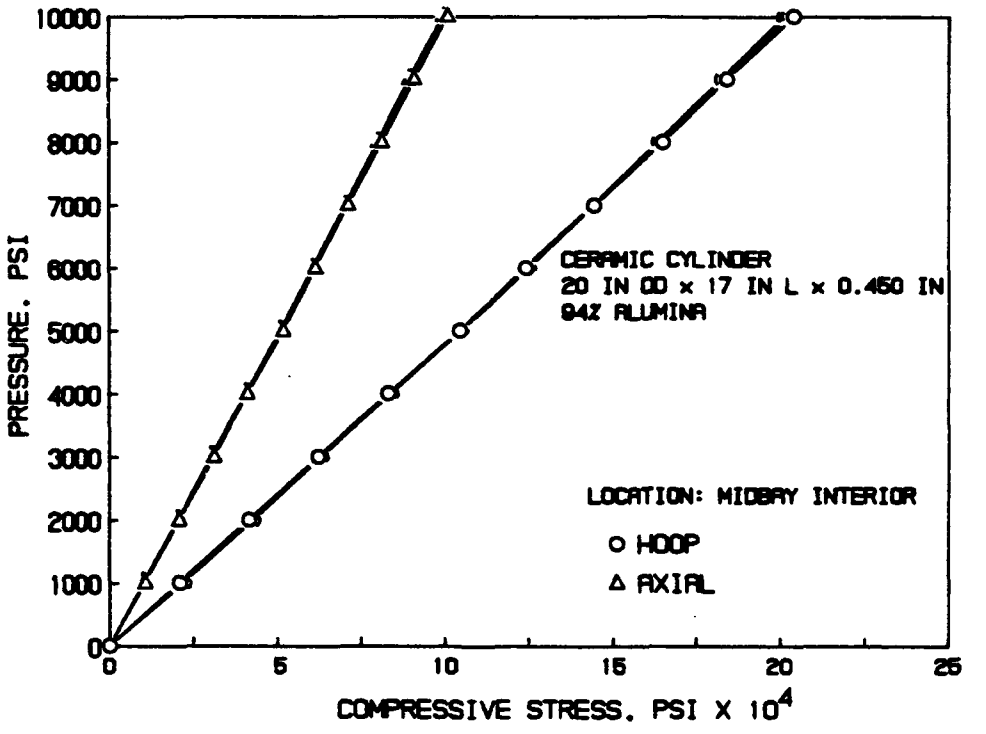

Figure A-18. Compressive stress on cylinder C, midbay.

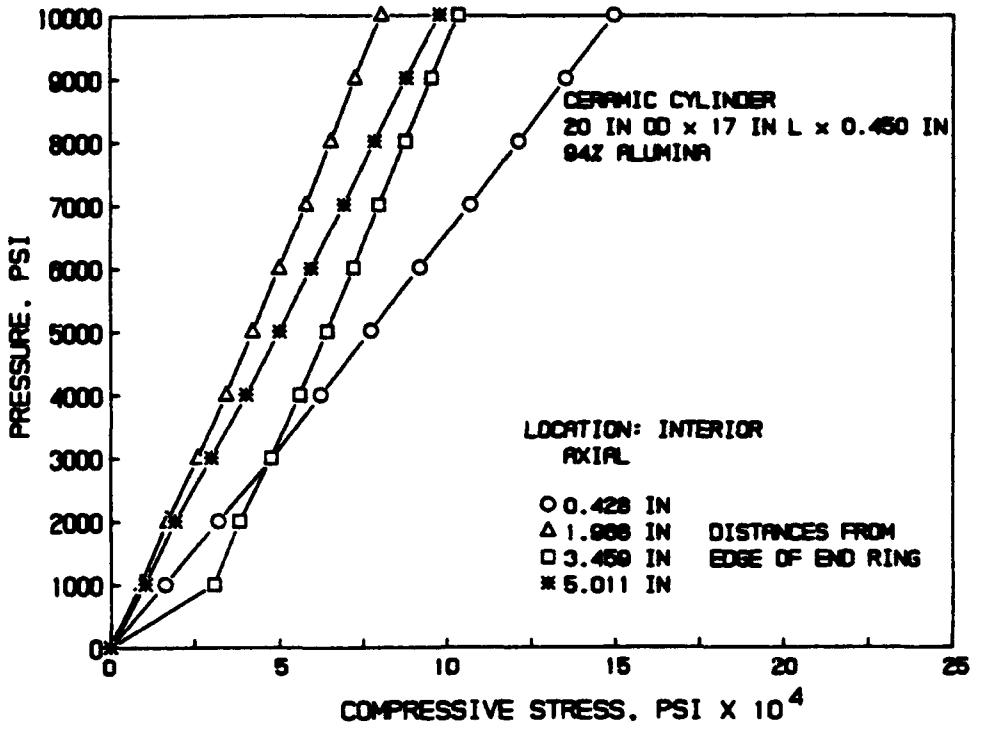

Figure A-19. Compressive stress on cylinder C, axial.

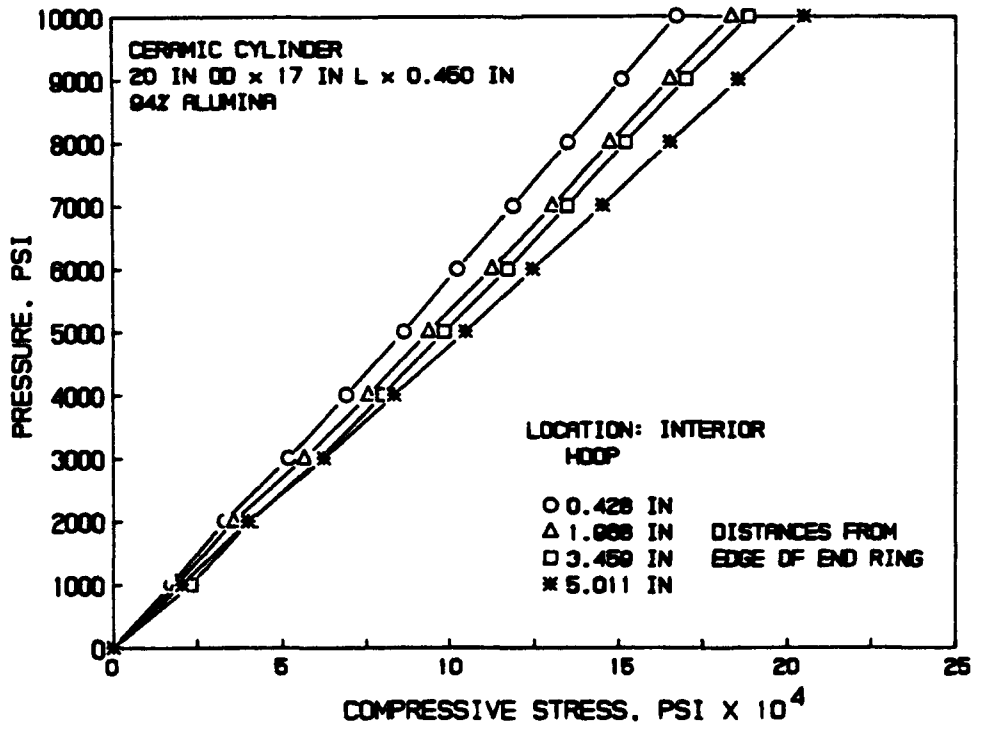

Figure A-20. Compressive stress on cylinder C, hoop.

Table A-1. Properties of alumina ceramics.

PROPERTIES*		UNITS	TEST	ALUMINA AD-85 Nom 85% Al_2O_3	AD-90 Nom 90% Al_2O_3	AD-94 Nom 94% Al_2O_3	AD-96 Nom 96% Al_2O_3	AD-99.5 Nom 99.5% Al_2O_3	AD-99.9% Nom 99.9% Al_2O_3
DENSITY		g/cc (#/cu. in.)	ASTM C20-83	3.41 (0.12)	3.6C (0.13)	3.70 (C.13)	3.72 (0.13)	3.89 (0.14)	3.96 (0.14)
SURFACE FINISH	AS-FIRED	MICROMETRES (MICROINCHES) CLA	PROFILOMETER (0.75mm cutoff)	1.6 (63)	1.6 (63)	1.6 (63)	1.6 (63)	0.9 (35)	0.5 (20)
	GROUND			1.0 (39)	0.5 (20)	1.3 (51)	1.3 (51)	0.5 (20)	0.9 (35)
	POLISHED			0.2 (8.0)	0.1 (3.9)	0.3 (12)	0.3 (12)	0.1 (3.9)	<0.03 (<1)
CRYSTAL SIZE	RANGE	MICROMETRES (MICROINCHES)	THIN SECTION	2-12 (79-473)	2-10 (79-394)	2-25 (79-985)	2-20 (79-788)	5-50 (197-1970)	1-6 (39-236)
	AVERAGE			6 (236)	4 (158)	12 (473)	11 (433)	17 (670)	3 (118)
WATER ABSORPTION		%	ASTM C373-72	0	0	0	0	0	0
GAS PERM.		—	"	0	0	0	0	0	0
COLOR		—	—	WHITE	WHITE	WHITE	WHITE	IVORY	IVORY
FLEXURAL STRENGTH (MOR)	20°C	MPa (psi x 10^3)	ASTM F417-78	317 (46)	338 (49)	352 (51)	358 (52)	379 (55)	552 (80)
ELASTIC MODULUS	20°C	GPa (psi x 10^6)	ASTM C848-78	221 (32)	276 (40)	296 (43)	303 (44)	372 (54)	386 (56)
SHEAR MODULUS		GPa (psi x 10^6)		96 (14)	117 (17)	117 (17)	124 (18)	152 (22)	158 (23)
BULK MODULUS		GPa (psi x 10^6)		138 (20)	158 (23)	165 (24)	172 (25)	228 (33)	228 (33)
TRANS. SONIC VEL.		m/sec. (ft/sec)		8.2 (27) x 10^3	8.8 (29) x 10^3	8.9 (29) x 10^3	9.1 (30) x 10^3	9.8 (32) x 10^3	9.9 (32) x 10^3
POISSON'S RATIO		—		0.22	0.22	0.21	0.2[illegible]	0.22	0.22
STIFFNESS/WEIGHT	20°C	GPa/g/cc	—	65	77	80	81	96	97
COMPRESSIVE STRENGTH	20°C	MPa (kpsi)	ASTM C773-82	1930 (280)	2482 (360)	2[illegible]03 (305)	2068 (300)	2620 (380)	3792 (550)
HARDNESS		GPa (kg/mm²)	—	9 (960)	10 (1058)	12 (1175)	11 (1088)	14 (1440)	15 (1551)
TENSILE STRENGTH	25	MPa (kpsi)	ACMA TEST #4	155 (22)	221 (32)	193 (28)	193 (28)	262 (38)	310 (45)
	1000°C			— (—)	103 (15)	103 (15)	96 (14)	— (—)	221 (32)
FRACTURE TOUGHNESS	K_{Ic}	MPa-m½	NOTCHED BEAM TEST	3-4	3-4	3-4	3-4	3-4	3-4
THERMAL CONDUCTIVITY	20°C	W/m°K (Btu-in/ft²-h-°F)	ASTM C408-82	16.0 (111)	16.7 (116)	22.4 (155)	24.7 (172)	35.6 (247)	38.9 (270)
COEFFICIENT OF THERMAL EXPANSION	25-1000°C	10-6/°C (10-6/°F)	ASTM C372-81	7.2 (4.0)	8.1 (4.5)	8.2 (4.6)	8.2 (4.6)	8.0 (4.6)	8.0 (4.5)
SPECIFIC HEAT	100°C	J/kg-°K (cal/g-°C)	ASTM C351-82	920 (0.22)	920 (0.22)	880 (0.21)	880 (0.21)	880 (0.21)	880 (0.21)
THERMAL SHOCK RESISTANCE	ΔTc	°C (°F)	—	300 (570)	300 (570)	300 (570)	250 (480)	200 (392)	200 (392)
MAXIMUM USE TEMPERATURE		°C (°F)	No-load conds.	1400 (2552)	1500 (2732)	[illegible]700 (3092)	1700 (3092)	[illegible]750 (3182)	[illegible]900 (3452)
DIELECTRIC STRENGTH	6.35mm	ac-kv/mm (ac-volts/mil)	ASTM-D116-76	9.4 (240)	9.2 (235)	8.7 (220)	8.3 (210)	8.7 (220)	9.4 (240)
	3.18mm			13.4 (340)	12.6 (320)	11.8 (300)	10.8 (275)	11.4 (290)	12.8 (325)
	1.27mm SPEC.			17.3 (440)	17.7 (450)	16.7 (425)	14.6 (370)	16.9 (430)	18.1 (460)
	0.64mm THICK.			21.6 (550)	22.8 (580)	21.6 (550)	17.7 (450)	22.8 (580)	23.2 (590)
	0.25mm			28.3 (720)	29.9 (760)	28.3 (720)	22.8 (580)	33.1 (840)	31.5 (800)
DIELECTRIC CONSTANT	1 kHz	25°C	ASTM D150-81	8.2	8.8	9.1	9.0	9.8	9.9
	1 MHz		ASTM D2520-81	8.2	8.8	9.1	9.0	9.7	9.8
	1 GHz			8.2	8.8	9.1	9.0	9.7	—
DISSIPATION FACTOR	1 kHz	25°C	ASTM D150-81	0.0014	0.0006	0.0007	0.0011	0.0002	0.0020
	1 MHz		ASTM D2520-81	0.0009	0.0004	0.0004	0.0001	0.0003	0.0002
	1 GHz			0.0014	0.0007	0.0010	0.0002	0.0002	—
LOSS INDEX	1 kHz	25°C	ASTM D150-81	0.011	0.005	0.007	0.010	0.002	0.020
	1 MHz		ASTM D2520-81	0.007	0.004	0.004	0.001	0.003	0.002
	1 GHz			0.010	0.005	0.009	0.002	0.002	—
VOLUME RESISTIVITY	25°C	ohm-cm²/cm	ASTM D1829-66	>10^{14}	>10^{14}	10^{14}	>10^{14}	>10^{14}	>10^{14}
	300°C			4.6 x 10^{10}	1.4 x 10^{11}	1.2 x 10^{11}	3.1 x 10^{11}	—	>10^{14}
	500°C			4.0 x 10^8	2.8 x 10^8	4.8 x 10^8	4.0 x 10^9	—	3.3 x 10^{12}
	700°C			7.0 x 10^6	7.0 x 10^6	2.1 x 10^7	1.0 x 10^8	—	9.0 x 10^9
	1000°C			—	8.5 x 10^5	5.0 x 10^5	1.0 x 10^6	—	1.1 x 10^7
Te VALUE		°C(°F)	TEMP AT WHICH RESISTIVITY IS 1 MEGOHM-CM	850 (1562)	960 (1760)	950 (1742)	1000 (1832)	—	1170 (2138)
CORROSION RESISTANCE	WEIGHT LOSS	mg/cm²/day	95% H_2SO_4 @20°C – NOTE 3	0.04	0.03	—	—	0.01	0.01
			95% H_2SO_4 @100°C – NOTE 3	1.0	0.5	—	—	0.1	0.1
IMPINGEMENT		—	NOTE 4	1.00	0.45	0.52	0.63	0.47	0.14
RUBBING		—	NOTE 4	1.00	0.36	—	0.75	—	0.55

Table A-2. Strains on cylinder A, Sheet 1.

Strains on Ceramic Cylinder 20 in OD x 30 in L x 0.685 in T
under Short Term Pressurization

Gage Locations

	Interior End A						Interior Midbay					
Pressure	1		2		3		4		5		6	
(Psi)	Hoop	Axial	Hoop	Axial	Hoop	Axial	Hoop	Axial	Hoop	Axial	Hoop	Axial
0	-11	0	0	0	0	0	11	-11	0	0	0	0
1000	-215	-43	-251	-22	-314	-43	-302	-87	-282	-65	-303	-65
2000	-506	-129	-545	-108	-607	-129	-625	-162	-585	-153	-607	-153
3000	-797	-225	-850	-194	-888	-214	-905	-303	-877	-261	-899	-251
4000	-1099	-279	-1133	-280	-1192	-300	-1217	-379	-1170	-359	-1213	-359
5000	-1390	-364	-1449	-356	-1473	-396	-1519	-487	-1452	-447	-1506	-447
6000	-1670	-439	-1721	-442	-1766	-471	-1821	-563	-1755	-545	-1809	-523
7000	-1950	-493	-2004	-506	-2037	-546	-2112	-682	-2047	-632	-2112	-621
8000	-2252	-579	-2298	-571	-2329	-654	-2402	-769	-2329	-730	-2416	-708
9000	-2532	-643	-2571	-646	-2611	-718	-2704	-856	-2622	-828	-2708	-795
10000	-2812	-707	-2854	-722	-2903	-814	-2973	-953	-2903	-937	-3012	-893
10000	-2812	-696	-2865	-711	-2903	-814	-2995	-964	-2882	-915	-2990	-861
0	22	21	22	11	0	21	22	0	87	87	65	76

NOTES: Specimen imploded after 453 cycles to 9000 psi
All strains are in microinches per inch
Electric resistance strain gages are CEA-06-125WT-350, Gage Factor 2.09
Ceramic Composition: 94 percent Alumina Ceramic
End Closures: Steel Hemispheres

Table A-2. Strains on cylinder A, Sheet 2.

Strains on Ceramic Cylinder 20 in OD x 30 in L x 0.685 in T
under Short Term Pressurization

Gage Locations

	Interior End B					
Pressure	7		8		9	
(Psi)	Hoop	Axial	Hoop	Axial	Hoop	Axial
0	0	0	11	0	-11	-11
1000	-251	-33	-240	-22	-316	-87
2000	-545	-120	-534	-120	-610	-173
3000	-828	-207	-817	-196	-893	-282
4000	-1122	-283	-1111	-294	-1198	-379
5000	-1405	-359	-1373	-370	-1492	-477
6000	-1699	-436	-1667	-468	-1786	-574
7000	-1983	-512	-1928	-556	-2070	-661
8000	-2266	-588	-2222	-643	-2364	-737
9000	-2549	-664	-2495	-730	-2647	-823
10000	-2832	-741	-2778	-828	-2941	-89[illegible]
10000	-2810	-708	-2756	-795	-2941	-856
0	76	87	76	87	-22	11

NOTES: Specimen imploded after 453 cycles to 9000 psi
All strains are in microinches per inch
Electric resistance strain gages are CEA-06-125WT-350,
Gage Factor 2.09
Ceramic Composition: 94 percent Alumina Ceramic
End Closures: Steel Hemispheres

Table A-3. Stresses on cylinder A, Sheet 1.

Stresses on Ceramic Cylinder 20 in OD x 30 in L x 0.685 in T
under Short Term Pressurization

Gage Locations

		<---------- Interior End A ----------						<---------- Interior Midbay ----------					
Pressure	1		2		3		4		5		6	
(Psi)	Hoop	Axial	Hoop	Axial	Hoop	Axial	Hoop	Axial	Hoop	Axial	Hoop	Axial
0	-472	-99	0	0	0	0	373	-373	0	0	0	0
1000	-9609	-3781	-10964	-3204	-13855	-4673	-13737	-6452	-12681	-5328	-13582	-5517
2000	-22865	-10091	-24349	-9541	-27197	-11001	-28267	-12578	-26470	-11832	-27414	-12030
3000	-36212	-16830	-38206	-15977	-40016	-17177	-41546	-21148	-39967	-19094	-40821	-18863
4000	-49651	-21866	-51119	-22215	-53829	-23604	-55613	-27218	-53417	-25937	-55262	-26324
5000	-62899	-28133	-65357	-28321	-66747	-30253	-69540	-34571	-66305	-32251	-68622	-32738
6000	-75584	-33872	-77798	-34460	-79990	-36109	-83177	-40551	-80184	-39184	-82302	-38727
7000	-88080	-38710	-90513	-39754	-92289	-41767	-96731	-48276	-93493	-45546	-96181	-45659
8000	-101808	-45119	-103709	-45190	-105786	-49029	-109953	-54620	-106471	-52289	-110004	-52129
9000	-114394	-50386	-116094	-50866	-118458	-54315	-123690	-61071	-119921	-59132	-123312	-58491
10000	-126980	-55653	-128917	-56675	-131847	-61062	-136102	-67655	-132955	-66338	-137234	-65433
10000	-126881	-55181	-129290	-56302	-131847	-61062	-137145	-68325	-131856	-65205	-136002	-63862
0	1133	1099	1043	670	189	901	944	198	4515	4515	3473	3845

NOTES: Specimen imploded after 453 cycles to 9000 psi
All stresses are in pounds per square inch
Ceramic Composition: 94 percent Alumina Ceramic
Material Properties: Poisson's Ratio 0.21, Modulus of Elasticity 41,000,000
End Closures: Steel Hemispheres

Table A-3. Stresses on cylinder A, Sheet 2.

Stresses on Ceramic Cylinder 20 in OD x 30 in L x 0.685 in T
under Short Term Pressurization

Gage Locations

		<---------- Interior End B ----------				
Pressure	7		8		9	
(Psi)	Hoop	Axial	Hoop	Axial	Hoop	Axial
0	0	0	0	0	0	0
1000	-11063	-3676	-10492	-3105	-14338	-6578
2000	-24457	-10056	-23985	-9957	-27722	-12915
3000	-37379	-16337	-36808	-15766	-40843	-20139
4000	-50674	-22245	-50301	-22617	-54798	-27047
5000	-63497	-28054	-62223	-28237	-68291	-33898
6000	-76801	-34004	-75716	-35089	-81775	-40707
7000	-89667	-39822	-87704	-41214	-94740	-46997
8000	-102490	-45631	-101098	-47594	-108035	-52905
9000	-115313	-51440	-113591	-53784	-120948	-59142
10000	-128145	-57292	-126612	-60537	-134243	-65050
10000	-126904	-55678	-125371	-58923	-133856	-63206
0	4043	4416	4043	4416	-845	274

NOTES: Specimen imploded after 453 cycles to 9000 psi
All stresses are in pounds per square inch
Ceramic Composition: 94 percent Alumina Ceramic
Material Properties: Poisson's Ratio 0.21,

Table A-4. Strains on cylinder B, Sheet 1.

Strains on Ceramic Cylinder 20 in OD x 30 in L x 0.585 in T
under Short Term Pressurization

Gage Locations

|<---------- Interior End A ----------->|<---------- Interior Midbay ---------->|

Pressure	1		2		3		4		5		6	
(Psi)	Hoop	Axial	Hoop	Axial	Hoop	Axial	Hoop	Axial	Hoop	Axial	Hoop	Axial
0	0	0	0	0	0	0	0	0	0	0	0	0
1000	-294	-172	-343	-189	-324	-202	-329	-117	-391	-122	-359	-121
2000	-590	-381	-645	-392	-627	-391	-677	-227	-746	-227	-709	-228
3000	-890	-591	-949	-594	-933	-580	-1027	-339	-1103	-333	-1064	-337
4000	-1190	-799	-1252	-794	-1234	-766	-1375	-451	-1458	-438	-1416	-445
5000	-1493	-907	-1558	-1006	-1560	-832	-1727	-566	-1820	-544	-1773	-554
6000	-1801	-1088	-1874	-1077	-1862	-1000	-2071	-678	-2174	-647	-2123	-661
7000	-2101	-1271	-2179	-1263	-2166	-1174	-2420	-793	-2536	-748	-2480	-768
8000	-2404	-1448	-2490	-1446	-2475	-1345	-2771	-909	-2903	-851	-2841	-877
9000	-2714	-1631	-2824	-1625	-2806	-1512	-3155	-1028	-3313	-948	-3241	-983
10000												

NOTES: Specimen imploded at 9700 psi
All strains are in microinches per inch
Electric resistance strain gages are CEA-06-125WT-350, Gage Factor 2.09
Ceramic Composition: 94 percent Alumina Ceramic
End Closures: Titanium Hemispheres

Table A-4. Strains on cylinder B, Sheet 2.

Strains on Ceramic Cylinder 20 in OD x 30 in L x 0.585 in T
under Short Term Pressurization

Gage Locations

Aluminum
|<---------- Interior End B ---------->|<---- End Cap --->|

Pressure	7		8		9		10	
(Psi)	Hoop	Axial	Hoop	Axial	Hoop	Axial	Hoop	Axial
0	0	0	0	0	0	0	0	0
1000	-316	-192	-336	-160	-322	-218	-262	35
2000	-614	-397	-635	-363	-622	-414	-563	58
3000	-914	-600	-937	-566	-924	-608	-865	69
4000	-1214	-805	-1242	-778	-1225	-806	-1164	74
5000	-1516	-1015	-1555	-840	-1541	-892	-1472	506
6000	-1821	-1096	-1853	-1019	-1845	-1074	-1771	608
7000	-2122	-1282	-2157	-1197	-2150	-1267	-2072	710
8000	-2440	-1503	-2471	-1475	-2462	-1512	-2361	803
9000	-2762	-1690	-2803	-1663	-2792	-1703	-2663	903
10000								

NOTES: Specimen imploded at 9700 psi
All strains are in microinches per inch
Electric resistance strain gages are CEA-06-125WT-350, Gage Factor 2.09
Ceramic Composition: 94 percent Alumina Ceramic
End Closures: Titanium Hemispheres

Table A-5. Stresses on cylinder B, Sheet 1.

Stresses on Ceramic Cylinder 20 in OD x 30 in L x 0.585 in T
under Short Term Pressurization

Gage Locations

		<---------- Interior End A ----------->	<---------- Interior Midbay ---------->				
Pressure	1		2		3		4		5		6	
(Psi)	Hoop	Axial	Hoop	Axial	Hoop	Axial	Hoop	Axial	Hoop	Axial	Hoop	Axial
0	0	0	0	0	0	0	0	0	0	0	0	0
1000	-14160	-10026	-16414	-11196	-15716	-11583	-15165	-7982	-17870	-8755	-16488	-8424
2000	-28738	-21656	-31196	-22623	-30415	-22418	-31083	-15834	-34042	-16456	-32464	-16166
3000	-43497	-33366	-46055	-34026	-45242	-33281	-47104	-23791	-50309	-24218	-48673	-24038
4000	-58238	-44989	-60853	-45333	-59828	-43970	-63039	-31729	-66482	-31919	-64743	-31841
5000	-72207	-52351	-75887	-57183	-74406	-49738	-79173	-39833	-82963	-39727	-81038	-39732
6000	-87048	-62889	-90080	-63074	-88872	-59664	-94936	-47735	-99075	-47333	-97014	-47474
7000	-101564	-73440	-104838	-73800	-103479	-69865	-110941	-55811	-115512	-54926	-113290	-55279
8000	-116155	-83761	-119826	-84450	-118273	-79983	-127041	-63948	-132181	-62649	-129756	-63206
9000	-131100	-94403	-135764	-95136	-133974	-90127	-144584	-72511	-150640	-70503	-147867	-71356
10000												

NOTES: Specimen imploded at 9700 psi
All stresses are in pounds per square inch
Ceramic Composition: 94 percent Alumina Ceramic
Material Properties: Poisson's Ratio 0.21, Modulus of Elasticity 41,000,000
End Closures: Titanium Hemispheres

Table A-5. Stresses on cylinder B, Sheet 2.

Stresses on Ceramic Cylinder 20 in OD x 30 in L x 0.585 in T
under Short Term Pressurization

Gage Locations

		<---------- Interior End B ---------->	Aluminum	<---- End Cap ---->		
Pressure	7		8		9		10	
(Psi)	Hoop	Axial	Hoop	Axial	Hoop	Axial	Hoop	Axial
0	0	0	0	0	0	0	0	0
1000	-15283	-11082	-15853	-9889	-15775	-12251	-2828	-611
2000	-29912	-22559	-30506	-21289	-30408	-23360	-6143	-1509
3000	-44608	-33968	-45288	-32717	-45109	-34401	-9515	-2545
4000	-59322	-45463	-60280	-44557	-59803	-45605	-12877	-3638
5000	-74167	-57190	-74263	-50036	-74131	-52140	-14699	62
6000	-87978	-63412	-88657	-60398	-88810	-62685	-17687	66
7000	-102564	-74101	-103300	-70771	-103630	-73710	-20699	62
8000	-118194	-86445	-119272	-85523	-119219	-87029	-23609	3
9000	-133690	-97366	-135205	-96577	-135094	-98194	-26639	-27

NOTES: Specimen imploded at 9700 psi
All stresses are in pounds per square inch
Ceramic Composition: 94 percent Alumina Ceramic
Material Properties: Ceramic: Poisson's Ratio 0.21,
Modulus of Elasticity 41,000,000
Aluminum Bearing Ring: Poisson's Ratio 0.34,
Modulus of Elasticity 10,000,000
End Closures: Titanium Hemispheres

Table A-6. Strains on cylinder C, Sheet 1.

Strains on Ceramic Cylinder 20 in OD x 17 in L x 0.450 in T
under Short Term Pressurization

Gage Locations

		<---------- Interior End A ----------						<---------- Interior Midbay ----------					
Pressure	D		E		F		A		B		C	
(Psi)	Hoop	Axial	Hoop	Axial	Hoop	Axial	Hoop	Axial	Hoop	Axial	Hoop	Axial
0	0	0	0	0	0	0	0	0	0	0	0	0
1000	-337	-272	-344	-293	-349	-622	-448	-157	-482	-142	-463	-142
2000	-656	-564	-670	-569	-660	-866	-902	-297	-934	-280	-916	-280
3000	-983	-847	-1017	-857	-1014	-1145	-1360	-438	-1383	-421	-1371	-420
4000	-1345	-1036	-1336	-1121	-1349	-1412	-1810	-583	-1836	-562	-1829	-562
5000	-1685	-1295	-1698	-1296	-1694	-1583	-2275	-726	-2287	-704	-2279	-706
6000	-2007	-1540	-2032	-1543	-2032	-1833	-2712	-863	-2734	-842	-2711	-845
7000	-2335	-1789	-2350	-1769	-2355	-2077	-3156	-1001	-3153	-980	-3148	-983
8000	-2656	-2032	-2671	-2006	-2677	-2315	-3595	-1138	-3578	-1114	-3570	-1119
9000	-2979	-2214	-2994	-2213	-2994	-2548	-4025	-1277	-4000	-1246	-3990	-1257
10000	-3307	-2517	-3324	-2432	-3311	-2776	-4454	-1416	-4424	-1387	-4395	-1395
0	37	14	33	15	41	-475	49	-1	66	-1	83	-9
10000	-3373	-2486	-3381	-2418	-3353	-2793	-4506	-1425	-4485	-1396	-4493	-1406
0	-4	-3	-2	-4	0	-504	-4	-8	0	-6	0	-12

NOTES: Specimen was subsequently cycled 50 times to 9000 psi without initiation of cracks
All strains are in microinches per inch
Electric resistance strain gages are CEA-06-125WT-350, Gage Factor 2.12
Ceramic Composition: 94 percent Alumina Ceramic
End Closures: Steel Hemispheres

Table A-6. Strains on cylinder C, Sheet 2.

Strains on Ceramic Cylinder 20 in OD x 17 in L x 0.450 in T
under Short Term Pressurization

Gage Locations

	|<---------- From Interior Midbay to End B ----------|						
Pressure	G		H		I		J	
(Psi)	Hoop	Axial	Hoop	Axial	Hoop	Axial	Hoop	Axial
0	0	0	0	0	0	0	0	0
1000	-448	-144	-524	-623	-408	-124	-338	-308
2000	-879	-267	-956	-721	-787	-229	-642	-608
3000	-1368	-411	-1436	-843	-1245	-346	-1020	-903
4000	-1828	-546	-1904	-950	-1667	-442	-1364	-1154
5000	-2298	-682	-2349	-1054	-2074	-542	-1705	-1440
6000	-2738	-808	-2791	-1156	-2485	-642	-2025	-1710
7000	-3191	-938	-3241	-1251	-2884	-738	-2350	-1988
8000	-3635	-1066	-3661	-1349	-3263	-828	-2671	-2259
9000	-4072	-1195	-4090	-1449	-3662	-923	-2991	-2520
10000	-4503	-1327	-4517	-1553	-4064	-1020	-3321	-2779
0	33	0	-64	-501	39	-2	6	-7
10000	-4534	-1333	-4462	-1559	-4105	-1010	-3322	-2719
0	-1	-5	-12	-506	-2	-7	-4	-6

NOTES: Specimen was subsequently cycled 50 times to 9000 psi without initiation of cracks
All strains are in microinches per inch
Electric resistance strain gages are CEA-06-125WT-350, Gage Factor 2.12
Ceramic Composition: 94 percent Alumina Ceramic
End Closures: Steel Hemispheres

Table A-7. Stresses on cylinder C, Sheet 1.

Stresses on Ceramic Cylinder 20 in OD x 17 in L x 0.450 in T
under Short Term Pressurization

Gage Locations

		<---------- Interior End A ----------						<---------- Interior Midbay ----------					
Pressure	D		E		F		A		B		C	
(Psi)	Hoop	Axial	Hoop	Axial	Hoop	Axial	Hoop	Axial	Hoop	Axial	Hoop	Axial
0	0	0	0	0	0	0	0	0	0	0	0	0
1000	-16905	-14702	-17394	-15666	-20572	-29822	-20630	-10769	-21953	-10432	-21138	-10261
2000	-33217	-30100	-33863	-30440	-36109	-43089	-41364	-20864	-42583	-20423	-41811	-20260
3000	-49792	-45184	-51340	-45919	-53806	-58245	-62278	-31037	-63112	-30515	-62588	-30364
4000	-67021	-56551	-67401	-60116	-70580	-72714	-82886	-41309	-83812	-40643	-83512	-40580
5000	-83937	-70722	-84504	-70882	-86918	-83156	-104119	-51631	-104435	-50796	-104110	-50809
6000	-99956	-84131	-101055	-84485	-103667	-96924	-124096	-61444	-124851	-60741	-123891	-60663
7000	-116267	-97766	-116730	-97043	-119719	-110299	-144383	-71362	-144066	-70434	-143878	-70518
8000	-132224	-111080	-132633	-110100	-135674	-123408	-164447	-81192	-163502	-80010	-163204	-80152
9000	-147717	-121796	-148352	-121888	-151369	-136257	-184143	-91028	-182791	-89473	-182461	-89854
10000	-164515	-137746	-164479	-134254	-167020	-148891	-203795	-100854	-202247	-99340	-201076	-99422
0	1713	934	1551	941	-2520	-20004	2093	398	2822	552	3479	362
10000	-167067	-137011	-166798	-134167	-168974	-149999	-206107	-101708	-204945	-100275	-205378	-100776
0	-199	-165	-122	-190	-4540	-21618	-244	-379	-54	-257	-108	-515

NOTES: Specimen was subsequently cycled 50 times to 9000 psi without initiation of cracks
All stresses are in pounds per square inch
Ceramic Composition: 94 percent Alumina Ceramic
Material Properties: Poisson's Ratio 0.21, Modulus of Elasticity 41,000,000
End Closures: Steel Hemispheres

Table A-7. Stresses on cylinder C, Sheet 2.

Stresses on Ceramic Cylinder 20 in OD x 17 in L x 0.450 in T
under Short Term Pressurization

Gage Locations

	|<---------- From Interior Midbay to End B ----------|						
Pressure	G		H		I		J	
(Psi)	Hoop	Axial	Hoop	Axial	Hoop	Axial	Hoop	Axial
0	0	0	0	0	0	0	0	0
1000	-20513	-10212	-23111	-30397	-18617	-8994	-17272	-16255
2000	-40107	-19370	-40250	-38014	-35819	-16911	-33013	-31861
3000	-62378	-29951	-60994	-47372	-56517	-26055	-51883	-47919
4000	-83325	-39884	-80058	-55763	-75482	-33973	-68899	-61783
5000	-104709	-49951	-98452	-63889	-93840	-41929	-86101	-77122
6000	-124716	-59319	-116999	-71966	-112369	-49920	-102259	-91585
7000	-145317	-68975	-134969	-79635	-130348	-57631	-118703	-106436
8000	-165514	-78464	-152107	-87252	-147415	-64905	-134912	-120952
9000	-185420	-87934	-170122	-95135	-165384	-72574	-150988	-135029
10000	-205095	-97478	-188301	-103217	-183501	-80356	-167476	-149110
0	1415	297	-2840	-21138	1655	266	194	-246
10000	-206479	-98014	-190114	-103844	-185169	-80296	-166978	-146546
0	-88	-223	-4643	-21721	-149	-318	-226	-293

NOTES: Specimen was subsequently cycled 50 times to 9000 psi without initiation of cracks
All stresses are in pounds per square inch
Ceramic Composition: 94 percent Alumina Ceramic
Material Properties: Poisson's Ratio 0.21, Modulus of Elasticity 41,000,000
End Closures: Steel Hemispheres

Table A-8. Strains on cylinder D.

Strains on Ceramic Cylinder 20 in OD x 30 in L x 0.685 in T
under Short Term Pressurization

Gage Locations on Interior Surface

	Above Separation		Edge of Separation		Below Separation		Edge of Separation		Away From Separation	
Pressure	1		2		3		4		5	
(Psi)	Hoop	Axial	Hoop	Axial	Hoop	Axial	Hoop	Axial	Hoop	Axial
0	0	0	0	0	0	0	0	0	0	0
1000	-304	-70	-300	-87	-307	-66	-301	-90	-264	-85
2000	-593	-142	-589	-175	-600	-135	-585	-178	-548	-174
3000	-897	-222	-893	-274	-909	-212	-887	-277	-848	-271
4000	-1203	-303	-1194	-369	-1215	-286	-1183	-372	-1140	-368
5000	-1506	-384	-1497	-468	-1524	-363	-1484	-471	-1437	-465
6000	-1807	-463	-1795	-561	-1826	-438	-1778	-566	-1732	-562
7000	-2105	-539	-2091	-654	-2126	-508	-2070	-658	-2021	-656
8000	-2404	-613	-2386	-746	-2427	-578	-2363	-750	-2313	-750
9000	-2706	-692	-2685	-841	-2731	-651	-2659	-846	-2608	-849
10000	-3006	-772	-2983	-936	-3033	-725	-2953	-940	-2899	-946
0	7	10	10	11	6	9	10	9	9	10
10000	-3003	-778	-2976	-945	-3030	-730	-2946	-945	-2922	-941

NOTES: All strains are in microinches per inch
Electric resistance strain gages are CEA-06-125WT-350, Gage Factor 2.09
Ceramic Composition: 94 percent Alumina Ceramic
End Closures: Steel Hemispheres
Separation 0.150 in long x 0.02 in wide x 0.032 in deep on interior surface at midbay

Table A-9. Stresses on cylinder D.

Stresses on Ceramic Cylinder 20 in OD x 30 in L x 0.685 in T
under Short Term Pressurization

Gage Locations on Interior Surface

	Above Separation		Edge of Separation		Below Separation		Edge of Separation		Away From Separation	
Pressure	1		2		3		4		5	
(Psi)	Hoop	Axial	Hoop	Axial	Hoop	Axial	Hoop	Axial	Hoop	Axial
0	0	0	0	0	0	0	0	0	0	0
1000	-13670	-5741	-13651	-6434	-13762	-5596	-13721	-6571	-12089	-6024
2000	-26714	-11432	-26839	-12811	-26951	-11195	-26695	-12904	-25072	-12399
3000	-40473	-17601	-40770	-19796	-40898	-17281	-40540	-19870	-38813	-19262
4000	-54328	-23832	-54536	-26582	-54689	-23211	-54091	-26611	-52211	-26052
5000	-68053	-30035	-68424	-33557	-68636	-29297	-67893	-33569	-65823	-32888
6000	-81675	-36135	-82043	-40230	-82265	-35234	-81359	-40291	-79350	-39706
7000	-95141	-42079	-95577	-46885	-95763	-40938	-94712	-46868	-92592	-46340
8000	-108633	-47946	-109059	-53488	-109304	-46652	-108108	-53453	-105963	-53002
9000	-122297	-54054	-122739	-60256	-123000	-52521	-121669	-60236	-119508	-59906
10000	-135885	-60188	-136376	-67015	-136620	-58415	-135125	-66916	-132863	-66687
0	390	492	528	562	338	440	510	476	476	510
10000	-135811	-60418	-136157	-67338	-136537	-58603	-134870	-67068	-133805	-66680

NOTES: All stresses are in pounds per square inch
Ceramic Composition: 94 percent Alumina Ceramic
Material Properties: Poisson's Ratio 0.21, Modulus of Elasticity 41,000,000
End Closures: Steel Hemispheres

Table A-10. Acoustic emissions during hydrostatic testing of 20-inch ceramic cylinder with surface defects.

Cycles	1	2	3	4	5	20
Pressure						
			Events			
0000	0	0	0	0	0	0
1000	46-14	14	1	0	2	0
2000	82-95	14	1	1	6	0
3000	154-239	15	2	1	6	1
4000	399-469	33	7	3	7	2
5000	559-607	42	9	6	7	5
6000	640-1282	68	17	17	11	8
7000	1484-1811	150	30	25	28	12
8000	2077-2351	301	77	50	64	16
9000	2569-2835	468	364	135	97	20
10000	3057-3294					

Notes:
1. Transducer: AET AC175 SN# 7664
   50 to 200 KHZ
2. Amplifier Setting:
   Rate: T Gain: 60 DB
   Threshold: Automatic
   Function: Events
   Scale: 1
3. Recorder:
   Channel "A" Events,
   200 Full Range,
   Channel "B" Rms,
   50 MV Full Scale,
   0.5 CM/Min Chart Speed

APPENDIX B: DESIGN OF LARGE-DIAMETER ALUMINA-CERAMIC HOUSINGS FOR 9,000 PSI SERVICE

FIGURES

APPENDIX B: DESIGN OF LARGE-DIAMETER ALUMINA-CERAMIC HOUSINGS FOR 9,000 PSI SERVICE

INTRODUCTION

This report has summarized the performance of 20-inch ceramic cylinders with different wall thicknesses, lengths, and types of defects. Based on the experimental data generated by the testing of the four cylinders with 20-inch OD in this program, and 22.5- and 12-inch diameters in other programs, a set of recommendations has been drawn up for the guidance of the engineer in designing ceramic housings.

These recommendations, validated experimentally on housings with 6-, 12-, and 20-inch diameters, apply to any size that can be fabricated today by the ceramic industry. The recommended designs of components for 20-inch-diameter housings are shown in appendix B, figures B-1 through B-10.

RECOMMENDATIONS

1. Ceramic with 94-percent alumina composition (table A-1) is well suited as a cost-effective structural material for construction of monocoque cylinders and hemispheres for external pressure housings with **guaranteed** 200-cycle fatigue life at design pressure, provided that the maximum design membrane stress in the ceramic component does **not** exceed −136,000 psi, and the axial pressure on plane-bearing surfaces does not exceed −68,000 psi. Increase of alumina content in the ceramic from 94- to 96-percent will increase the **guaranteed** cyclic fatigue life beyond 200 cycles. To date, the magnitude of improvement has not been quantified experimentally.
2. Monocoque configuration is the preferred shape for cylinders. It minimizes fabrication cost and facilitates a uniform stress field along the length of the cylinder.
3. The hemispheres are to be provided at the equator with a cylindrical rim and at the pole with a reinforcement around the penetration to prevent maximum design stress from exceeding −136,000 psi.
4. To achieve the guaranteed 200-cycles fatigue life, the ends of the monocoque cylinders must be bonded with epoxy to Mod 1 end caps, preferably fabricated from the corrosion-resistant titanium alloy Ti-6Al-4V, or, as a second choice, from high-strength aluminum 7178-T6 or 7075-T6 alloys. These aluminum alloys perform well, but only in applications where the housing is taken apart after each dive and flushed with tap water. The thickness of epoxy interlayer underneath the ceramic plane-bearing surface must be controlled within the 0.005- to 0.015-inch range. The adhesive and its application is described in appendix A, Bonding Procedure.
5. The Mod 1 end cap is defined by the height of the twin circular flanges. In order to be effective in reduction of tensile radial stress on the ceramic plane-bearing surface and the associated extension of its cyclic fatigue life, the height (h) of the flange must be $\leq 2.7\ t$, where t is the thickness of the ceramic cylinder.
6. The sealing of Mod 1 end caps can be achieved in several ways. All of the methods shown in figure 58 have been used and were found to be acceptable. The boot seal design utilizes a lighter, less expensive configuration of the Mod 1 end cap.
7. To provide ceramic hemispheres with the same guaranteed fatigue life as the ceramic cylinders, the thickness of their cylindrical rim at the equator must match that of the cylinder and also must be adhesive bonded to Mod 1 end caps.
8. The entire payload inside the cylinder must be attached to a framework supported by, and fastened to, the ears on Mod 1 end caps.
9. The preferred technique for fastening hemispheres to cylinders is by split wedge bands.
10. All penetrations should be located in the hemispheres.

11. The dimensions of the monocoque cylinder for 9,000-psi design pressure with an S.F. of 1.5 based on buckling and S.F. of 2.2 on material strength are $t/D_o = 0.034$ and $L/D_o = 1.5$. The W/D of such a cylinder equipped with Mod 1 end caps is 0.5.

12. The length of the cylindrical housing may be extended by incorporating additional cylinder sections that are supported and joined by intermediate circular joint ring stiffeners fabricated from titanium or aluminum.

13. The quality control (QC) for all ceramic components must include, as a minimum:

    a. Dimensional check

    b. Dye penetrant inspection

    c. Ultrasonic NDT, consisting of a C scan performed at a 0.01-inch index rate for detection and location of inclusions ≥ 0.030 inch. Indications of ≥ 0.05 of an inch shall be X-rayed. Presence of inclusions > 0.03 inch located within 0.1 of an inch of the plane-bearing surface, or inclusions > 0.1 of an inch anywhere in the ceramic component shall be the cause for its rejection.

Recommended Bonding Procedure:

1. Sand interior of end cap flanges with 80 grit paper.

2. Clean with methyl ethyl ketone, or equivalent solvent.

3. Etch interior surface of titanium end cap for 30 minutes by brushing on: SEMCO PASA-GEL 107 sand, or sandblast interior surface of aluminum end cap.

4. Wash off etching compound with tap water and air dry (a forced-air heater is acceptable).

5. Turn the end cap upside down, place it on a table, and spray all the exterior surfaces with a mold release to make subsequent removal of spilled epoxy easier (DEVCON Silicon Type Liquid Release Agent does an excellent job).

6. Mix components of epoxy (100 parts resin CIBA Ceigy 610 and 70 parts hardener CIBA Geigy 283), degas by applying vacuum for 30 minutes, and pour the mixture into the end cap space, filling it to a depth of approximately 0.25 of an inch.

7. Cut a cardboard gasket with same OD and ID as cylinder from 0.01-inch-thick 125-pound-weight cellulose file-folder material. Subsequently divide the gasket into approximately 1-inch-wide segments (instead of cutting the gasket into segments, one may punch 0.25-inch-diameter holes into the gasket centerline at 1-inch intervals).

8. Place gasket segments on top of the epoxy layer inside the end cap on approximately 1.250-inch centers (i.e., width of space between segments is equal to to approximately 0.25 inches).

9. Push the individual gasket segments into the layer of epoxy with a pointed rod until they are totally submerged and come to rest on the bottom of the end cap.

10. Place pencil marks around the exterior surface of the cylinder 2 inches away from its end.

11. Pour additional epoxy mixture into the end cap until the depth of epoxy reaches 0.5 of an inch.

12. Insert the ceramic cylinder vertically into the epoxy-filled end cap, gently forcing the cylinder downward until the pencil marks are barely visible above the edge of the end cap. In some cases, if the cylinder becomes wedged in an inclined position, rock the upper end of the cylinder from side to side while applying over 100 pounds of downward force to free the lower end of the cylinder.

13. After the seating is completed, immediately inspect the condition of the end cap. If in some places the epoxy level inside the annular spaces did not reach the top of the end cap, additional epoxy should be injected at those locations into the annular space with a syringe until the epoxy overflows.

14. Place a 24-inch by 24-inch by 1-inch plywood panel on top of the cylinder and load it with weights totaling at least 100 pounds. Do not disturb the setup for about 6 hours at 70°F ambient temperature.

15. After 6 to 8 hours, remove the weight, turn the cylinder over, and remove all the surplus epoxy from the exterior surfaces of the end cap while the epoxy is still soft and easy to remove. Place the cylinder into its original position and let the epoxy harden overnight in the end cap.

16. Repeat the procedure on the other end of the cylinder.

PROVEN DESIGN FOR 20-INCH-DIAMETER HOUSING ASSEMBLIES

The extensive testing performed in the present and preceding 20-inch-diameter ceramic housing programs, as well as on the early 12-inch-diameter programs, generated sufficient test data to allow the formulation of designs for 20-inch-diameter housing assemblies whose structural performance can be considered qualified for service to 9,000 psi with a guaranteed minimum 200-cycle fatigue life.

The recommended designs of components for the 20-inch housing assemblies allow the engineer to configure the housing assembly to meet budgetary and operational requirements. The engineer can increase the buoyancy of the housing assembly by increasing the number of cylindrical sections from one to two-or-more sections, and by using ceramic instead of titanium hemispherical bulkheads. Some minor increases in buoyancy and a major reduction in cost also can be achieved by substituting aluminum for titanium in the end caps and joint stiffeners.

In general, high-strength aluminum alloys may be substituted in the fabrication of end caps, stiffeners, and even hemispheres if the operational scenario for the underwater vehicles calls for only brief submersion (i.e., <24 hours) followed by disassembly and thorough rinsing in tap water. In applications where the submersion is long, or brief, but without subsequent rinsing, titanium must be used.

The dimensions of end caps remain the same regardless of whether they are to be fabricated from aluminum or titanium (figures B-3 and B-6). This is not the case with ring stiffeners (figures B-7, B-8, B-9, and B-10) or hemispherical bulkheads (figure B-16). Their dimensions vary to compensate for the difference in the modulus of elasticity for these materials.

Maximum buoyancy of the cylindrical housing assembly is achieved by using the lighter, but more expensive, ceramic hemispherical bulkheads and the lighter and cheaper, but less corrosion-resistant, aluminum end caps and joint stiffeners.

Minimum acquisition cost of the housing assembly is achieved by using the less corrosion resistant, but less expensive, aluminum hemispherical bulkheads, end caps, and joint stiffeners.

Maximum buoyancy at lowest lifetime cost is achieved by using the lighter, but more expensive, ceramic hemispherical bulkheads and the heavier and more expensive, but more corrosion-resistant, titanium end caps and joint stiffeners.

Some further savings in weight can be achieved by using joint stiffener rings with holes drilled through their webs. These holes also are useful as conduits for electric cables and hydraulic lines connecting payload components situated in different cylinder sections of the housing assembly. Because the holes reduce the load-carrying ability of joint stiffener rings, their use is not recommended in housing assemblies with more than two cylinder sections.

Further savings in weight can be generated by reducing the wall thickness of the cylinder at midbay. This, however, requires a reduction in length of individual cylinder sections to maintain the specified minimum S.F. of 1.5 based on buckling. Thus, cylinders with t = 0.585 inch and L = 22 inch equipped at ends with 2-inch-wide ring stiffeners of 0.685-inch thickness provide a W/D of 0.43. Cylinders with t = 0.455 inch and L = 15 inch equipped at ends with 2-inch-long ring stiffeners of 0.455-inch thickness provide a W/D of 0.36. Because of significant reduction in cyclic fatigue

life associated with this type of cylinder design, they are recommended only for applications where the specified fatigue life is less than 10 cycles.

To aid the engineer in selecting components for the 20-inch-diameter housing assemblies, their designs are shown in figures B-1 through B-18 and their drawing number references shown in figures B-19 and B-20. When properly assembled, these housings have a guaranteed fatigue life in excess of 200 dives to design depth.

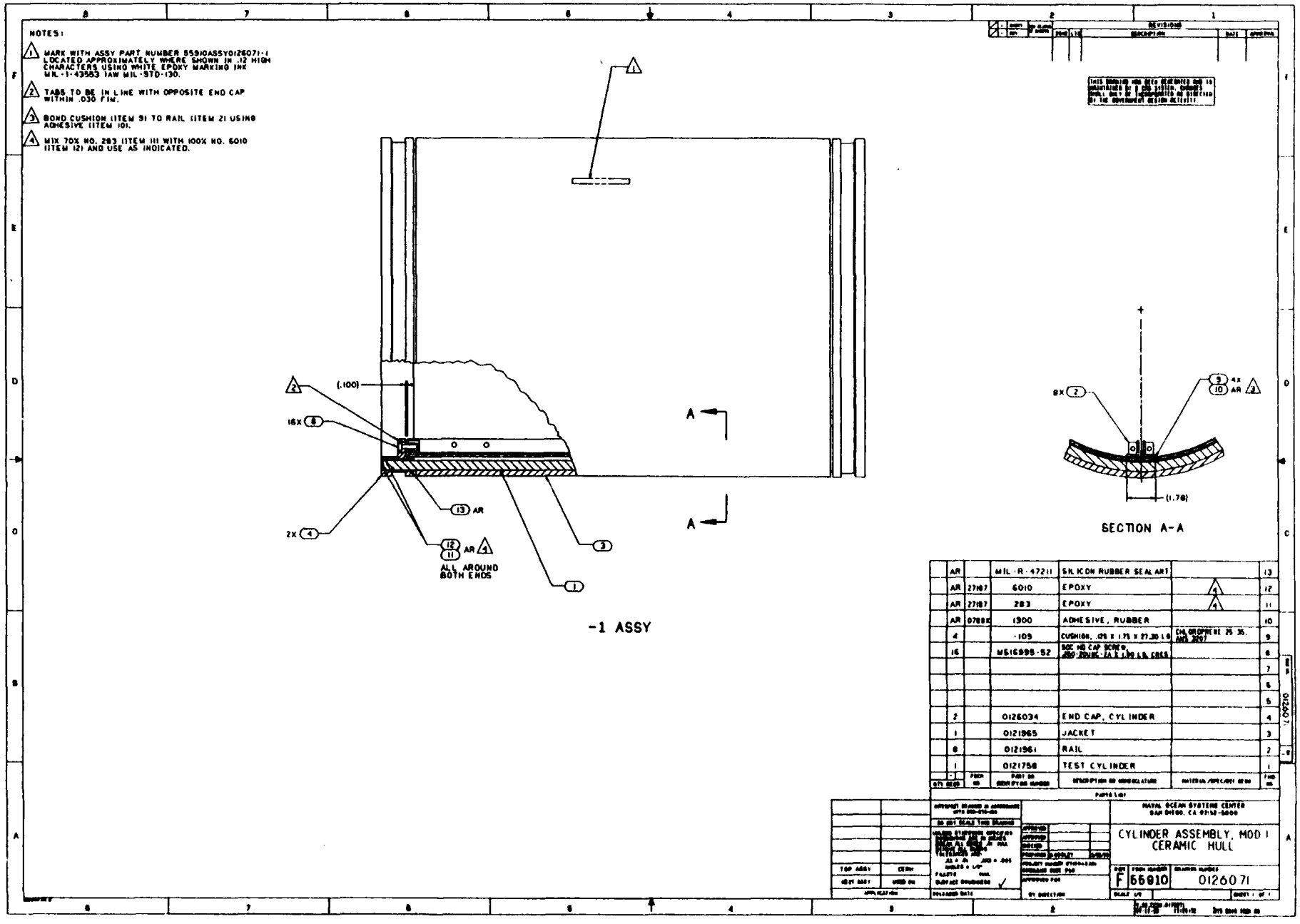

Figure B-1. Mod 1 ceramic hull cylinder assembly.

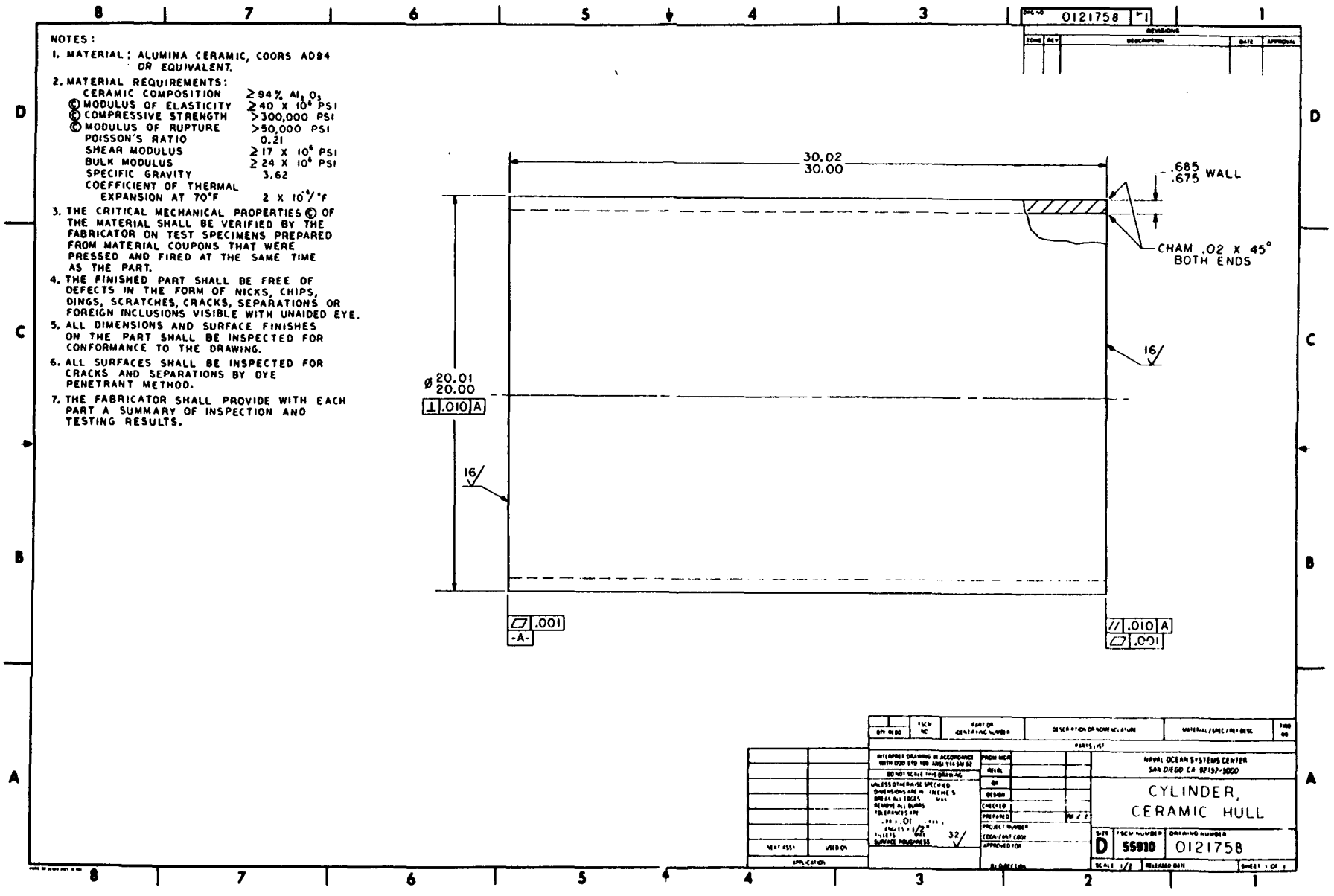

Figure B-2. Ceramic hull cylinder.

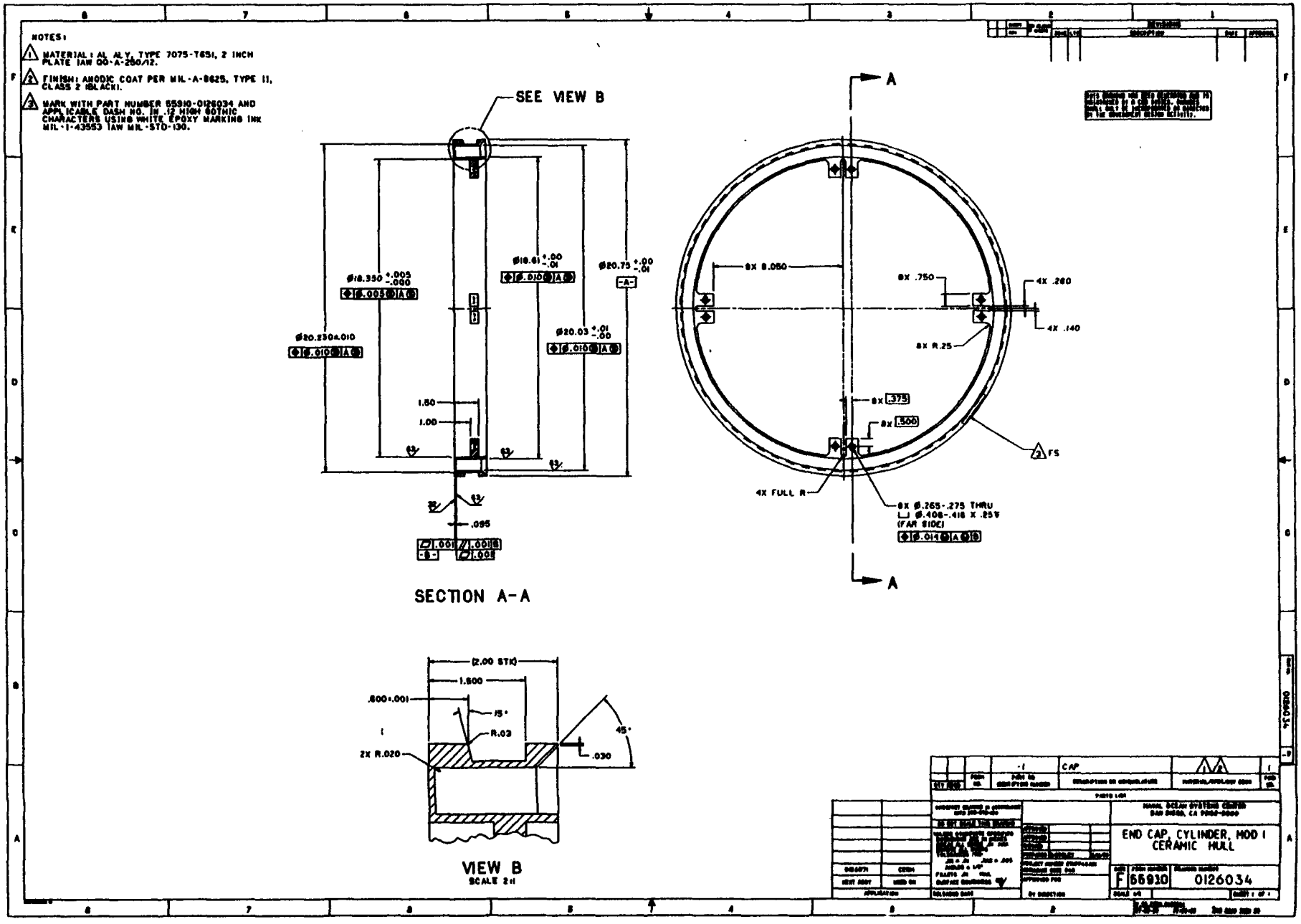

Figure B-3. Mod 1 ceramic hull cylinder end cap.

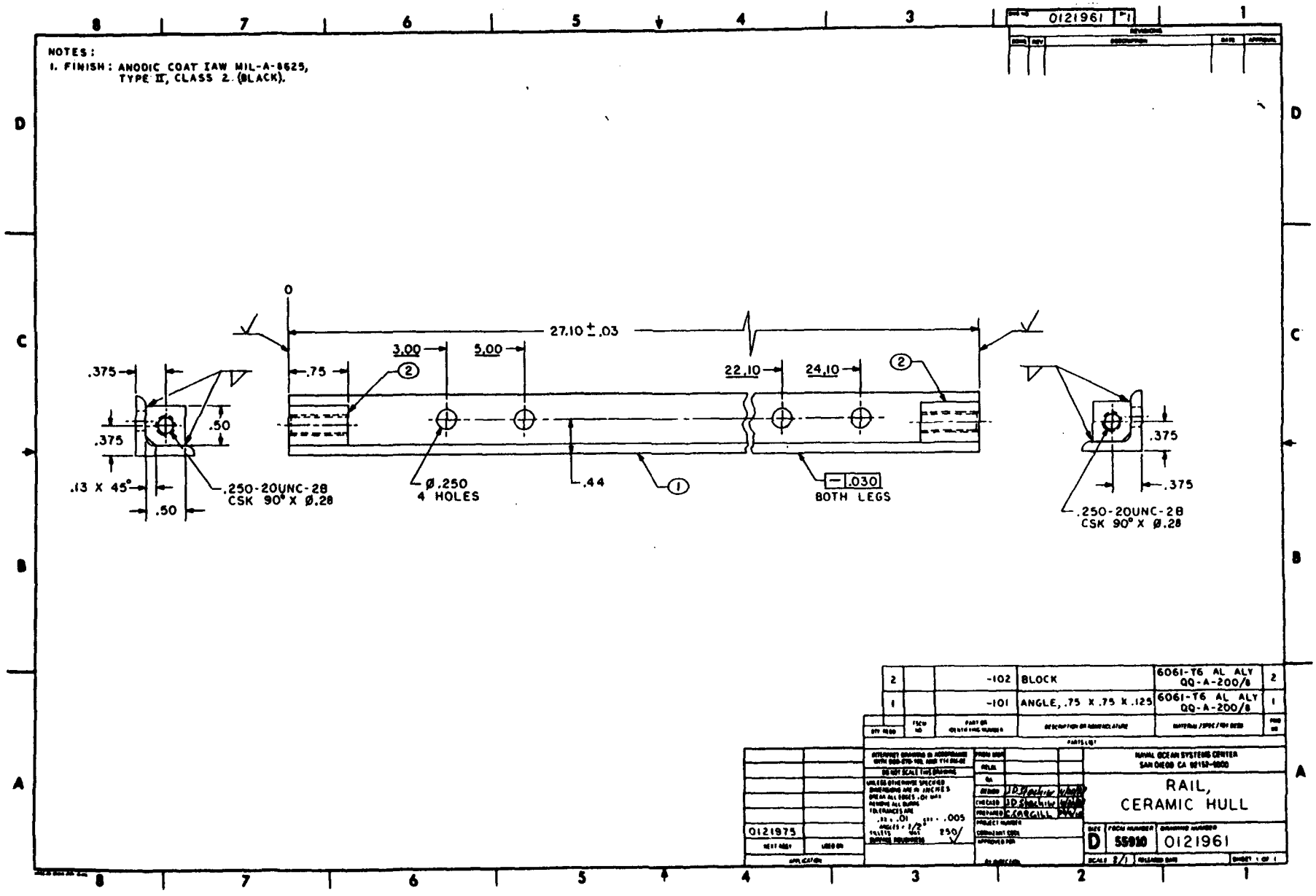

Figure B-4. Ceramic hull rail (6061-T6 alloy).

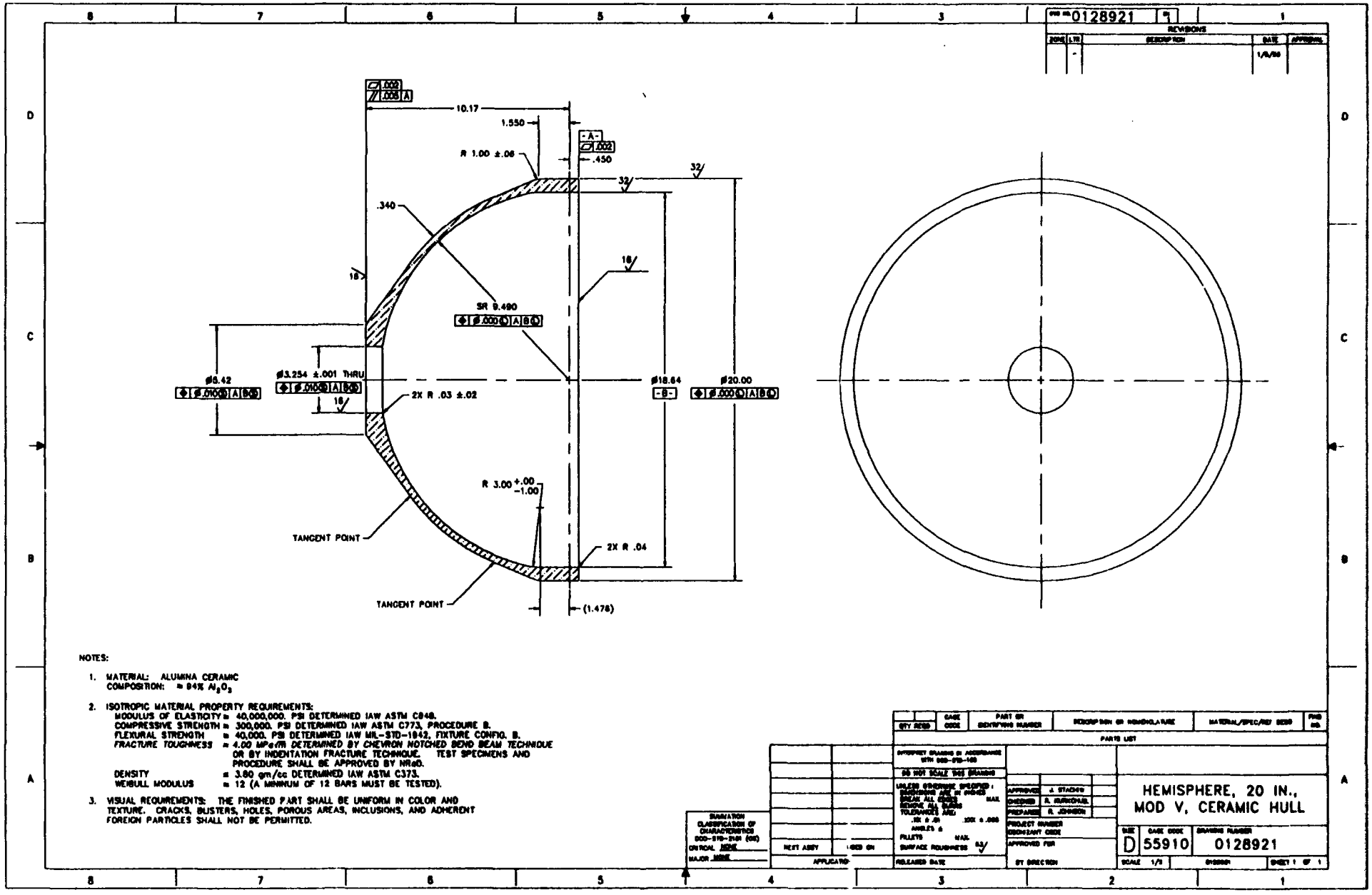

Figure B-5. Mod V ceramic hull 20-inch hemisphere.

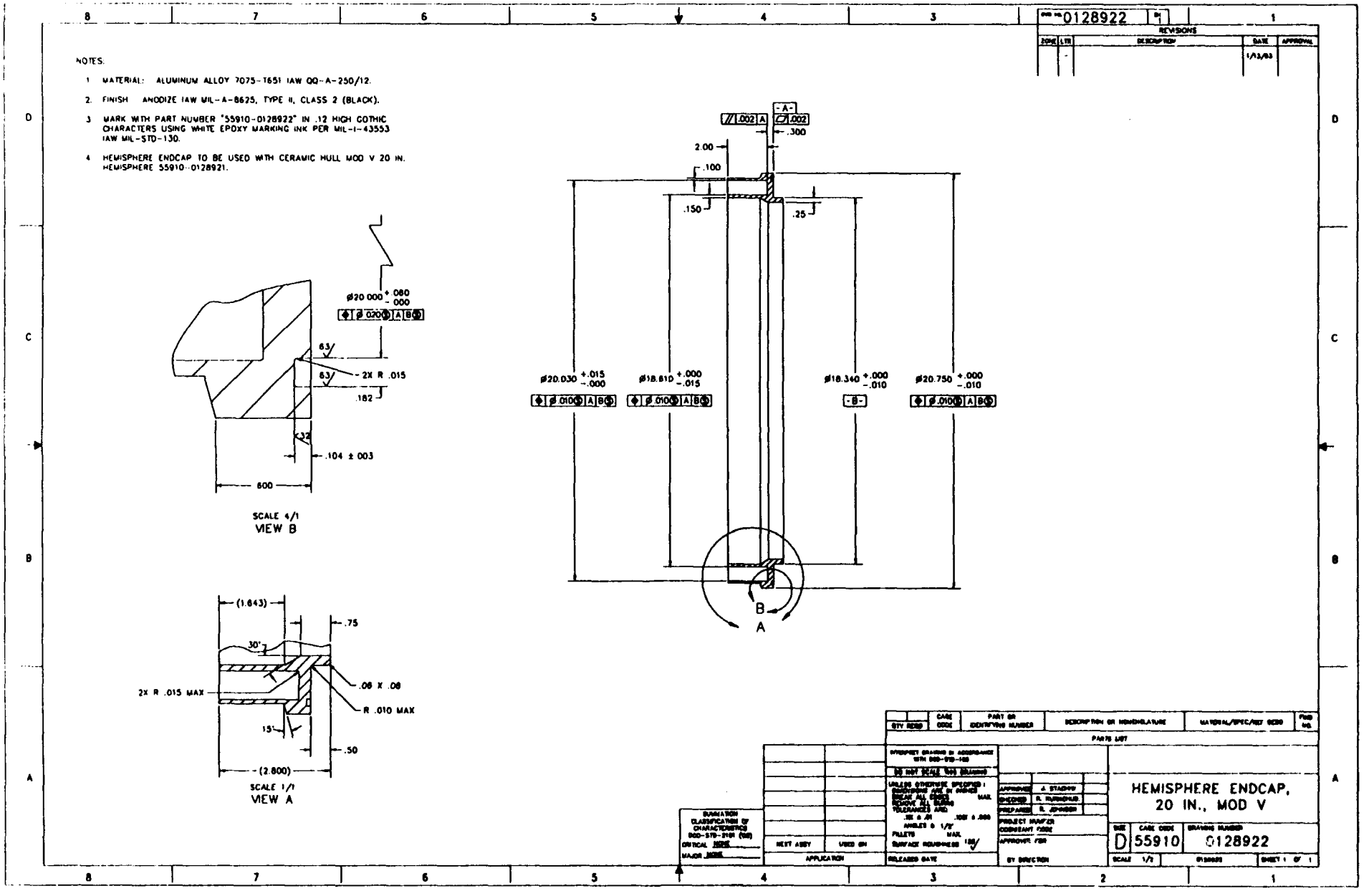

Figure B-6. Mod V 20-inch hemisphere end cap.

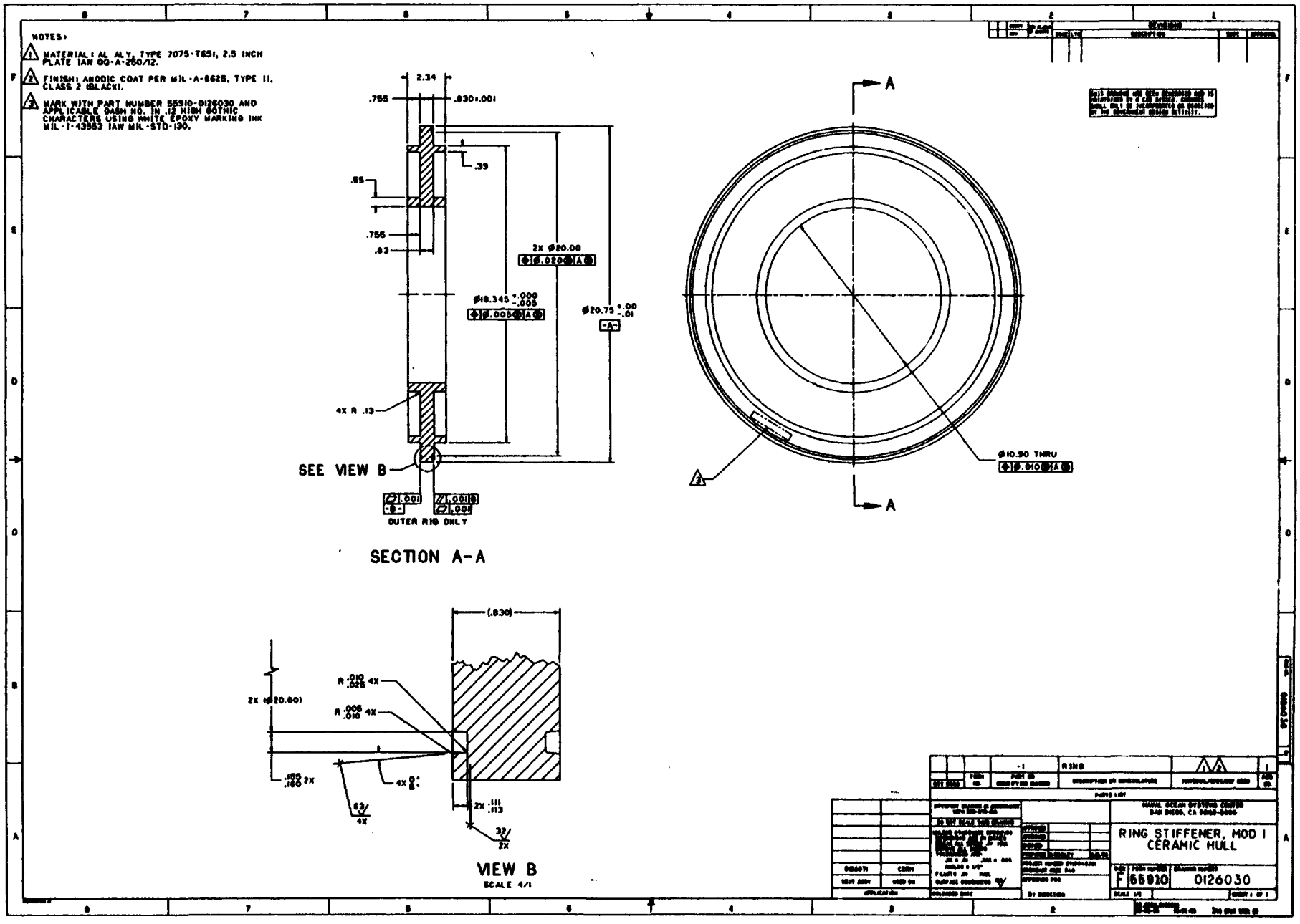

Figure B-7. Mod 1 ceramic hull solid aluminum ring stiffener.

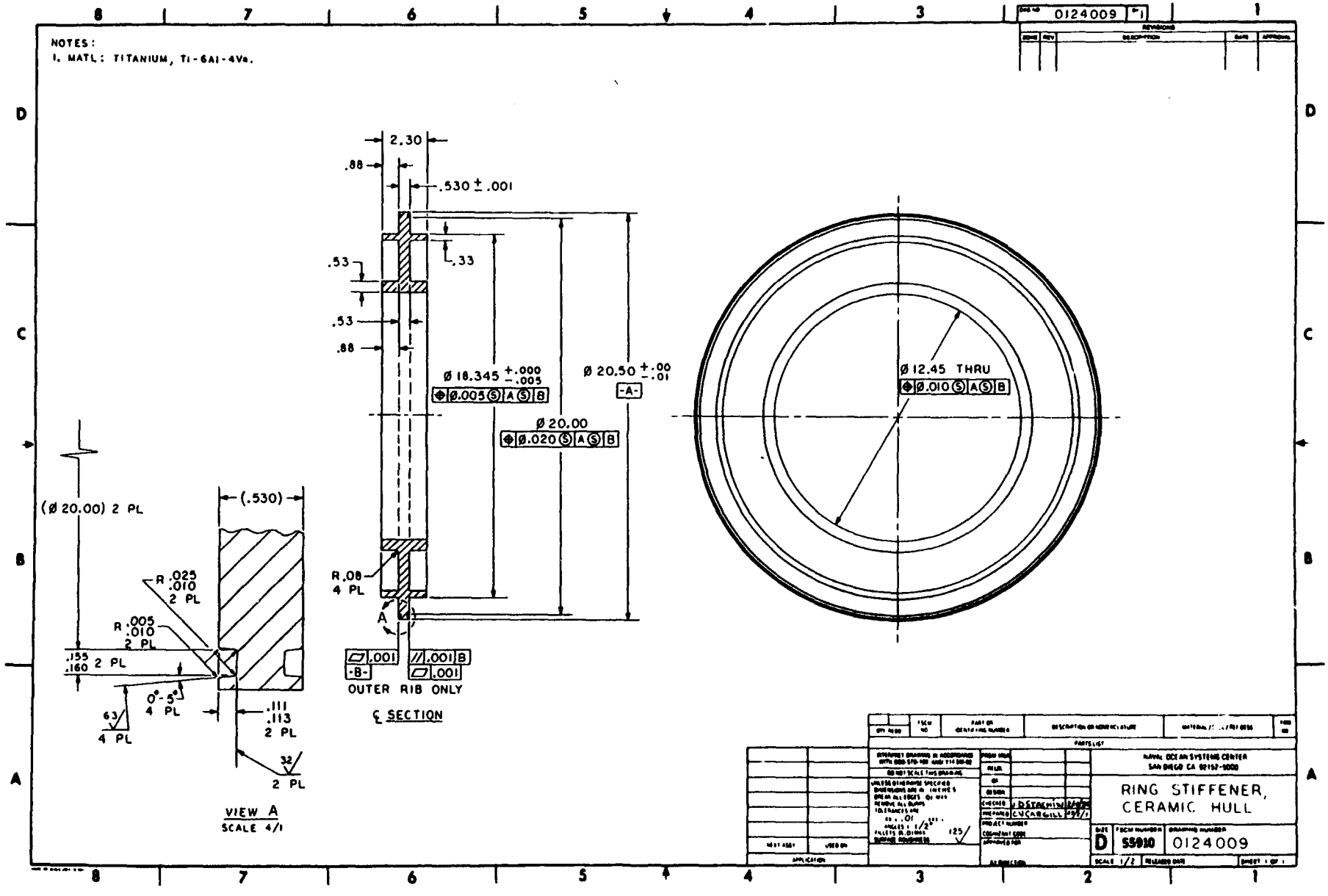

Figure B-8. Ceramic hull solid titanium ring stiffener.

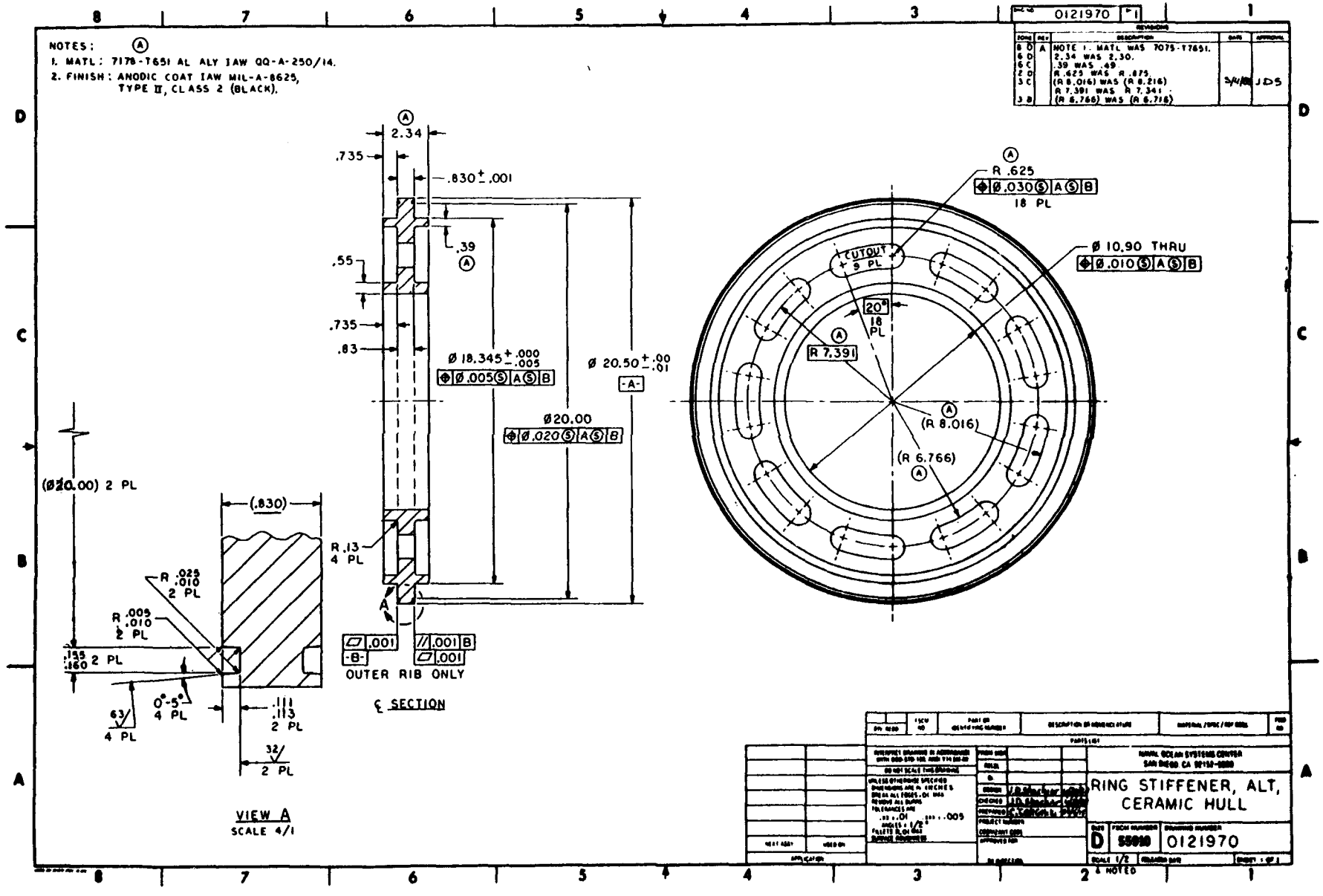

Figure B-9. Ceramic hull perforated aluminum ring stiffener.

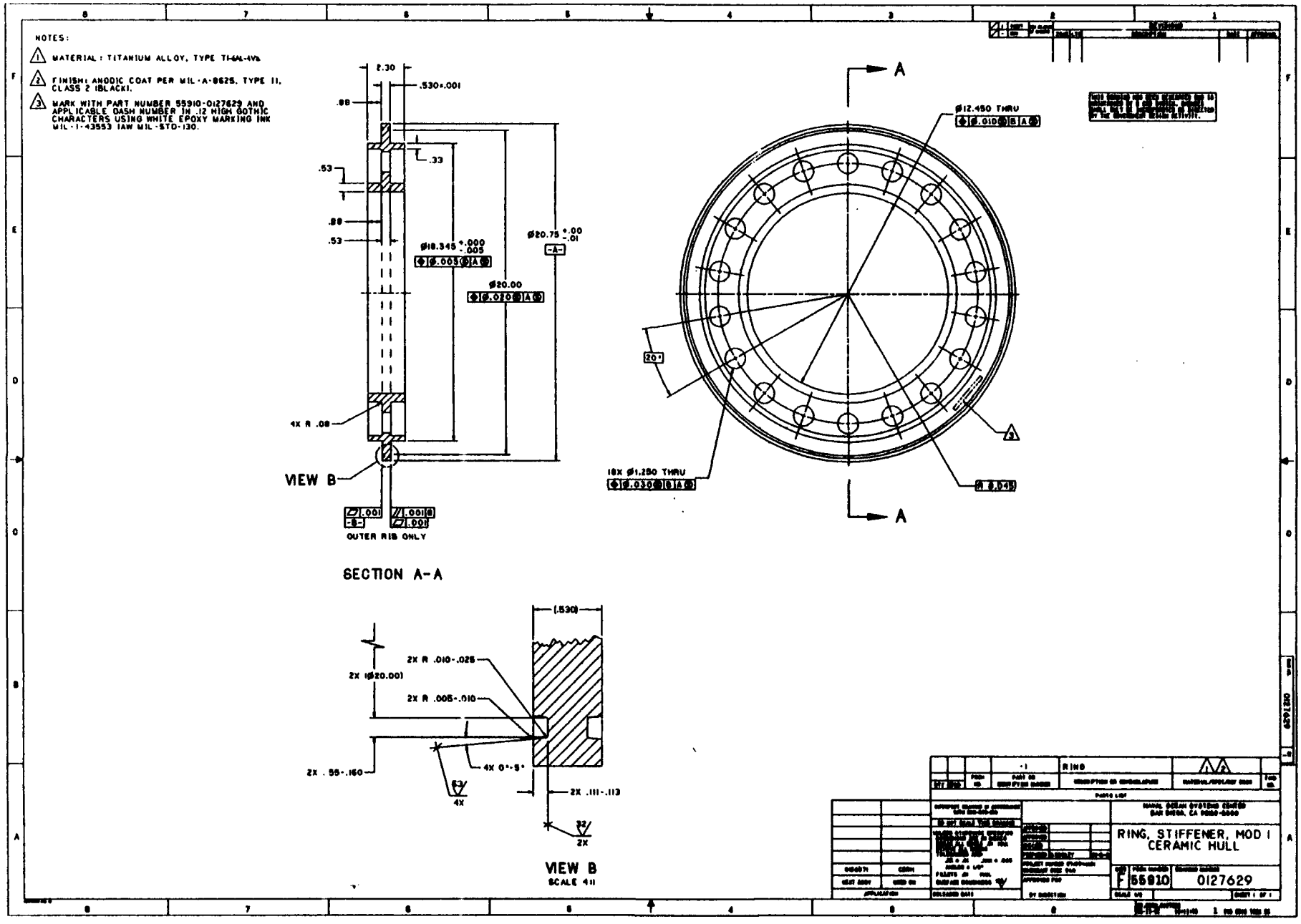

Figure B-10. Mod 1 ceramic hull perforated aluminum ring stiffener.

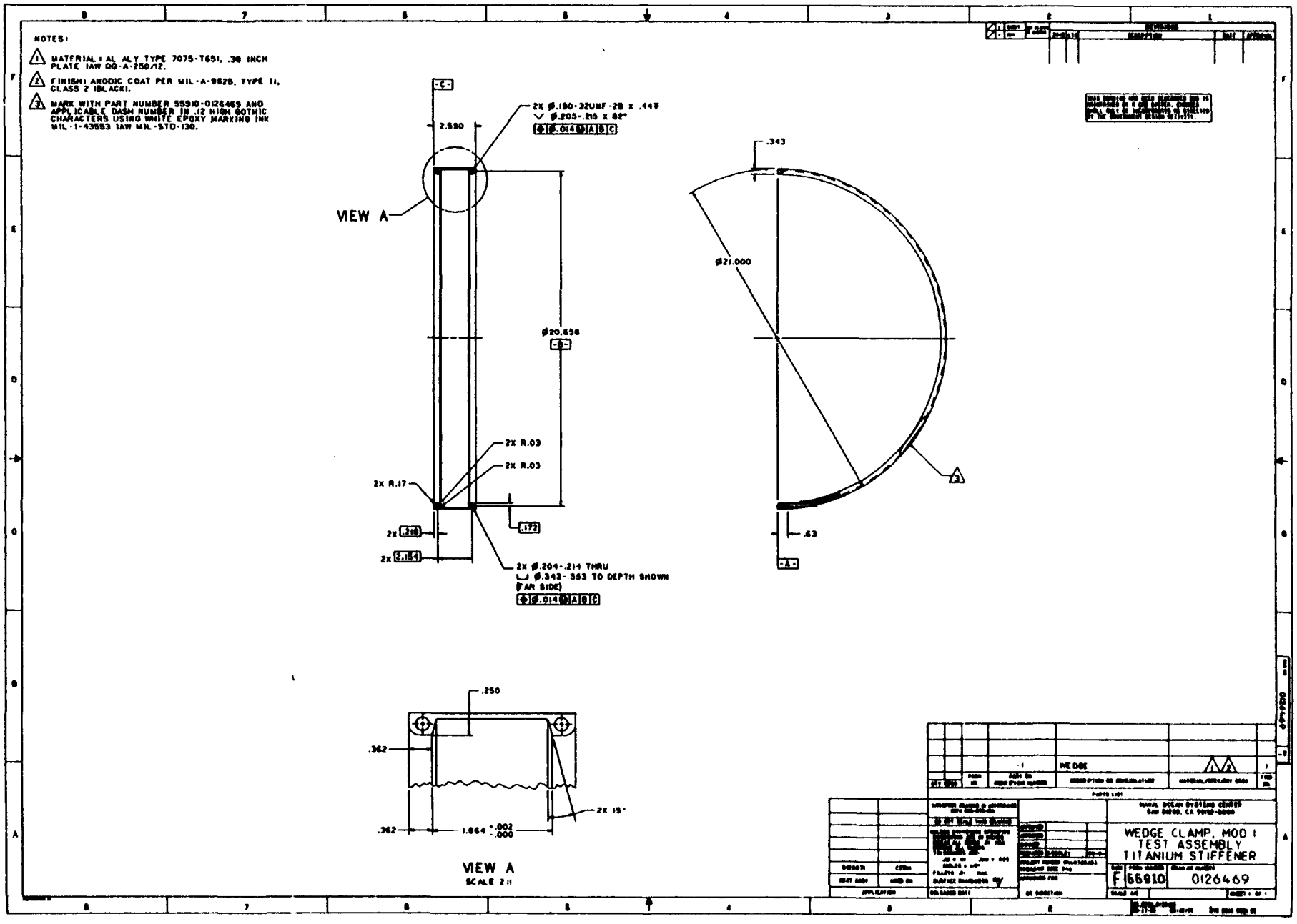

Figure B-11. Mod I test assembly wedge clamp for titanium stiffener.

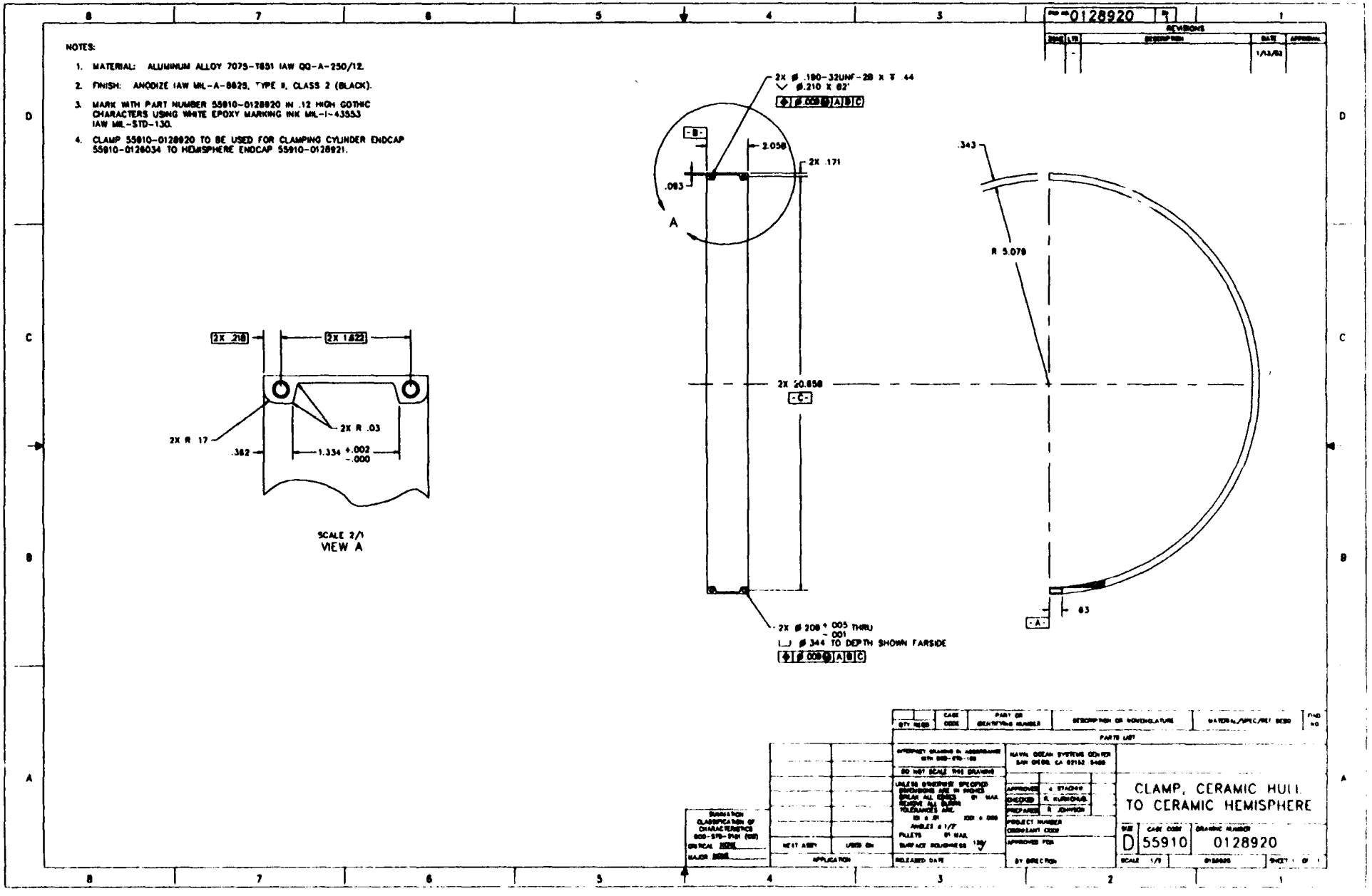

Figure B-12. Ceramic hull to ceramic hemisphere clamp.

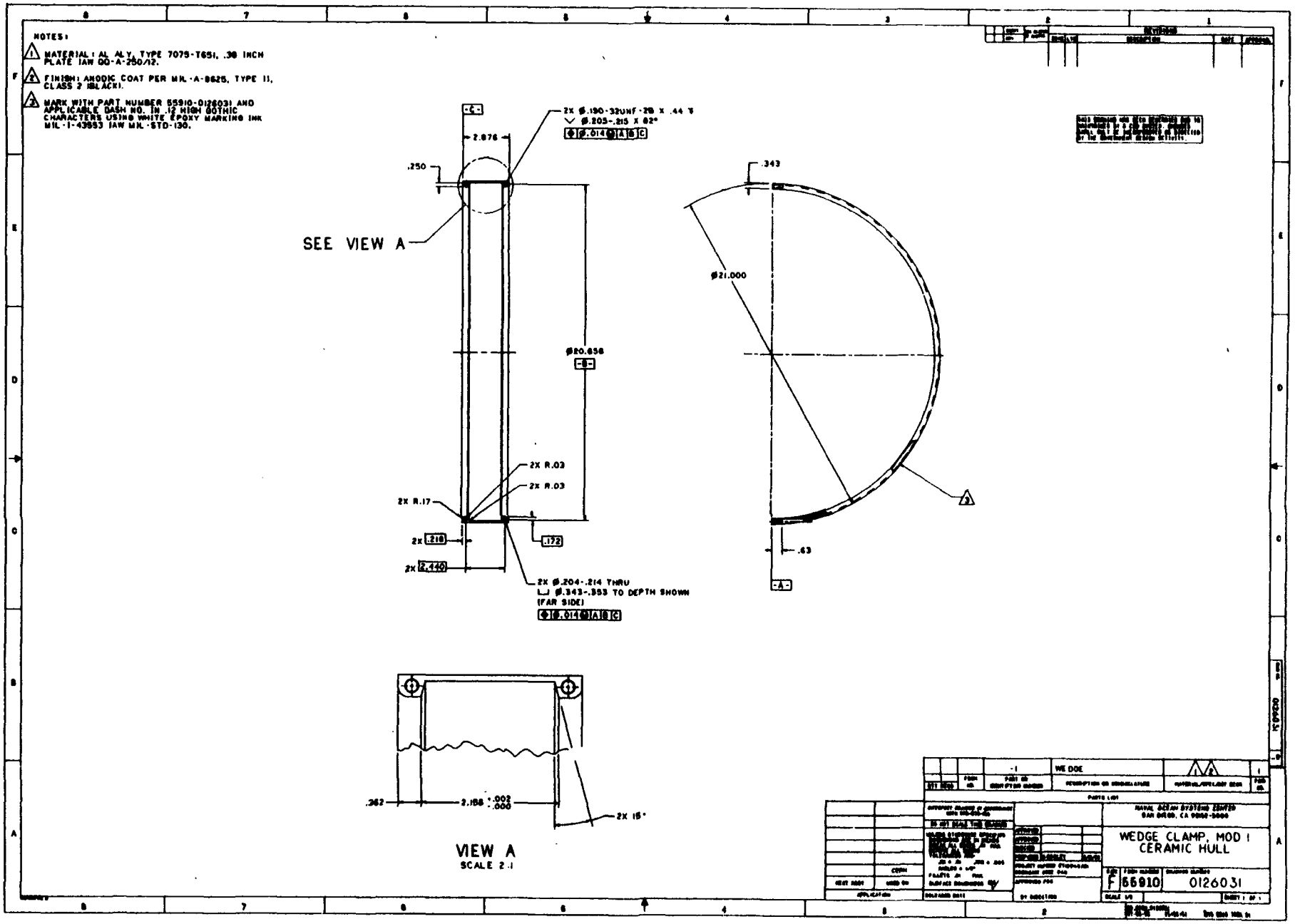

Figure B-13. Mod I ceramic hull wedge clamp for aluminum stiffener.

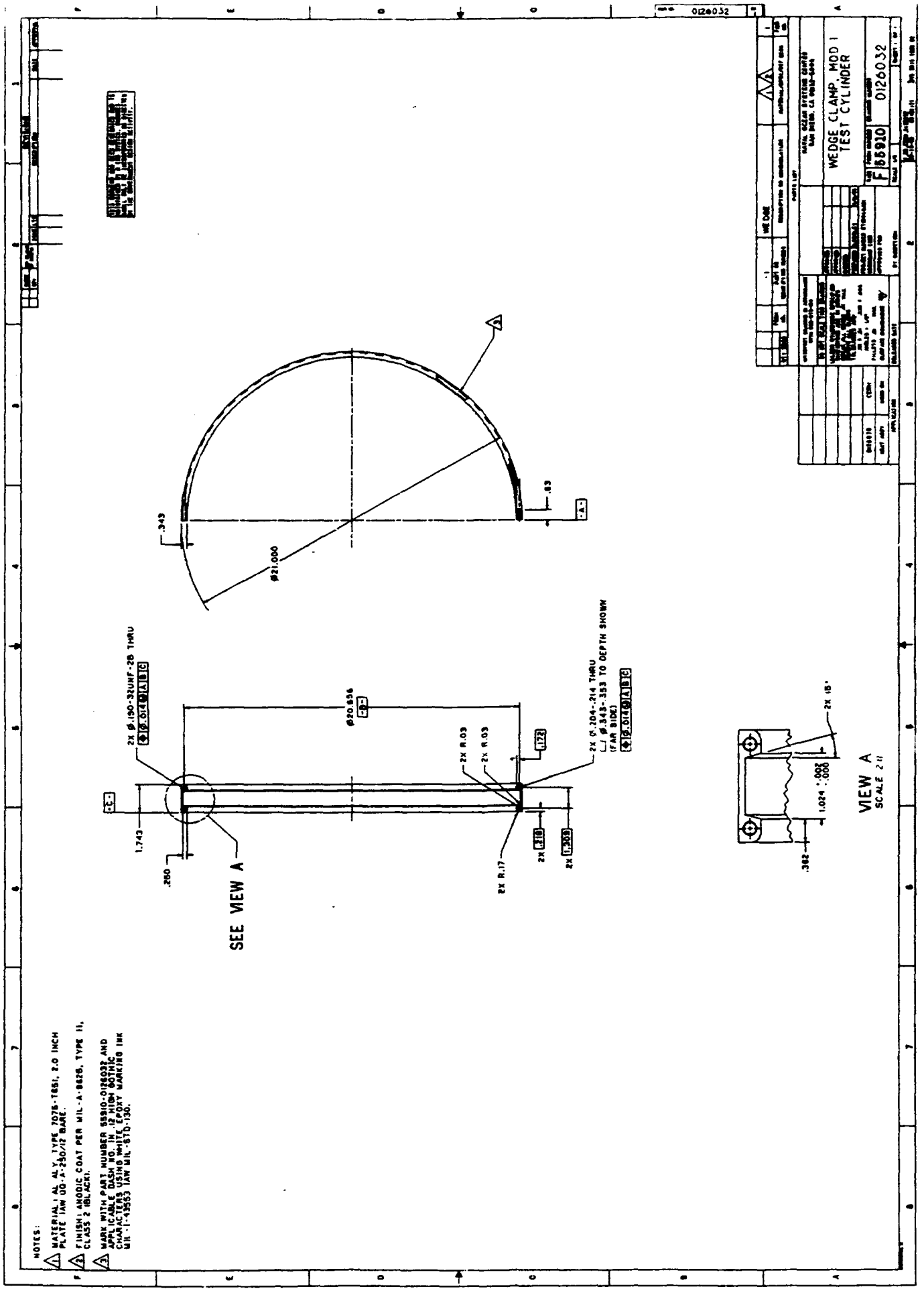

Figure B-14. Mod I test cylinder wedge clamp for metallic hemisphere.

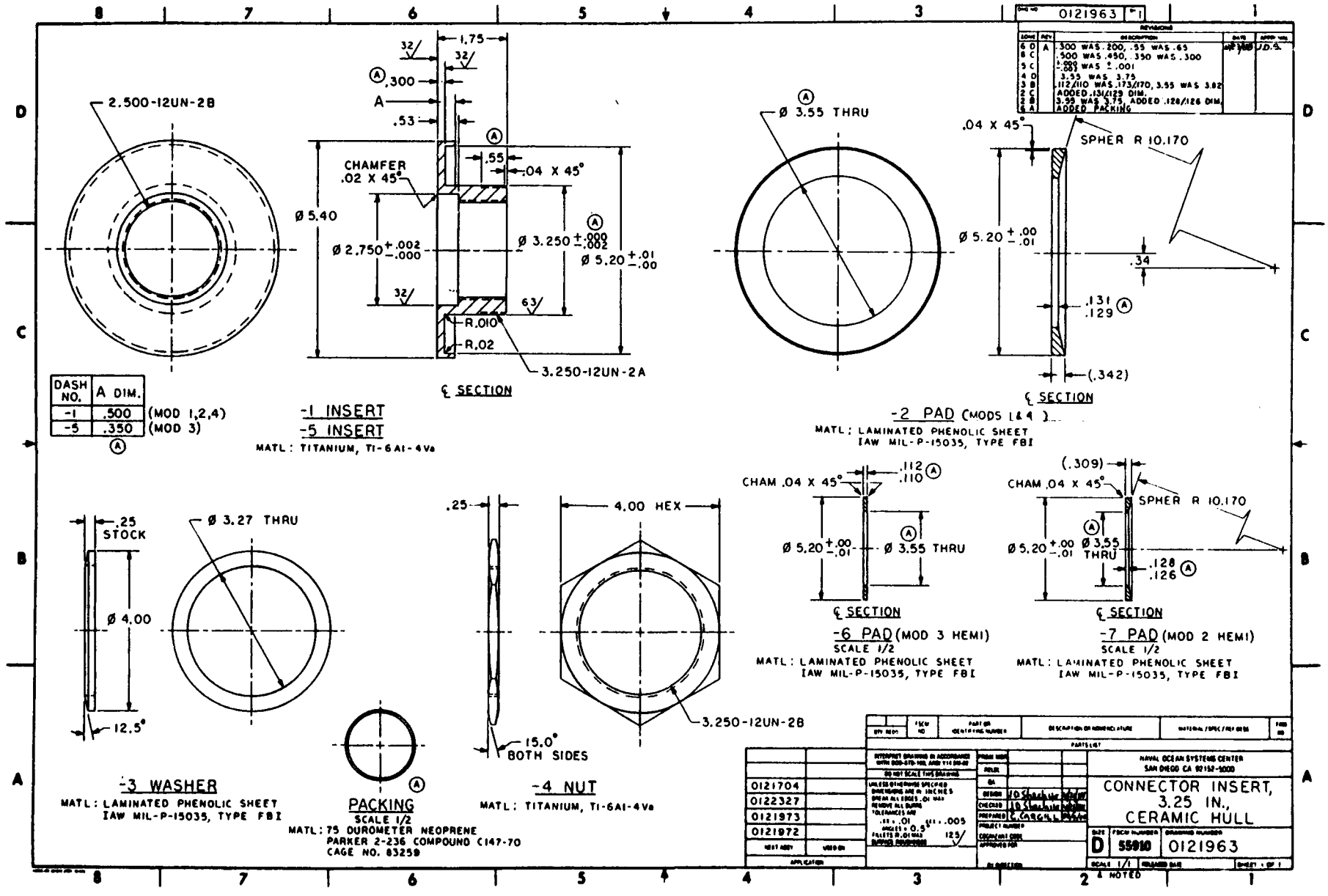

Figure B-15. Ceramic hull 3.25-inch connector insert for ceramic hemisphere.

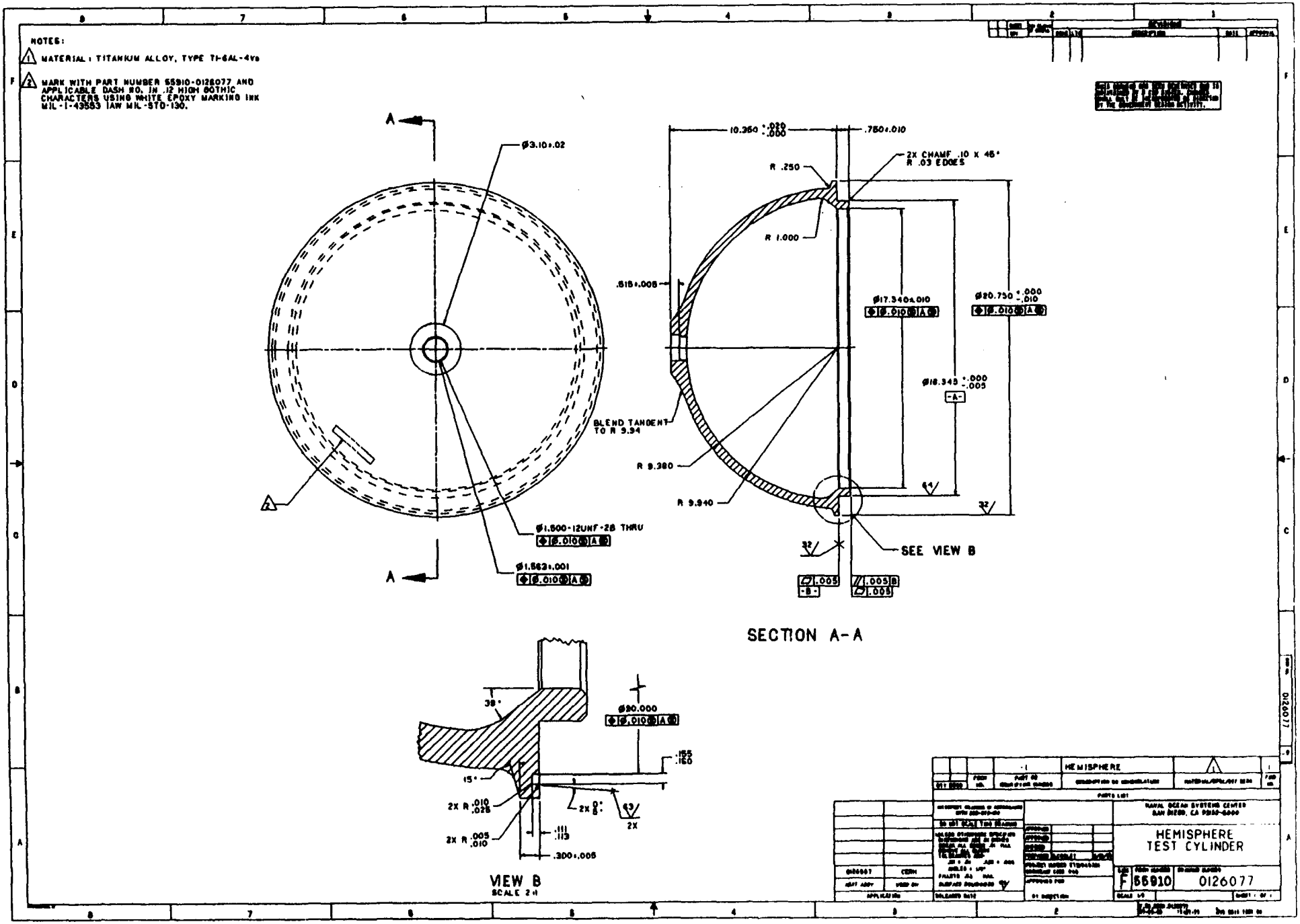

Figure B-16. Test cylinder titanium hemisphere.

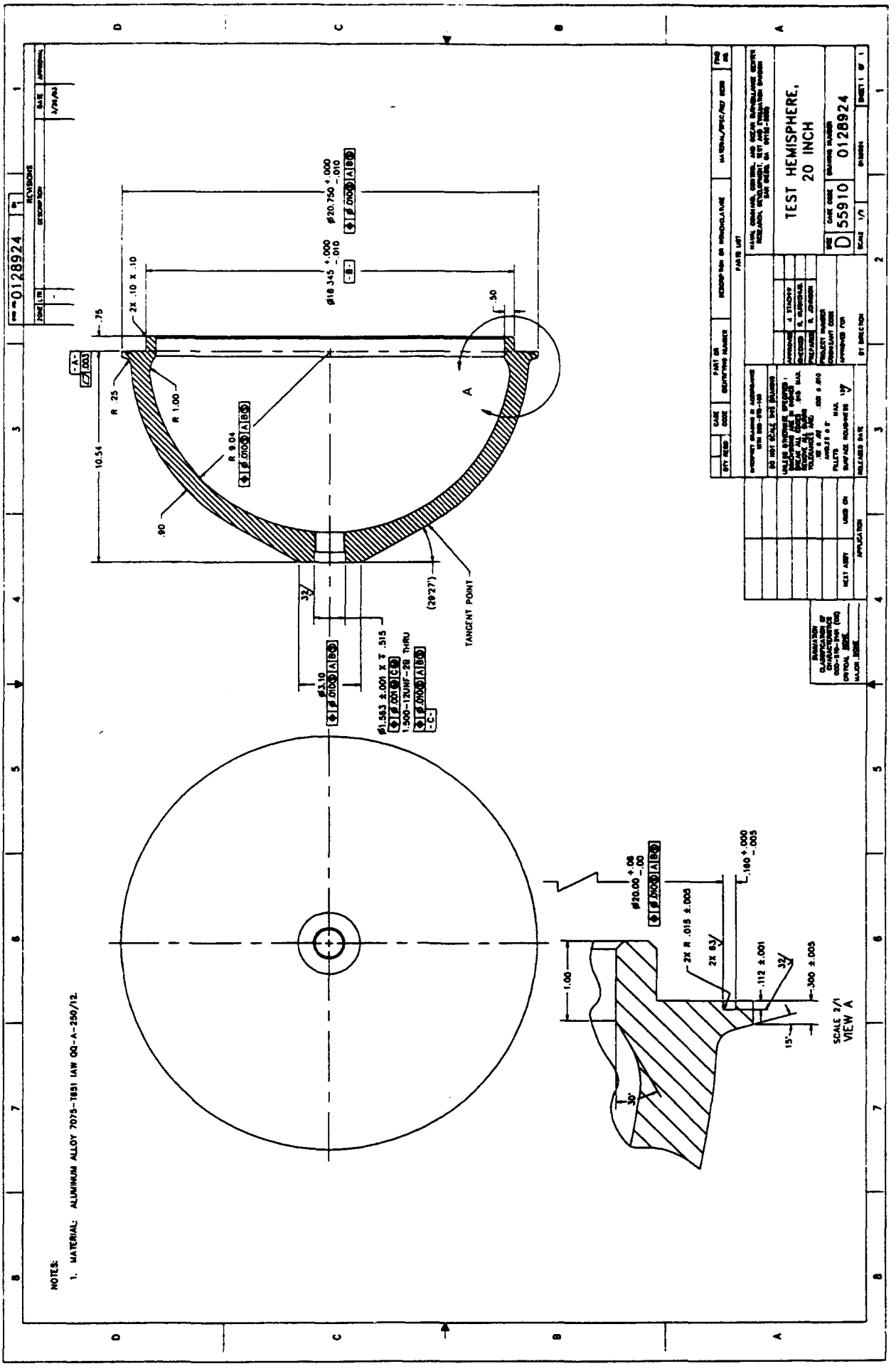

Figure B-17. Aluminum 20-inch test hemisphere.

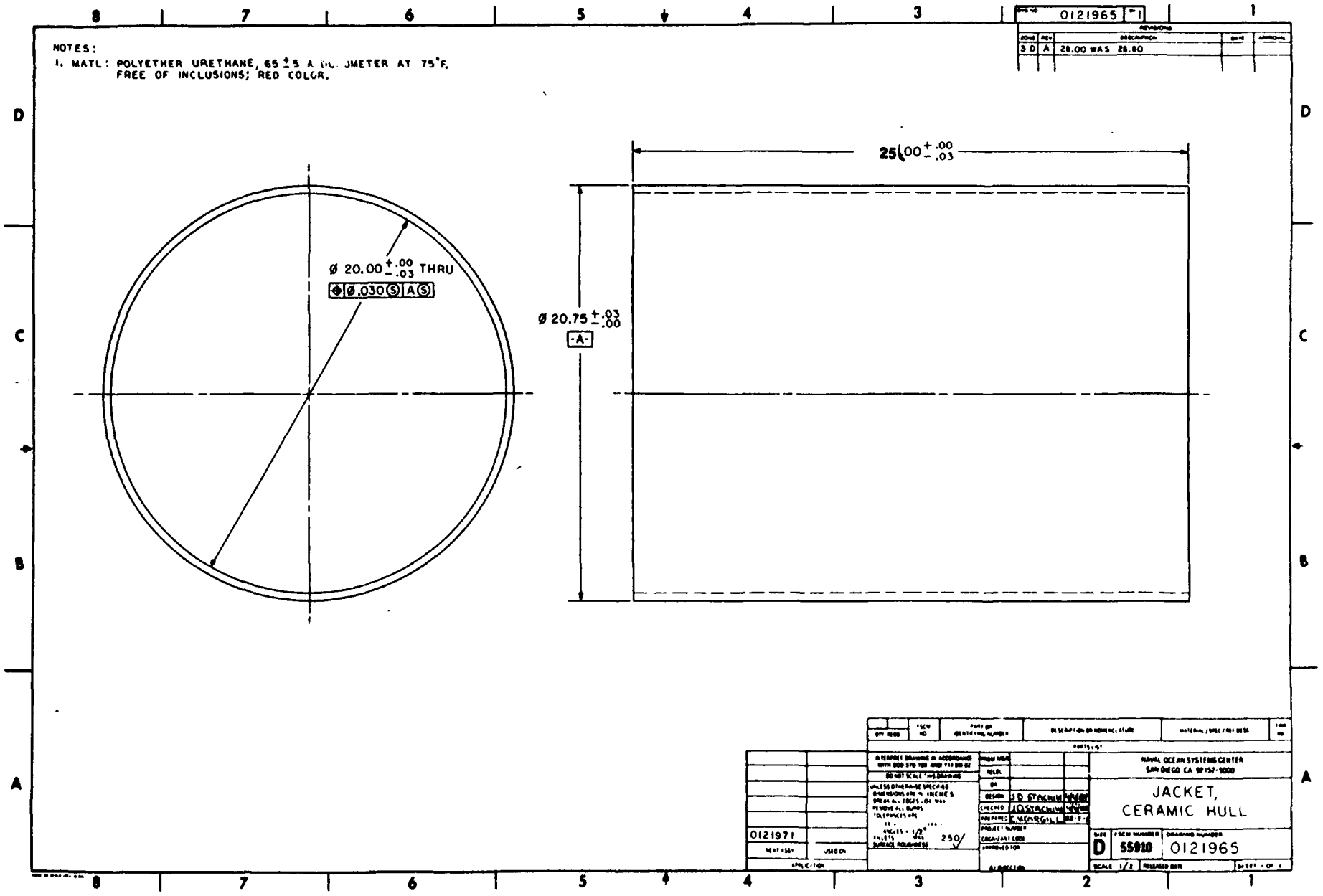

Figure B-18. Ceramic hull polyurethane jacket.

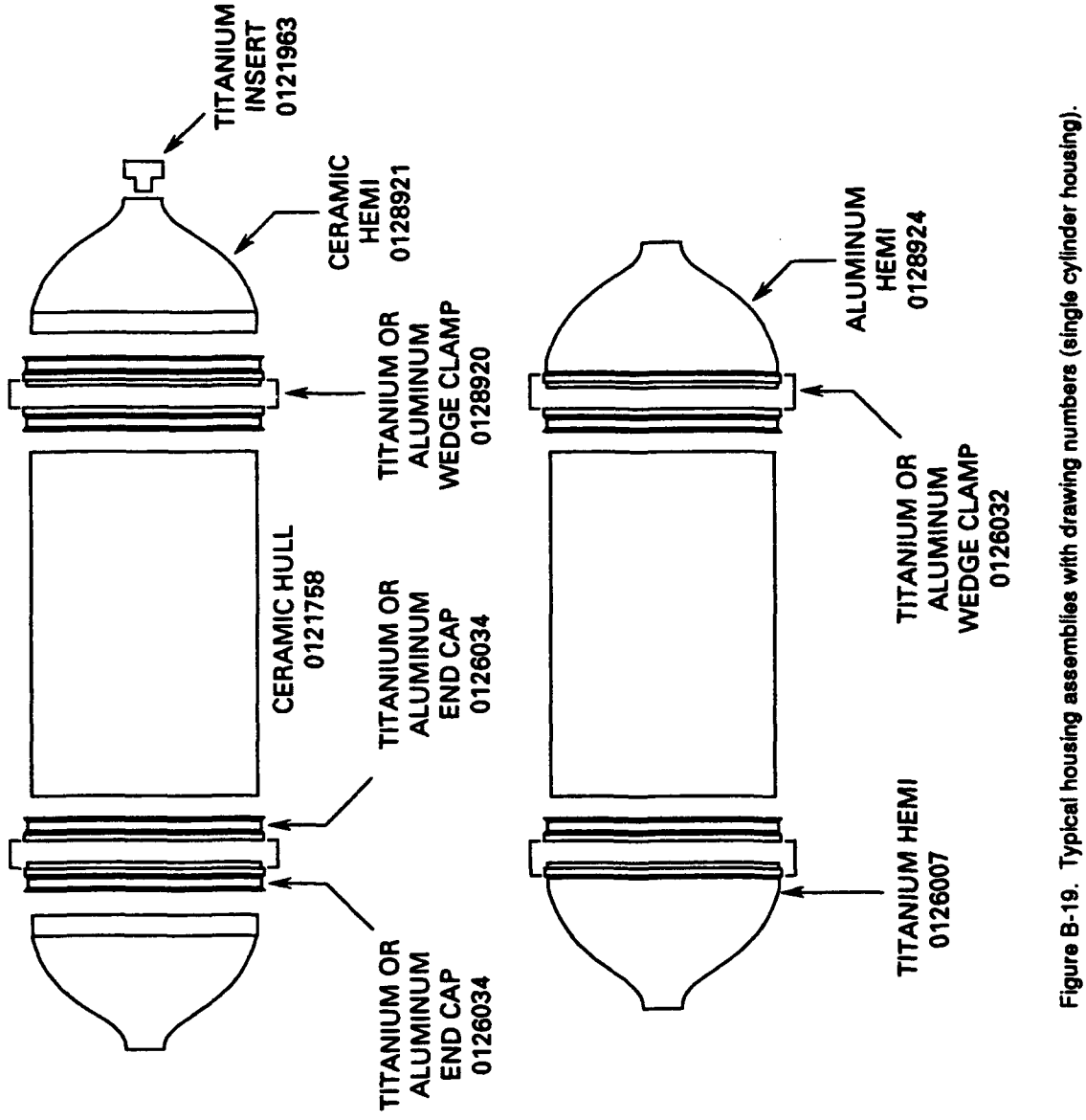

Figure B-19. Typical housing assemblies with drawing numbers (single cylinder housing).

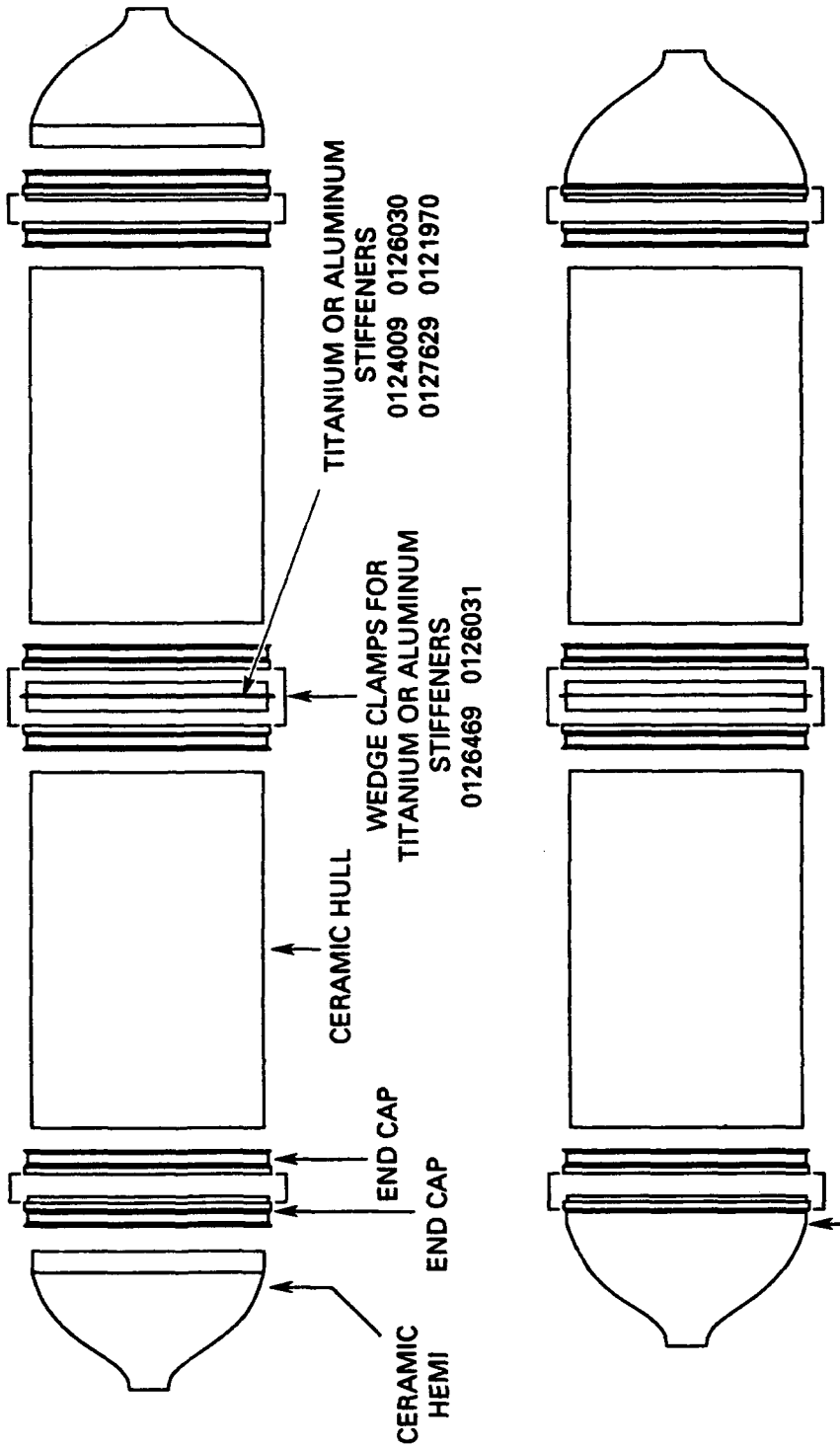

Figure B-20. Typical housing assemblies with drawing numbers (multiple cylinder housing).

REPORT DOCUMENTATION PAGE

Form Approved
OMB No. 0704-0188

1. AGENCY USE ONLY *(Leave blank)*	2. REPORT DATE	3. REPORT TYPE AND DATES COVERED
	August 1993	Final

4. TITLE AND SUBTITLE

ADHESIVE BONDED JOINT WITH IMPROVED CYCLIC FATIGUE LIFE FOR ALUMINA-CERAMIC CYLINDERS AND HEMISPHERES
Fourth Generation Housings

5. FUNDING NUMBERS

PE: 0603713N
PROJ: S0397
ACC: DN302232

6. AUTHOR(S)

J. D. Stachiw

7. PERFORMING ORGANIZATION NAME(S) AND ADDRESS(ES)

Naval Command, Control and Ocean Surveillance Center (NCCOSC)
RDT&E Division
San Diego, CA 92152–5000

8. PERFORMING ORGANIZATION REPORT NUMBER

TR 1587

9. SPONSORING/MONITORING AGENCY NAME(S) AND ADDRESS(ES)

Naval Sea Systems Command
Washington, DC 20362

10. SPONSORING/MONITORING AGENCY REPORT NUMBER

11. SUPPLEMENTARY NOTES

12a. DISTRIBUTION/AVAILABILITY STATEMENT

Approved for public release; distribution is unlimited.

12b. DISTRIBUTION CODE

13. ABSTRACT *(Maximum 200 words)*

A series of 20-inch-diameter monocoque cylinders of 94-percent alumina-ceramic have been pressure tested to determine their structural performance under repeated pressurizations to 9,000 psi external design pressure when their ends are encapsulated in epoxy-filled Mod 1 titanium or aluminum end caps.

Naval Ocean Systems Center (NOSC) Type Mod 1 titanium end caps provided an order-of-magnitude improvement in cyclic fatigue life for the ceramic cylinders over previously tested Mod 0 end caps. The cyclic fatigue life of 20-inch OD by 18.63-inch ID by 30-inch L by 0.685-inch t ceramic cylinders with 0.5-inch weight/displacement ratio, the ends of which were encapsulated with epoxy adhesive in Mod 1 titanium end caps, exceeded 400 cycles to 9,000 psi that generated inside the cylinder compressive membrane stresses of 136,000 psi magnitude in hoop and 68,000 psi in axial direction.

At these stress levels, the shell of the monocoque cylinder can tolerate imperfections in the shape of spherical ($\leq$0.063-inch) and oblong cavities ($\leq$0.063-inch by 0.187-inch) located below, or on, the shell surface, provided that they are at least two inches away from the ends. The payload-carrying ability of 94-percent alumina-ceramic monocoque cylinders with above dimensions is approximately four-times larger, then, of rib-stiffened titanium cylinders with the same external dimensions and pressure rating.

14. SUBJECT TERMS

ceramics
external pressure housing
ocean engineering

15. NUMBER OF PAGES
119

16. PRICE CODE

17. SECURITY CLASSIFICATION OF REPORT	18. SECURITY CLASSIFICATION OF THIS PAGE	19. SECURITY CLASSIFICATION OF ABSTRACT	20. LIMITATION OF ABSTRACT
UNCLASSIFIED	UNCLASSIFIED	UNCLASSIFIED	SAME AS REPORT

21a. NAME OF RESPONSIBLE INDIVIDUAL	21b. TELEPHONE *(include Area Code)*	21c. OFFICE SYMBOL
J. D. Stachiw	(619) 553–1875	Code 9402

THE AUTHORS

DR. JERRY STACHIW is Staff Scientist for Marine Materials in the Ocean Engineering Division. He received his undergraduate engineering degree from Oklahoma State University in 1955 and graduate degree from Pennsylvania State University in 1961.

Since that time he has devoted his efforts at various U.S. Navy Laboratories to the solution of challenges posed by exploration, exploitation, and surveillance of hydrospace. The primary focus of his work has been the design and fabrication of pressure resistant structural components of diving systems for the whole range of ocean depths. Because of his numerous achievements in the field of ocean engineering, he is considered to be the leading expert in the structural application of plastics and brittle materials to external pressure housings.

Dr. Stachiw is the author of over 100 technical reports, articles, and papers on design and fabrication of pressure resistant viewports of acrylic plastic, glass, germanium, and zinc sulphide, as well as pressure housings made of wood, concrete, glass, acrylic plastic, and ceramics. His book on "Acrylic Plastic Viewports" is the standard reference on that subject.

For the contributions to the Navy's ocean engineering programs, the Navy honored him with the Military Oceanographer Award and the NCCOSC's RDT&E Division honored him with the Lauritsen-Bennett Award. The American Society of Mechanical Engineers recognized his contributions to the engineering profession by election to the grade of Life-Fellow, as well as the presentation of Centennial Medal, Dedicated Service Award and Pressure Technology Codes Outstanding Performance Certificate.

Dr. Stachiw is past-chairman of ASME Ocean Engineering Division and ASME Committee on Safety Standards for Pressure Vessels for Human Occupancy. He is a member of the Marine Technology Society, New York Academy of Science, Sigma Xi and Phi Kappa Honorary Society.